JPRS L/10238

7 January 1982

Translation

OPERATION MODES OF WATER-MODERATED WATER-COOLED NUCLEAR POWER REACTORS

By

F. Ya. Ovchinnikov, et al.

FBIS FOREIGN BROADCAST INFORMATION SERVICE

NOTE

JPRS publications contain information primarily from foreign newspapers, periodicals and books, but also from news agency transmissions and broadcasts. Materials from foreign-language sources are translated; those from English-language sources are transcribed or reprinted, with the original phrasing and other characteristics retained.

Headlines, editorial reports, and material enclosed in brackets [] are supplied by JPRS. Processing indicators such as [Text] or [Excerpt] in the first line of each item, or following the last line of a brief, indicate how the original information was processed. Where no processing indicator is given, the information was summarized or extracted.

Unfamiliar names rendered phonetically or transliterated are enclosed in parentheses. Words or names preceded by a question mark and enclosed in parentheses were not clear in the original but have been supplied as appropriate in context. Other unattributed parenthetical notes within the body of an item originate with the source. Times within items are as given by source.

The contents of this publication in no way represent the policies, views or attitudes of the U.S. Government.

APPROVED FOR RELEASE: 2007/02/09: CIA-RDP82-00850R000500020007-7

JPRS L/10238

7 January 1982

OPERATION MODES OF WATER-MODERATED WATER-COOLED NUCLEAR POWER REACTORS

Moscow EKSPLUATATSIONNYYE REZHIMY VODO-VODYANYKH ENERGETICHESKIKH YADERNYKH REAKTOROV in Russian 1979 (signed to press 3 Jul 79)

[Chapters 2.4, 3.2, 3.3, 4.1, 4.2, 4.3, 5.3, 7.1, 7.2, and Appendix, 8.4, 11.1, 11.2, 12.4, and table of contents from book "Operation Modes of Water-Moderated Water-Cooled Nuclear Power Reactors", by Fedor Yakovlevich Ovchinnikov, Lev Ivanovich Golubev (deceased), Vyacheslav Dmitriyevich Dobrynin, Victor Ivanovich Klochkov, Vladimir Vladimirovich Semenov and Valentin Mikhaylovich Tsybenko, Atomizdat, 4,100 copies, 288 pages]

CONTENTS

[Text]

2.4. Special Features of Neutron Physics Characteristics of the Core of VVER-1000

The dimensions of the core of the VVER-1000 [water-moderated water-cooled power reactor] exceed substantially the dimensions of the core for VVER-440. Fuel assemblies are larger than the fuel assemblies of VVER-440 and contain 317 fuel elements each arranged with a somewhat larger lattice pitch. The basic design parameters of the core, assemblies and fuel elements are given below:

Basic Design Characteristics of the Core of VVER-1000

Equivalent radius of the core -- 156.0 cm
Core height (working state) -- 355.0 cm
Core volume -- 27.0 m^3
Ratio of the moderator area to the fuel area in the core cross section -- 2.00

Design Characteristics of VVER-1000 Assembly of the V Block of NVAES [Novovoronezhskaya Nuclear Electric Power Station]

"Box-wrench" size of assembly -- 238 mm
Spacing of assemblies -- 241 mm
Thickness of assembly wall -- 1.5 mm (with 25% surface perforation)
Height of assembly with a bunch of control rods or SVP [rods with a burnable absorber] -- 4665 mm
Number of fuel elements in the assembly -- 317
Spacing of fuel elements -- 12.75 mm
Number of guiding channels for regulating rods -- 12
Number of channels for energy release indicators -- 1
Dimensions of guiding channels and the channel for the energy release indicator -- 12.6 X 0.85 mm
Size of the central tube -- 10.3 X 0.65 mm
Material of guiding channels, the channel for energy release measurements, and the central tube -- zirconium alloy

Characteristics of Fuel Elements of Assemblies in VVER-1000

Size of fuel element jacket -- 9.1 X 0.69 mm
Material of the fuel element jacket -- zirconium alloy
Diameter of fuel pellet -- 7.6 mm
Diameter of axial hole in fuel pellet - 1.4 mm

Material of pellet -- UO_2
Enrichment of make-up fuel, %:
in a two-year cycle -- 3.3
in a three-year cycle -- 4.4
Weight of UO_2 load in one fuel element -- 1575 g

Characteristics of a Regulating Rod and Rods with a Burnable Absorber (SVP)

Dimensions of the envelope of the regulating rod and SVP -- 8.2 X 0.6 mm
Envelope material -- stainless steel
Diameter of the core of the regulating rod and SVP -- 7 mm
Material of the core of the regulating rod -- Eu_2O_3 + aluminum alloy
Material of SVP core -- boron in a zirconium matrix
Concentration of natural boron in the material of SVP -- 1%

The achievement of the prescribed burnup fraction of fuel with permissible specific thermal loads is determined entirely by the length of time the fuel elements stay in the core. The operation time of fuel elements in VVER-440 is three years. A three-year run was also adopted for the main fuel reloading mode in VVER-1000. Due to high specific loads in the core of this reactor in the above-mentioned mode, an average calculated burnup fraction of 39,800 Mw X day/T U is achieved, which is approximately 30% greater than the average fuel burnup fraction achieved in VVER-440. For the first loadings of the core of the first VVER-1000, it is planned to use a two-year-run mode. In this case, the fuel burnup fraction will be 26,500 Mw·day/T U and will not exceed the achieved limits.

After an experimental study of part of the fuel elements kept in the reactor until a burnup of 45,000 Mw·day/T U, the VVER-1000 reactor is changed to a three-year run; in this case, the fuel component of the electric energy drops (according to calculations) by approximately 15% in comparison with a two-year cycle. The enrichment of the makeup fuel is 3.3% (in the two-year cycle) and 4.4% (in the three-year cycle).

Properties of the fuel elements are adjusted over the cross section of the assembly, since an increase in the enrichment and the dimensions of the assemblies of VVER-1000 leads to an increase in the nonuniformity of heat release in it. For example, in an assembly with a fuel of 4.4%-enrichment, the variation factor for the fuel elements is 1.22. The arrangement of fuel elements with uranium of lower enrichment (3.6%) in a peripheral row and in corner spots of the next row lowers the variation factor to 1.16.

The 109 assemblies have movable regulating rods (clusters) which are intended (by analogy with SUZ assemblies in VVER-440): a) for rapid stopping of the nuclear reactions; b) for automatic regulation in order to maintain the reactor power at the prescribed level or for changing it from one power level to another; c) for compensating rapid changes in reactivity by changing their position in the core.

For the core variant with a three-year run, rods were installed in 42 peripheral assemblies with a burnable absorber (with respect to the mass of 1% of natural boron) -- SVP. SVP rods are intended for lowering the breeding properties in the peripheral assemblies with a fuel enrichment of 4.4% at the beginning of the run.

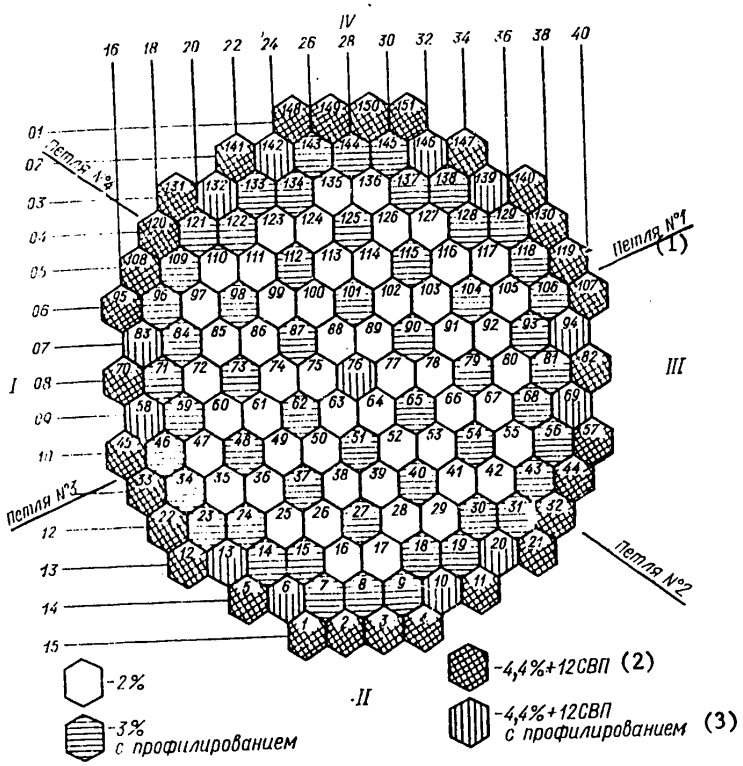

Figure 2.10. Cartogram of the first fuel loading of the VVER-1000 core of the V block of NVAES with assemblies with various degrees of enrichment of the fuel (three reloadings per run) for a three-year burnup cycle.
Key: 1. loop
2. SVP
3. with adjustment

The cartogram of the first fuel loading of the core of the VVER-1000 of the V block of NVAES for a three-year cycle is shown in 2.10. The core consists of assemblies with fuel enrichment of 2% (54 items), 3% with adjustment of energy release by the fuel elements with enrichment of 2.4% (54 items), 4.4% + 12 SVP with adjustment of energy release by the fuel elements with enrichment of 3.6% (13 items), 4.4% + 12 SVP (30 items). At the time of fuel reloading, the assemblies are rearranged in the core according to a definite scheme, and SVP consisting of assemblies with initial enrichment of 4.4% are removed.

The basic operation characteristics of VVER-1000 in the three-year cycle are:

average burnup fraction between reloadings -- $10.9\text{-}13.8 \times 10^3$ Mw·days/T U (for an operation length of 240-300 effective days);

maximum power variation factors of assemblies -- $k_q = 1.29 \div 1.35$;

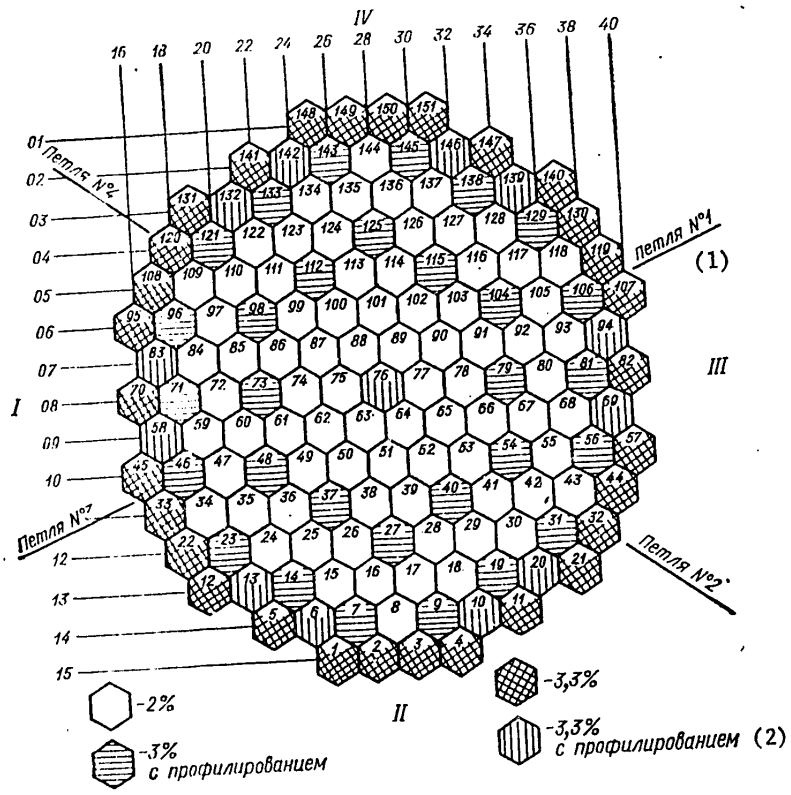

Figure 2.11. Cartogram of the first fuel loading of the VVER-1000 core of the V block of NVAES with assemblies with various degrees of fuel enrichment (two reloadings per run) for a two-year burnup cycle.
Key: 1. loop
2. with adjustment

initial boron concentration in the heat-transfer agent of the I circuit c_B = 1.39 ÷ 1.80 v B/kg H_2O.

The cartogram of the first fuel loading of the core of VVER-1000 of the V block of NVAES for the two-year cycle is shown in Figure 2.11. The core consists of assemblies with fuel enrichment of 2% (78 items), 3% with adjustment of energy release by the fuel elements with enrichment of 2.4% (30 items), 3.3% with adjustment of energy release by the fuel elements with enrichment of 2.4 and 3% (13 items), 3.3% (30 items).

The basic operation characteristics in the two-year cycle are:

average burnup fraction between reloadings -- 11.3-13.35X10^3 Mw·day/t U (for operation lengths of 250 ÷ 290 effective days);

maximum power variation factor of assemblies $k_q = 1.31 \div 1.37$;

initial boron concentration in the heat-transfer agent of the I circuit -- $c_B = 1.15 \div 1.45$ g B/kg H_2O.

For adjusting energy release, fuel elements of lower enrichment are installed in the peripheral row of the cells and in the corner cells of the following row: for assemblies with enrichment of 3% -- fuel elements with enrichment of 2.4%, and for assemblies with enrichment of 4.4% -- 3.6%. For assemblies with enrichment of 3.3%, energy release is adjusted by installing fuel elements with enrichment of 2.4% in three corner cells of the peripheral row and in the corner cells of the next row, and in the remaining cells of the peripheral row -- fuel elements with enrichment of 3%.

3.2. Coefficients of Reactivity of the Reactor

The reactivity and, consequently, the reactivity excess of VVER depend greatly on the temperature of the core. As a rule, VVER reactivity drops as the temperature rises, specifically, when its power rises (this phenomenon is used for ensuring safety in controlling the reactor). Changes in the reactivity when the core temperature rises are caused by a number of phenomena occurring in the moderator-coolant and in the fuel. First of all, it is the decrease in the water density with temperature rise which leads to a decrease in the number of atoms of the moderator in a unit volume and, as a result of this, to a decrease in the moderating ability of the water. As a result of this, as well as due to an increase in the kinetic energy of the nuclei of the moderator (hydrogen), when the water temperature rises, there occurs ruggedization of the spectrum of neutrons leading to changes in the neutron cross sections of the nuclei of the fuel, the heat-transfer agent and structural materials and, consequently, the neutron-physics characteristics of the core lattice. Moreover, the rise of the fuel temperature increases the resonance capture of neutrons by the ^{238}U isotope (Doppler effect).

When the core temperature rises, the following effects play the most important role: 1) decrease in the cross section of neutron absorption in water governed by the law 1/v; 2) decrease in the cross section of scattering and density of water and decrease in the moderating ability of the water connected with this; 3) decrease in the cross section of absorption and fission of uranium and transuranium elements; 4) increase of the resonance capture of neutrons in the fuel (Doppler effect); 5) decrease in the cross section of absorption of neutrons by zirconium and niobium.

Some of these effects make a positive contribution and some a negative contribution to the total temperature effect. Effect 1 makes a positive contribution due to decreased absorption of neutrons in the water. The decrease in the moderating ability of the water gives a negative component which, as a rule, exceeds all positive components of the temperature effect. Effects 3 and 4 also decrease the core reactivity. Effect 5 contributes a small positive component to the temperature effect.

An additional influence on the temperature effect of reactivity is connected with the accumulation of plutonium isotopes during the fuel burnup. Isotopes ^{239}Pu and ^{241}Pu have large cross section of fission and absorption at a neutron energy of about 0.3 eV. Isotopes ^{240}Pu and ^{242}Pu have a strong absorption resonance at an energy of approximately 1 eV. As the core temperature rises, the resonances of plutonium isotopes widen, but the inverse influence of resonance blocking is greater in this case. As a result of this, the accumulation of plutonium isotopes makes a positive contribution to the temperature effect of reactivity.

In calculating the neutron-physics chatacteristics of VVER, several coefficients of reactivity characterizing temperature and some other effects are introduced. As a rule, these are: 1) water temperature coefficient of reactivity k_1; 2) fuel temperature coefficient of reactivity k_2; 3) water coolant pressure coefficient of reactivity k_3; 4) water density coefficient of reactivity k_4; 5) power coefficient of reactivity k_5; 6) coefficient of reactivity with respect to the concentration of boric acid in the coolant k_6.

The temperature coefficient of reactivity k_1 is defined as the ratio of the change in the reactivity of the reactor to the change in the average temperature of water and is designated as $\partial\rho/\partial t_{H_2O}$. It allows also for the changes in the density of the water as its temperature changes, i.e., coefficient k_4 is a component of k_1.

The fuel temperature coefficient of reactivity k_2 characterize the changes in the reactivity of the reactor when the average temperature of the fuel changes and is designated by $\partial\rho/\partial t_{UO_2}$.

The sum of the water and fuel temperature coefficients of reactivity is the temperature coefficient of reactivity of the reactor $\partial\rho/\partial t$ and is defined as the change in the reactivity with changes in the average temperatures of the water and fuel in the reactor which are identical when the core works at zero power.

It is evident that in experiments on a reactor, it is practically impossible to determine the water temperature and fuel temperature coefficients separately. As a rule, the total temperature effect is determined when working at a negligibly small power and heating the water with main circulation pumps or outside sources of heat. Coefficients k_1 and k_2 can be estimated separately only by calculations or in indirect experiments using critical assemblies.

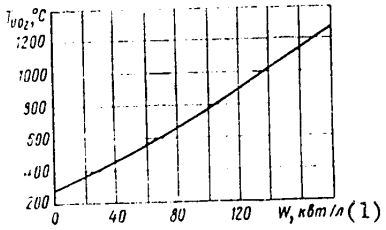

Figure 3.2. Dependence of the average fuel temperature of VVER-440 on the specific power (at t_{H_2O} = 285 degrees C)
Key: 1. kw/l

When the power of the reactor increases, there occurs an additional rise in the fuel temperature which becomes higher than the temperature of the coolant (Figure 3.2). Moreover, there appears a temperature drop between the center and the surface of the fuel element. The increase in the fuel temperature results in an additional decrease of reactivity due to the Doppler effect. This decrease in reactivity is called power effect, for which a special coefficient is introduced: $k_5 = \partial\rho/\partial N$. The power coefficient of reactivity is determined experimentally by measuring the changes

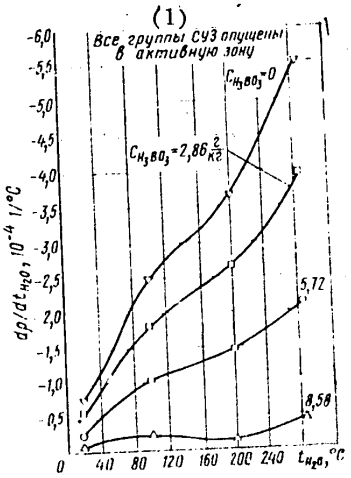

Figure 3.3. Dependence of the water temperature coefficient of reactivity on the coolant temperature for VVER-440 of the IV block of NVAES.
Key: 1. All SUZ [control and safety rods] groups are lowered into the core.

in the reactivity during gradual increases in the power of the reactor with a constant water temperature.

The power and temperature coefficients of reactivity do not remain constant in the entire interval of working temperatures of the reactor. As the water temperature rises, the absolute value of the negative water temperature coefficient of reactivity k_1 increases, while the coefficient of reactivity k_2 decreases (Figures 3.3 and 3.4).

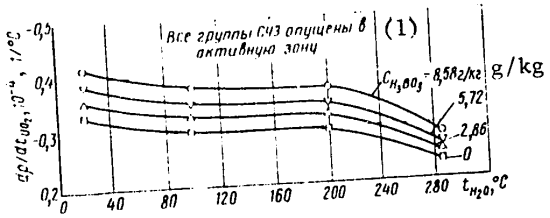

Figure 3.4. Dependence of the fuel temperature coefficient of reactivity on the coolant temperature for VVER of the IV block of NVAES.
Key: 1. All SUZ groups are lowered into the core.

During the loading of the reactor, the water and fuel temperature coefficient of reactivity increases with respect to its absolute value, which is a re ult of the accumulation of plutonium and fission fragments and the decrease in the concentration of boric acid.

The coolant pressure coefficient of reactivity in VVER is small, because water is a weakly compressed liquid. However, when pressure in circuit I increases sharply, for example, during preparations for the startup, it is possible to have a reactivity release sufficient for causing the runaway of the reactor. In this connection, as well as for reasons of strength, the pressure increase rate in circuit I is normalized.

Boric acid is introduced into the coolant for even distribution of the absorber over the core. The coefficient of reactivity with respect to the concentration of boric acid in the coolant k_6 is defined as $\partial\rho/\partial C_{H_3BO_3}$. The values of the coefficients of reactivity for the reactors of the Novovoronezhskaya AES are given in Tables 3.1 and 3.2.

Table 3.1

Coefficients of Reactivity of VVER-365 and VVER-440 of NVAES (for the beginning of the run)

(1) Коэффициент реактивности	(2) ВВЭР-365*		ВВЭР-440, IV блок (3)	
	20 °C	260 °C	20 °C2*	285 °C3*
(4) По температуре топлива, 10^{-4} °C^{-1}	—0,33	—0,25	—0,38	—0,32
(5) По температуре воды, 10^{-4} °C^{-1}	—(1÷2)	—(3÷4)	—0,001	—1,286
(6) По плотности воды, $(г/см^3)^{-1}$	—	0,18÷0,25	—0,102	0,06
(7) По мощности реактора, 10^{-4} 1/%	—	—1,5	—	—1,7
(8) По содержанию борной кислоты в воде, 10^{-2} кг/г H_3BO_3	—2,87	—2,42	—2,18	—1,86

*In the absence of boric acid in the water.

2*$C_{H_3BO_3}$=7.7 g/kg.

3*$C_{H_3BO_3}$=5.0 g/kg; N - 100%.

Key: 1. Coefficient of reactivity
2. VVER-365*
3. VVER-440, IV block
4. Fuel temperature, 10^{-4} $^{o}C^{-1}$
5. Water temperature, 10^{-4} $^{o}C^{-1}$
6. Water density, $(g/cm^3)^{-1}$
7. Reactor power, 10^{-4} 1/%
8. Boric acid content in the water, 10^{-2} kg/g H_3BO_3

Undesirable release of reactivity is possible in some instances, for example, when circulation loops of the reactor are turned on during the startup or after repairs with a lower water temperature or with a lower concentration of boric acid. For example, the work [26] examines a calculated model of VVER behavior when the water temperature at the entrance to the core is lowered. When the input temperature dropped from 266 to 232 degrees, reactivity $\rho \simeq 0.002$ was released in one fourth part of the zone whose values decreased to 0.001 in six seconds. In published literature, they examined some cases of supplying colder water in an operating reactor which was in a critical state [27]. At the AES "Dresden-2" (U.S.A.), where a boiling-type reactor was installed, there were instances of the delivery of colder water into the reactor when a reserve circulation pump was faultily turned on and the flow rate of feed water increased spontaneously. The release of reactivity due to the lowering of the water temperature in the reactor caused in both cases the runaway of the reactor and the triggering of the safety system.

Table 3.2

Coefficients of Reactivity of the Core of the Reactor VVER-1000 of the V Block of NVAES

(1) Коэффициент реактивности	(2) Состояние активной зоны	(3) Первая загрузка, T=3 года/T=2 года	(4) Стационарный трехлетний топливный цикл
(5) По температуре воды, 10^{-4} град$^{-1}$	Холодное (10)	—0,100/0,86	0,100—(—0,30)
	Горячее (11)	—0,50/0,605	—1,00—(—3,50)
	Рабочее: начало работы (12)	—1,00/—0,346	—1,50—(—4,00)
	($N_{тепл}$=100%) конец работы (13)	—3,50/—6,30	
(6) По плотности воды, (г/см^3)$^{-1}$	Холодное	—0,150/—0,126	—0,13—(—0,04)
	Горячее	—0,040/—0,030	0,06—0,15
	Рабочее: начало работы	—0,040/—0,005	0,10—0,20
	($N_{тепл}$=100%) конец работы	0,160/0,282	
(7) По температуре топлива, 10^{-5} град$^{-1}$	Холодное	—3,00/—3,39	—3,00—(—3,50)
	Горячее	—2,50/—3,02	—2,50—(—3,00)
	Рабочее: начало работы	—2,00/—2,69	—2,00—(—2,50)
	($N_{тепл}$=100%) конец работы	—2,30/—2,36	
(8) По мощности реактора, 10^{-4} 1/%	Рабочее: начало работы (12)	—1,40/—2,00	—(1,2—1,4)÷—
	($N_{тепл}$=100%) конец работы (13)	—1,50/—2,90	—(1,5—2,0)
(9) По содержанию бора, (г B/кг H_2O)$^{-1}$	Холодное	—0,120/—0,150	—0,095—(—0,105)
	Горячее	—0,095/—0,100	—0,075—(—0,085)
	Рабочее: начало работы	—0,090/—0,105	—0,070—(—0,080)
	($N_{тепл}$=100%) конец работы	—0,095/—0,110	

Key: 1. Coefficient of reactivity
2. State of the core
3. First loading, T = 3 years/T = 2 years
4. Steady-state three-year fuel cycle
5. Water temperature, 10^{-4} degrees^{-1}
6. Water density (g/cm^3)$^{-1}$
7. Fuel temperature, 10^{-5} degrees^{-1}
8. Reactor power, 10^{-4} 1/%
9. Boron content (g B/kg H_2O)$^{-1}$
10. Cold
11. Hot
12. Working: beginning of work
13. (N_{heat} = 100%) end of work

Compensation of the reactivity excess of boric acid makes it possible to reduce the nonuniformity of energy release over the core and, consequently, to increase the permissible power of the reactor and the fuel burnup fraction.

The decrease in the nonuniformity of energy release is determined by the fact that boric acid solution changes the neutron-physics characteristics of the entire core, while absorbing rods act chiefly on the neighboring areas of the core.

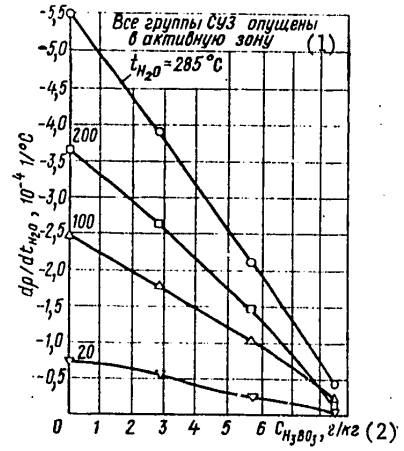

Figure 3.5. Dependence of the water temperature coefficient of reactivity on the concentration of boric acid in the coolant for VVER-440 of the IV block of NVAES.
Key: 1. All SUZ groups are lowered into the core
2. g/kg

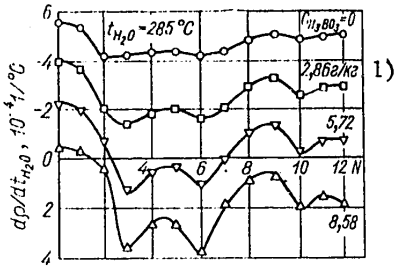

Figure 3.6. Effects of the removal of SUZ groups of assemblies on the water temperature coefficient of reactivity for VVER-440 of the IV block of NVAES (along the X-axis -- the number of the SUZ group removed from the core).
Key: 1. g/kg

However, when compensating reactivity with boric acid, it is necessary to consider the fact that the absolute value of the negative temperature coefficient of reactivity of the VVER decreases. This is caused by the decrease in the density of the boric acid solution as the temperature rises, which leads to a decrease in the concentration of the absorbing nuclei of ^{10}B in the unit volume of the coolant. This effect intensifies when the concentration of boric acid is increased (Figure 3.5).

The presence of boric acid in the coolant increases somewhat the absolute value of the negative fuel temperature coefficient of reactivity, since the absorption cross section of the ^{10}B isotope follows the law 1/v and, moreover, the absorption chiefly

of low-energy thermal neutrons leads to the ruggedization of the neutron spectrum. However, the influence of boric acid on the fuel temperature coefficient of reactivity is considerably lower than its influence on the water temperature coefficient of reactivity. The water temperature coefficient of reactivity depends also on the position of the SUZ groups (Figure 3.6).

At high concentrations of boric acid, the temperature coefficient of reactivity can become positive. The presence of a positive temperature coefficient of reactivity in VVER-type reactors at sufficiently high concentrations of boric acid was observed at a number of foreign AES. For example, the "Jose Cabrera" reactor (Spain), at the concentration of boric acid of 2.054 $g_{H_3BO_3}$/kg in the hot state without power had a positive temperature coefficient equal to $1.206 \cdot 10^{-4}$ degrees C^{-1} [28].

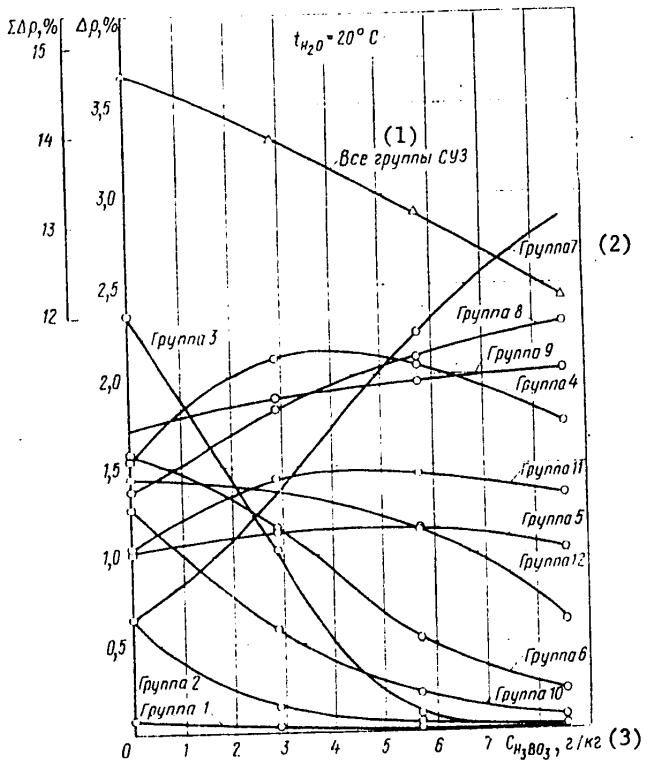

Figure 3.7. Dependence of the integral effectiveness of SUZ groups of VVER-440 of the IV block of NVAES on the concentration of boric acid.

Key: 1. All SUZ groups
2. Group
3. g/kg

It is evident that operation of a reactor with a positive temperature coefficient of reactivity is extremely undesirable because its control and safety conditions become complicated. Therefore, when calculating a VVER, the value of the concentration of boric acid ensuring a stable negative temperature coefficient is selected.

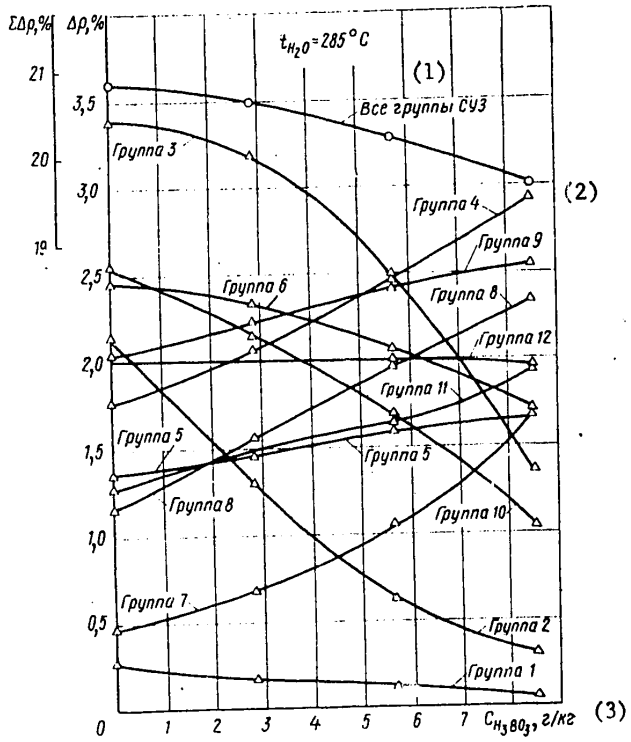

Figure 3.8. Dependence of the integral effectiveness of the groups of SUZ assemblies of the VVER-440 of the IV block of NVAES on the concentration of boric acid at operating temperature.
Key: 1. All SUZ groups
2. Group
3. g/kg

When a reactor operates with boric acid in the coolant, it is necessary to consider also the changes in the effectiveness of the SUZ assemblies from the concentration of boric acid (Figures 3.7, 3.8). In the presence of boric acid, the overall effectiveness of the groups of SUZ assemblies decreases, however, changes in the effectiveness of individual groups resulting from an increased concentration of boric acid are very different in nature, which is determined by the arrangement of the groups of assemblies in the core in relation to one another and order of their setting. It should be mentioned that the effectiveness of group No 12 (see Figure 3.8) which was selected as a controlling group of SUZ in the VVER-440 reactor of the IV block of Novovoronezhskaya AES at an average operating temperature of the coolant of 285 degrees C, remains practically constant in the entire interval of operating concentrations of boric acid.

When calculating the effect of boric acid on reactivity in the course of the run, it is necessary to consider the changes in the isotopic composition of boron due to the burnup of ^{10}B.

Boric acid introduced into the first loop at the beginning of the run circulates in a closed loop and, practically, is not replaced (it is only gradually removed as the fuel burns up). In this connection, its absorbing ability decreases, which has to be taken into consideration.

Changes in the amount of the ^{10}B isotope can be described by the following differential equation:

$$\frac{dN}{dT} + \sigma_a \varphi \frac{T_{a.3}}{T_{конт}} N + \frac{N_0}{T_0} = 0, \qquad (3.10)$$

where N -- concentration of the nuclei of the ^{10}B isotope in the coolant, cm^{-3}; σ_a -- microscopic absorption cross section of ^{10}B, cm^2; φ -- average density of the thermal neutron flux in the reactor, neutron/(cm^2Xsec); $T_{a.3}/T_{КОНТ}$ -- ratio of the passage time of a unit volume of the coolant through the core of the reactor to the passage time of the same volume through the entire first loop, including the core of the reactor; N_0 -- concentration of ^{10}B nuclei at the beginning of the loading of the reactor, cm^{-3}; T_0 -- total time of loading at nominal power, ef, sec; T -- current time, sec.

In the equation (3.10), the term N_0/T_0 allows for the removal of boric acid in the process of fuel burnup. It is assumed that the amount of the removed boric acid depends linearly on the effective time of the reactor's operation. The solution of the equation (3.10) has the following form:

$$\frac{N}{N_0} = \exp(-\sigma_a \varphi T_{a.3} T/T_{конт}) - \qquad (3.11)$$

$$- \frac{T_{конт}}{T_0 \sigma_a \varphi T_{a.3}} [1 - \exp(-\sigma_a \varphi T_{a.3} T/T_{конт})].$$

The relation $T_{a.3}/T_{КОНТ}$ can be taken to be approximately equal to $V_{a.3}/n_{петл}$ $V_{петл} + V_{a.3}$, where $V_{петл}$ -- coolant volume in one circulation loop of the reactor: $V_{a.3}$ -- coolant volume in the core of the reactor; $n_{петл}$ -- number of loops of the reactor. If the load works for 300 effective days, the burnup of the ^{10}B isotope can reach 10% of the initial content and result in a lower effectiveness of boric acid with respect to reactivity.

3.3. Requirements for the VVER Control and Safety System

The control and safety system (SUZ) is the main system for ensuring nuclear safety of the VVER reactor. It has two independent systems based on different principles, namely: a system of mechanical members of SUZ (SUZ assemblies) and a boron regulation system.

The SUZ system performs the following functions: 1) controls the power of the reactor; 2) compensates slow changes in reactivity; 3) performs emergency and planned shutdowns of the reactor.

The fulfillment of these functions is ensured if the following requirements for the SUZ system are satisfied: 1) reliable and sufficiently rapid compensation of changes in reactivity connected with power control; 2) insurance of the compensation of reactivity excess for fuel burnup in the course of the loading work of the reactor, as well as compensation of the poisoning effects of the reactor by samarium and xenon; at the same time, the temperature and power effects of reactivity during the changes of the reactor power from zero to the nominal value must be compensated; 3) in a cold unpoisoned state of the core, during the reloading of nuclear fuel, the effectiveness of SUZ must be sufficiently great for reliable damping of the reactor with a safe depth of subcriticality; 4) the effectiveness of the control members of the SUZ and the rate of reactivity release must exclude the possibility of uncontrolled runaway of the reactor; 5) when the power of the reactor drops to zero, the SUZ system must ensure the necessary subcriticality in a stopped hot reactor. In this case, it is necessary to consider possible failure of one of several SUZ drives with jamming of the absorbers in the upper position and the possibility of spontaneous removal of the SUZ absorbers from the core; 6) the speed of the introduction of negative reactivity in emergency conditions must ensure the damping of the reactor in the shortest possible time determined by the drop of the reactor power and ensuring the safety of the jackets of the fuel elements of the core.

The main causes of changes in the reactivity of VVER reactors and their contribution to the changes in reactivity in percentages are given below [29]:

Doppler effect	1.4-1.6
Changes of average water temperature	0-1.0
Changes in the average water density	0-0.1
Control area	0.5
Operation reserve	0.1
Overall effectiveness necessary for controlling the power of the reactor	2.0-3.3

Fuel burnup	3.0-10.0
Poisoning by xenon and samarium	3.0
Shutdown cooling	4.0-5.0
Subcriticality during reloading	2.0-10.0
Overall effectiveness necessary for the compensation of slow changes in reactivity	17.0-28.0
Power changes during shutdown	1.4-2.7
Subcriticality of a hot reactor	1.0
Effectiveness of one absorber jammed in the upper position	1.0
Overall effectiveness necessary for the shutdown of the reactor	3.4-4.7

In VVER, the boron regulation system compensates slow changes in reactivity in the course of the run, and the system of mechanical control members controls the power of the reactor in nonsteady-state conditions and compensates reactivity during planned and emergency shutdowns.

The system of mechanical members of SUZ ensures the introduction of negative reactivity into the reactor under emergency conditions at a rate of about 2% reactivity per second and ensures the release of reactivity during regulation at a rate of not over 0.22% reactivity per second.

Table 3.3

Excesses of Reactivity of the Core and Effects of Its Changes for VVER-440 of the IV Block of NVAES (first loading)

Параметр (1)	(2) Мощность, %	ρ, %	Δρ, %
Запас реактивности при: (3)			
20 °C	—	17,77	—
100 °C	—	16,95	—
150 °C	—	16,53	—
200 °C	—	16,07	—
285 °C	—	14,10	—
(4) Температурный эффект при 20—285 °C	—	—	3,67
(5) Мощностной эффект	0—100	—	1,60
(6) Стационарное отравление ^{135}Xe	100	—	2,53
» » ^{149}Sm	100	—	0,65
(7) Запас реактивности на выгорание	100	9,32	—
(8) Эффективность кассет СУЗ при:			
20 °C	—	—	14,66
285 °C	—	—	20,82

Key: 1. Parameter
2. Power
3. Reactivity excess at:
4. Temperature effect at
5. Power effect
6. Steady-state poisoning
7. Reactivity excess compensating the burnup
8. Effectiveness of SUZ assemblies at:

Table 3.3 shows the excesses of reactivity and effects of its changes for the reactor of the IV block of NVAES.

The SUZ assembly of VVER-440-type reactors consists of two parts: upper -- absorber, lower -- nuclear fuel. When setting up an SUZ assembly, the absorber is removed from the core and the fuel part replaces it. Thus, the lifting of an SUZ assembly releases the reactivity of the reactor both by reducing the absorption of neutrons, and the by increasing the mass of the fuel in the core. The SUZ absorbers have a hexahedral jacket with "black" walls for thermal neutrons. The jacket contains inserts of borated steel which absorb thermal and partially epithermal neutrons. The presence of water within the absorber ensures opacity to fast neutrons. The SUZ absorber serves as a neutron trap: fast neutrons are slowed down in the water and absorbed by boron without emerging beyond the limits of the absorber; thermal neutrons are absorbed in the borated inserts when they are passing through the walls of the absorber. If the absorber is removed from the core and the hexahedral water cavity is left, the latter will also fulfill the role of a neutron trap. The effectiveness of the water cavity is about 70% of the effectiveness of the SUZ absorber [30]. This effect is used during fuel reloading: before removing the absorber of the SUZ, two or three working fuel assemblies around it are unloaded in order to create water cavities which compensate to some degree the unloading of the absorber from the core and act as an absorber during the removal of the fuel part of the SUZ assembly from the reactor.

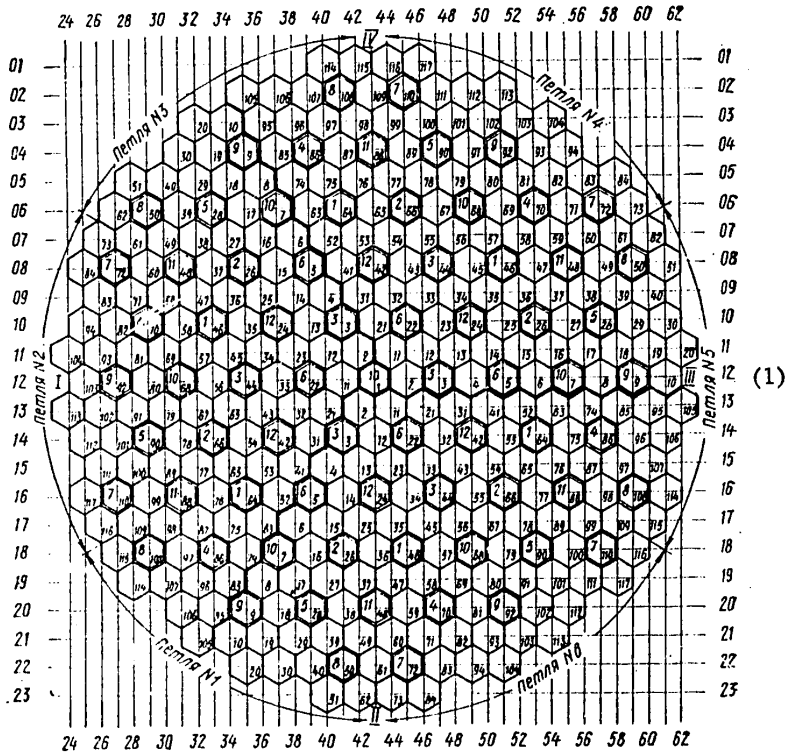

Figure 3.9. Cartogram of the arrangement of SUZ assembly groups in the VVER-440 of the III block of NVAES.
Key: 1. Loop

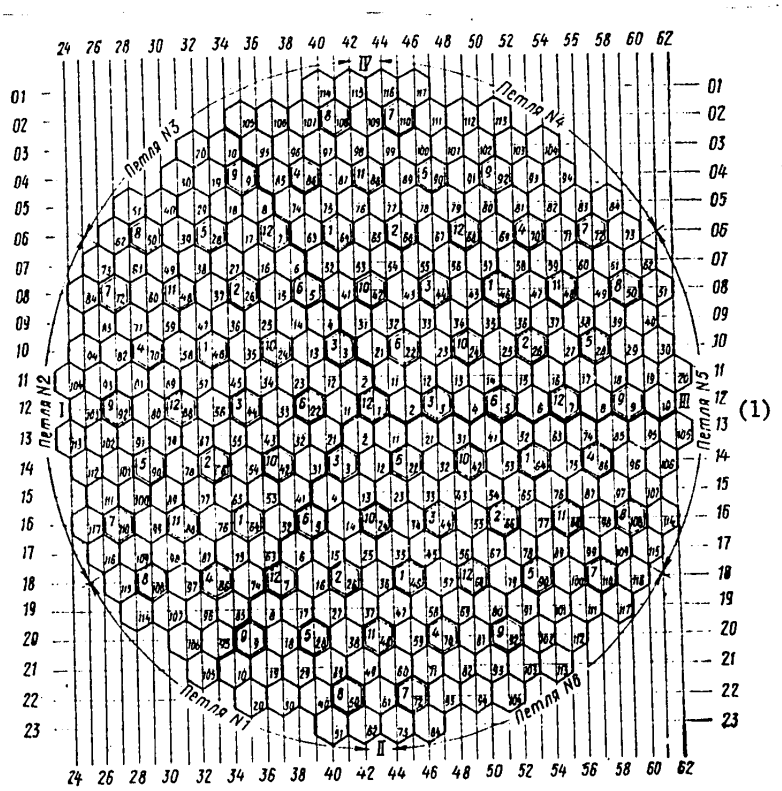

Figure 3.10. Cartogram of the arrangement of SUZ assembly groups in the VVER-440 of the IV block of NVAES.
Key: 1. Loop

The effectiveness of SUZ assemblies depends chiefly on their location in the core and on the core temperature. As the fuel in the core burns up, as well as during the burnup of the ^{10}B isotope in the absorbers of the SUZ assemblies, their effectiveness changes. When a reactor is designed, the optimal order of successive setting of SUZ groups is calculated for a definite number of assemblies in a group. The criterion for determining the order of the setting of SUZ groups is the insurance of minimal nonuniformity of energy release over the radius and height of the core. It is taken into consideration that the reactivity excess for the burnup is compensated almost fully by boric acid, therefore, all SUZ groups are in the upper position with the exception of the last XII working group.

Figures 3.9-3.11 show cartograms of the arrangement of SUZ groups in the cores of VVER-440 of the III and IV block of NVAES, as well as Kol'skaya AES. The VVER core in the plane is divided into three computation sectors with a 120 degree angle at the vertex. The neutron-physics computations of the VVER are done, as a rule, for one sector on the assumption that the properties are repeated with a periodicity of 120 degrees in the remaining sectors. In each computation sector, the design numbers

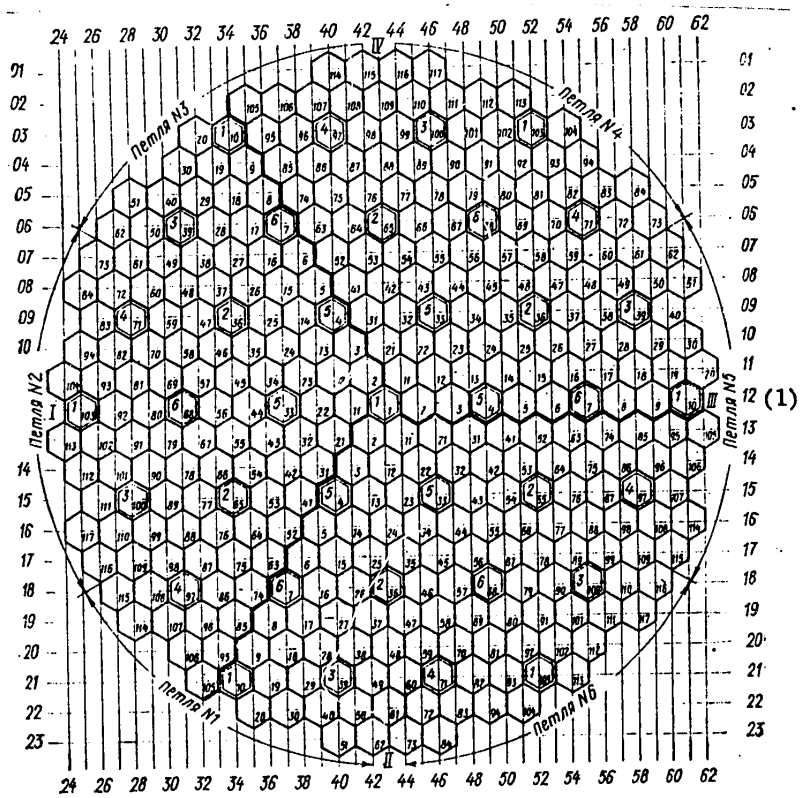

Figure 3.11. Cartogram of the arrangement of SUZ assembly groups in the VVER-440 of Kol'skaya AES.
Key: 1. Loop

of the assemblies are indicated. The cores of the reactors of the III and IV blocks of NVAES contain 73 SUZ assemblies which are divided into 12 groups. In the core of the VVER-440 reactor of the III block, the controlling group is group No 12 which contains six assemblies with design numbers 24 and 42. Since the VVER-440 of the IV block uses nuclear fuel with a greater enrichment than in the III block, the composition of the controlling group No 12 was changed in order to reduce the nonuniformity of energy release. SUZ assemblies with design numbers 1, 7, 68 from group No 10 were included in it, and assemblies with design numbers 24, 42 were transferred to group No 10.

The core of the VVER-440 of Kol'skaya AES has only 37 SUZ assemblies. Unlike the VVER-210, which also has 37 of them, the assemblies are spaced farther apart and, accordingly, they are displaced toward the periphery of the core. This is due to the zone loading of the VVER-440 and a higher enrichment of the fuel. Tables 3.4 and 3.5 show the values of the effectiveness of the SUZ assembly groups at various temperatures for VVER-440 of NVAES.

Table 3.4

Effectiveness of SUZ Groups of VVER-440 of the III block of NVAES (first loading, no boric acid in the coolant)

(1) Номер вводимой группы	(2) Расчетные номера кассет	20 °C		100 °C		180 °C		285 °C	
		ρ, %	Δρ, %	ρ, %	Δρ, %	ρ, %	Δρ, %	ρ, %	Δρ, %
(3) Все группы внизу	—	—3,93	—	—6,18	—	—9,22	—	—15,94	—
1	46, 64	—3,38	0,55	—5,62	0,56	—8,67	0,55	—14,02	1,92
2	26, 66	0,74	4,12	—1,48	4,14	—4,03	4,64	—8,25	5,77
3	3, 44	3,89	3,15	1,88	3,36	—0,267	3,763	—4,19	4,06
4	70, 86	4,94	1,05	3,01	1,13	1,009	1,276	—2,818	1,375
5	28, 90	5,81	0,87	4,02	1,01	2,072	1,063	—1,614	1,204
6	5, 22	7,45	1,64	5,86	1,84	4,14	2,068	1,051	2,665
7	72, 110	8,01	0,56	6,41	0,55	4,71	0,57	1,59	0,539
8	50, 108	9,22	1,21	7,67	1,26	5,97	1,26	2,26	0,67
9	9, 92	10,56	1,34	9,16	1,49	7,54	1,57	3,82	1,56
10	1, 7, 68	12,05	1,49	10,84	1,68	9,46	1,92	6,41	2,59
11	48, 88	13,70	1,65	12,59	1,75	11,39	1,93	8,49	2,08
12	24, 42	14,70	1,00	13,78	1,19	12,71	1,32	10,295	1,805

Key: 1. Number of the group being set up
2. Design numbers of assemblies
3. All lower groups

Table 3.5

Effectiveness of SUZ groups of VVER-440 of the IV block of NVAES (first loading, no boric acid in coolant)

(1) Номер вводимой группы	(2) Расчетные номера кассет	20 °C		100 °C		200 °C		285 °C	
		ρ, %	Δρ, %	ρ, %	Δρ, %	ρ, %	Δρ, %	ρ, %	Δρ, %
(3) Все группы внизу	—	3,116	—	1,682	—	—1,779	—	—6,720	—
1	46, 64	3,196	0,08	1,765	0,083	—1,647	0,132	—6,445	0,275
2	26, 66	3,837	0,641	2,436	0,671	—0,478	1,169	—4,309	2,136
3	3, 44	6,179	2,342	4,864	2,428	2,444	2,922	—0,934	3,375
4	70, 86	7,681	1,502	6,429	1,565	4,130	1,686	0,834	1,768
5	28, 90	8,683	1,002	7,478	1,049	5,323	1,193	2,175	1,341
6	5, 22	10,237	1,554	9,117	1,639	7,335	2,012	4,633	2,458
7	72, 110	10,878	0,641	9,768	0,651	7,913	0,578	5,109	0,476
8	50, 108	12,225	1,347	11,154	1,386	9,262	1,349	6,264	1,155
9	9, 92	13,947	1,722	12,941	0,787	11,225	1,963	8,289	2,025
10	24, 42	15,207	1,260	14,281	1,340	13,087	1,853	10,825	2,536
11	48, 88	16,340	1,033	15,452	1,171	14,317	1,239	12,102	1,277
12	1, 7, 68	17,772	1,432	16,949	1,497	16,066	1,749	14,104	2,002

Key: 1. Number of the group being set up
2. Design numbers of assemblies
3. All lower groups

Table 3.6

Effectiveness of SUZ groups VVER-440 of the IV block of NVAES at various concentrations of boric acid in the coolant (first loading)

(1) Номер вводимой группы	(2) Концентрация борной кислоты, г/кг H_3O																	
	20 °C				100 °C				200 °C				285 °C					
	0	2,86	5,72	8,58	0	2,86	5,72	8,58	0	2,86	5,72	8,58	0	2,86	5,72	8,58
1	0,08	0,041	0,024	0,016	0,083	0,047	0,028	0,018	0,132	0,082	0,053	0,036	0,275	0,193	0,132	0,094
2	0,641	0,057	0,151	0,029	0,671	0,184	0,072	0,037	1,169	0,424	0,172	0,086	2,136	1,302	0,642	0,324
3	2,342	1,027	0,110	0,024	2,428	1,237	0,176	0,035	2,922	2,185	0,856	0,161	3,375	3,197	2,502	1,398
4	1,502	2,091	2,057	1,713	1,565	2,106	2,324	1,884	1,686	2,129	2,677	2,613	1,768	2,066	2,482	2,957
5	1,002	1,109	1,105	1,012	1,049	1,162	1,176	1,093	1,193	1,328	1,415	1,402	1,341	1,471	1,602	1,699
6	1,554	1,155	0,502	0,232	1,639	1,277	0,747	0,321	2,012	1,750	1,328	0,811	2,458	2,321	2,077	1,730
7	0,641	1,351	2,253	2,866	0,651	1,288	2,156	2,822	0,578	1,022	1,731	2,552	0,476	0,698	1,072	1,616
8	1,347	1,811	2,098	2,276	1,386	1,836	2,138	2,331	1,349	1,830	2,227	2,506	1,155	1,531	1,967	2,361
9	1,722	1,863	1,952	2,024	1,787	1,929	2,023	2,094	1,963	2,147	2,279	2,373	2,025	2,240	2,428	2,572
10	1,260	0,579	0,211	0,089	1,340	0,689	0,278	0,120	1,853	1,247	0,682	0,331	2,536	2,129	1,694	1,084
11	1,033	1,415	1,441	1,308	1,171	1,451	1,523	1,413	1,239	1,523	1,750	1,789	1,277	1,493	1,651	1,966
12	1,432	1,34	1,154	0,615	1,497	1,423	1,258	0,957	1,749	1,734	1,643	1,480	2,002	2,040	2,037	1,981

Key: 1. Number of the group being set up
2. Boric acid concentration, g/kg H_2O

The effectiveness of SUZ assembly groups depends also on the concentration of boric acid in the reactor. Table 3.6 shows the values of their effectiveness at various concentrations of boric acid for VVER-440 of the IV block of NVAES.

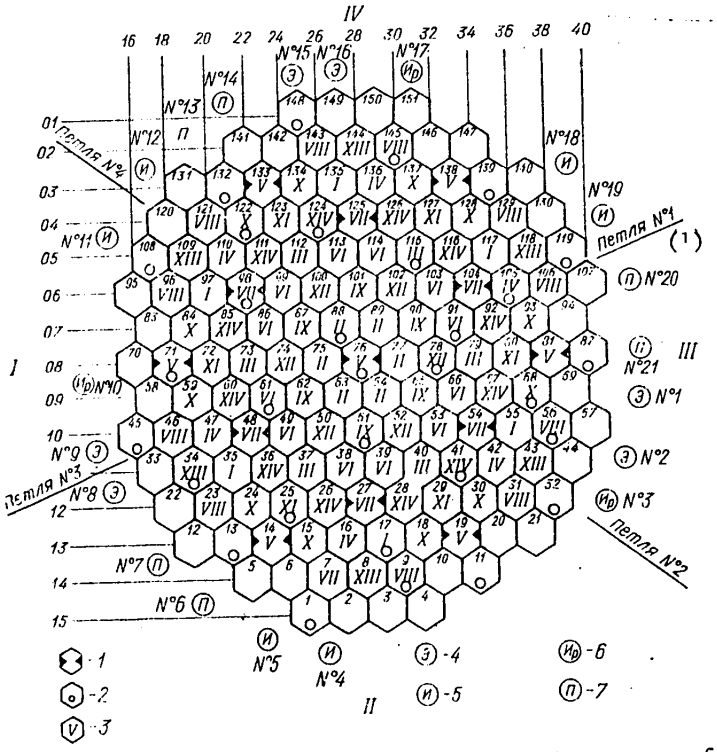

Figure 3.12. Cartogram of the arrangement of the groups of SUZ absorbers and neutron measuring channels in the core and the ionization chanbers of the SUZ of the VVER-1000 reactor of the V block of NVAES:
1 -- assemblies with SUZ absorbers filled to one half by absorbing materials; 2 -- assemblies with neutron measuring channels; 3 -- number of the group of SUZ absorbers; 4 -- energy-range ionization chambers; 5 -- startup-range ionization chanbers; 6 -- standby startup-range ionization chambers; 7 -- intermediate-range ionization chambers.
Key: 1. loop

The mechanical control and safety system in VVER-1000 of the V block of NVAES consists of 109 drives each of which is capable of moving a bunch (cluster) of twelve absorber rods (core material -- Eu_2O_3 in a matrix of an aluminum alloy) inside the assembly within the limits of the core. The SUZ drives combined into groups (Figure 3.12) move the clusters simultaneously.

The mechanical system of SUZ is intended for compensating rapid changes in the reactivity (temperature, power, and poisoning effects). Slow changes in the reactivity (fuel burnup) are compensated by changing the concentration of the boric acid solution in the coolant. For emergency situations, there is a high-speed boron injection system.

The total effectiveness of the mechanical system of the SUZ of VVER-1000 must be not less than the sum of the following effects:

Doppler effect of fuel when the power of the reactor changes from 0 to 100% -- 0.013;

changes in the average water temperature of the first circuit when the power changes from 0 to 100% -- 0.014;

changes in the steam content in individual jets of the coolant in the core when the power changes from 0 to 100% -- 0.002;

effective reserve for nonsteady-state xenon poisoning and leveling of energy release -- 0.015;

effectiveness of a jammed bunch of absorbers -- not over 0.010;

initial subcriticality after the triggering of the safety system -- 0.010.

In order to allow for errors in the neutron-physics computations, the necessary effectiveness of SUZ is taken 20% higher than the total sum of the above reactivity effects and must be not less than 0.077.

4.1. Distribution of Energy Release in the Core

The distribution of energy release in the core is characterized by energy release variation factors which must be known for determining the permissible thermal power of the reactor (see section 5.3).

It is customary to consider the energy release variation factors with respect to the radius, height, and volume of the core. According to the definition, the energy release variation factor in the i-th assembly over the radius of the core $k_{r,i}$ is equal to

$$k_{r,i} = Q_i/\bar{Q}, \qquad (4.1)$$

where Q_i -- power of the i-th assembly; $\bar{Q}$ -- average power of the assembly in the core.

For boron-regulated reactors, the maximum value of k_r^{max} varies within the limits of 1.2-1.4, and for reactors with regulation by mechanical members of SUZ -- within the limits of 1.5-2.1.

The small variation of energy release in boron-regulated reactors makes it possible to remove a great amount of thermal power from the core. The variation factors of energy release in the core are calculated on a computer for the entire run (see section 7.2). Experimental values of $k_{r,i}$ are determined on the basis of water temperature measurements at the outlet from the assemblies and the coolant temperature at the inlet to the reactor. The values of the variation factors are computed by the formula

$$k_{r,i} = \frac{t_i^{вых} - \sum_{j=1}^{m} t_j^{вх} G_j \Big/ \sum_{j=1}^{m} G_j}{\sum_{i=1}^{n} t_i^{вых} g_i \Big/ \sum_{i=1}^{n} g_i - \sum_{j=1}^{m} t_j^{вх} G_j \Big/ \sum_{j=1}^{m} G_j} \cdot \frac{g_i}{\frac{1}{n}\sum_{i=1}^{n} g_i}, \qquad (4.2)$$

where $t_i^{вых}$ -- water temperature at the outlet from the i-th assembly; $t_j^{вх}$ -- water temperature at the inlet to the reactor from the j-th circulation loop; G_j -- mass velocity in the j-th circulation loop; g_i -- mass velocity in the i-th assembly; m -- number of circulation loops; n -- number of fuel assemblies in the core.

For measuring the water temperature at the outlet from the assemblies, VVER are equipped with a temperature monitoring system. Temperature measurements are done by thermocouples which are sufficiently efficient in a wide temperature range under the conditions of neutron and gamma irradiation. Chromel-copel and platinum-platinorhodium (10% Rh) thermocouples are used most widely. In VVER-440, the outlet water temperature is monitored for about two thirds of the assemblies of the ıtire core, and in VVER-1000 -- at the outlet of all assemblies. The water temperature at the inlet to the core is measured in the circulation loops. Depending on the steam load of the steam generators, the number of working loops, and the hydraulic resistance, certain deviations of the inlet temperature in the loops are possible. In practical calculations, the water temperature at the inlet to the core is taken to be equal to the average value for all working loops of the reactor. In averaging, differences in the water flow rate in the loops are taken into considerations.

The flow rate of the coolant through the assemblies of the core are determined on the basis of the hydraulic characteristics of the assemblies (see section 5.2). The power of the assemblies under operating conditions is calculated by the energy release variation factors at a known average power of the assemblies of the core. The distribution of energy release over the height of the core is usually obtained by calculations for the entire run (see section 7.2). Experimental distribution of energy release is determined in special measuring channels with the aid of the sensors of the in-pile monitoring system. From 12 to 36 measuring channels are installed in the core of VVER-440. The measuring channel is a stainless steel tube with the lower end plugged up passing through the lid of the reactor into the central tube of the working assembly. In the VVER-1000 assemblies, the detectors of the in-pile monitoring system (VRK) are arranged not in the central tube, but in a special channel of energy release measurements. The VVER-1000 reactor of the V block of NVAES has 31 measuring channels connected to the VRK system (see Figure 3.12).

The distribution of the neutron flux density and energy release along the height are measured by activation and emission detectors, as well as by ionization chambers [31]. Calibrated copper wires with a constant mass per unit length are used as activation detectors. The wire is irradiated in the measuring channel in the course of time sufficient for its saturation by the ^{64}Cu isotope, after which it is removed from the core and cooled for a while for the decomposition of the short-lived copper isotopes. The distribution of beta-activity through the length of the wire measured after this will correspond to the distribution of the neutron flux density with the height of the measuring channel at the moment of the irradiation of the wire.

In VVER, emission detectors -- direct charge detectors (DPZ) -- are used widely. The operating principle of DPZ is based on the appearance of an electric potential in a detector consisting of an emitter and a collector during the beta-decomposition of the neutron-sensitive emitter. Rhodium and vanadium are usually used as DPZ emitters. DPZ are small and sufficiently simple secondary devices. A drawback of the direct charge detector is their rather great inertia. In the series-produced VVER-440, each measuring channel has four rhodium DPZ 250 mm long and one vanadium DPZ 2500 mm long. Rhodium detectors are intended for measuring the distribution of the neutron flux density with the height of the channel, and vanadium detectors are intended for measuring the total neutron power in the channel. Moreover, the distribution of the neutron flux density with the height can be measured by moving the DPZ along the length of the channel.

For practical monitoring working conditions of the fuel elements, it is necessary to know the energy release distribution whose correlation with the density distribution of the thermal neutron flux changes as the fuel burns up. At the initial moment of burnup, the neutron flux density and the specific energy release are connected by the relation

$$W = \varphi_0 \sigma_{25}^f N_{25}^0, \qquad (4.3)$$

where σ_{25}^f -- fission cross section of ^{235}U; N_{25}^0 -- initial concentration of ^{235}U nuclei.

Allowing for the accumulation of ^{239}Pu and ^{241}Pu and ^{235}U burnup, the relation (4.3) assumes the form

$$W = \varphi (\sigma_{25}^f N_{25} + \sigma_{39}^f N_{39} + \sigma_{41}^f N_{41}), \qquad (4.4)$$

where σ_{39}^f and σ_{41}^f -- fission cross sections of ^{239}Pu and ^{241}Pu; N_{25}, N_{39} and N_{41} -- concentration of ^{235}U, ^{239}Pu and ^{241}Pu nuclei, respectively.

In order to proceed from the measured density distribution of the thermal neutron flux to the distribution of energy release, it is necessary to perform conversions which, as a rule, are done on the computer and allow for the burnup of ^{235}U and accumulation of plutonium isotopes. For this purpose, information from DPZ is loaded into the computer which promptly processes the data and informs the operator about the results of measurements with consideration for the burnup of the DPZ emitter. In order to simplify the computation programs of information (controlling) electronic computers, it is desirable to use, in addition to the detectors measuring the density of the thermal neutron flux, detectors whose indications characterize directly the energy release in the fuel elements surrounding the channel. Energy release in fuel elements is characterized unambiguously by the flux density of fast or resonance neutrons which can be measured with the aid of modernized DPZ or ionization chambers. For example, a DPZ with an emitter of silver surrounded by a cadmium jacket for cutting off thermal neutrons registers chiefly the density of the flux of resonance neutrons which, in the final analysis, is proportional to the energy release in the surrounding fuel elements.

Reduction of the factors of variation along the radius k_r and the height kz and the volume factor of variability $k_V = k_r k_z$ is of great practical significance from the view point of the possibility of increasing the reactor power and the fuel burnup fraction. Therefore, the work on the leveling of VVER power is being done continuously.

In VVER, a zonal principle of load assembling is used (see section 7.1), which makes it possible to level energy release along the radius of the core and, in combination with boron regulation, to reduce the volume nonuniformity of energy release.

In the process of fuel burnup, there occurs additional self-leveling of energy release due to the nonuniformity of burnup proportional to energy release, and due to the nonuniformity of the manifestation of the poisoning effect and the power effect of reactivity. For an example, Figure 4.1 shows the changes in the calculated and experimental values of maximum variation factors of energy release k_q^{max} and k_r^{max}

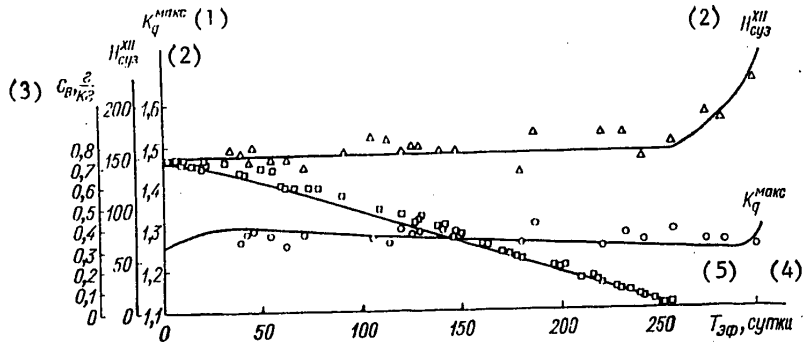

Figure 4.1. Changes in the maximum energy release variation factors during the work of the first loading of VVER-440 of the IV block (curves -- calculated data; dots -- experimental data).

Key: 1. Maximum
2. SUZ
3. g/kg
4. days
5. $T_{effective}$

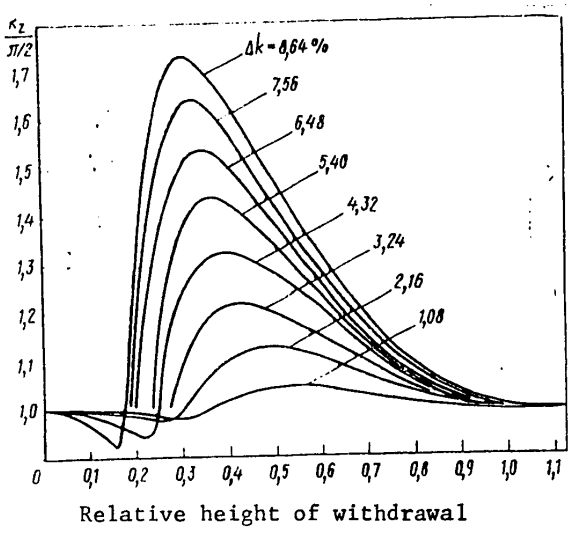

Figure 4.2. Dependence of the height factor of energy release variation on the height of withdrawal of mechanical members of SUZ with different integral effectiveness ($\frac{K_z}{\pi/2}$ = 1 for cosine distribution of energy release along the height of the core)

for the first fuel loading of the VVER-440 of the IV block of NVAES. The values of the variation factors decrease in the course of the loading operation. Some increase in the variation factors at the end of the run is due to the gradual withdrawal of the controlling group of SUZ from the core. There is a particularly strong dependence of the height distribution of energy release on the presence of partially inserted SUZ assemblies. Figure 4.2 shows theoretical dependence of the height variation of energy release of the core on the withdrawal height of the SUZ assemblies having different effectiveness [6]. The withdrawal of "light" groups creates the least nonuniformity.

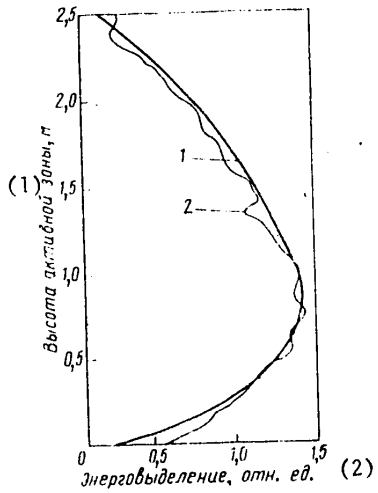

Figure 4.3. Energy release distribution along the height of the measuring channel of the VVER-440 of the III block of NVAES (1 -- computation; 2 -- measurement). Channel in the cell 13-30; power in the reactor 55%; withdrawal height of the 12-th group 127 cm; $C_{H_3BO_3}$ = 2.79 g/kg H_2O.
Key: 1. Core height, m
2. Energy release, per unit value

Figure 4.3 shows the distribution curve of energy release obtained in the measuring channel of the VVER-440 of the III block.

In conclusion, let us note that the leveling of energy release increases the probability of the appearance of xenon oscillations (see section 4.3). Xenon oscillations are the effect of periodic redistribution of power over the core volume caused by the feedback between the power and concentration of ^{135}Xe.

In VVER-440, the probability of xenon oscillations is small and if such oscillations occur, they are aperiodic in nature, have a small amplitude, and attenuate rapidly.

A distinguishing characteristic of VVER-1000 is the possibility of the occurrence of spatial xenon oscillations of power in the volume of the core. The probability of the occurrence of xenon oscillations increases as the dimensions of the reactor increase in the case of disturbances in the distribution of power. The greatest

field disturbances in VVER-1000 occur in the operation mode with changes in the level of power, for example, the lowering of power from 100 to 50% for a while with subsequent increase to 100% (Figure 4.4). The figure shows clearly the appearance of deformation in the axial distribution of the neutron flux caused by transitional xenon processes and the shifting of the SUZ regulating members.

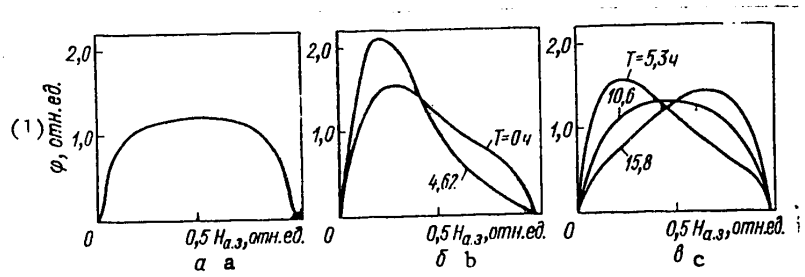

Figure 4.4. Axial density distribution of the neutron flux in VVER-1000 under the condition of changing loads: a -- reactor power 100%, regulating rods are withdrawn from the core; b -- reactor power lowered to 50%, regulating rods are lowered to the height of the core equal to 0.4; c -- reactor power increased to 100% after working at a power level of 50% in the course of 5.3 hours.

Key: 1. per unit value

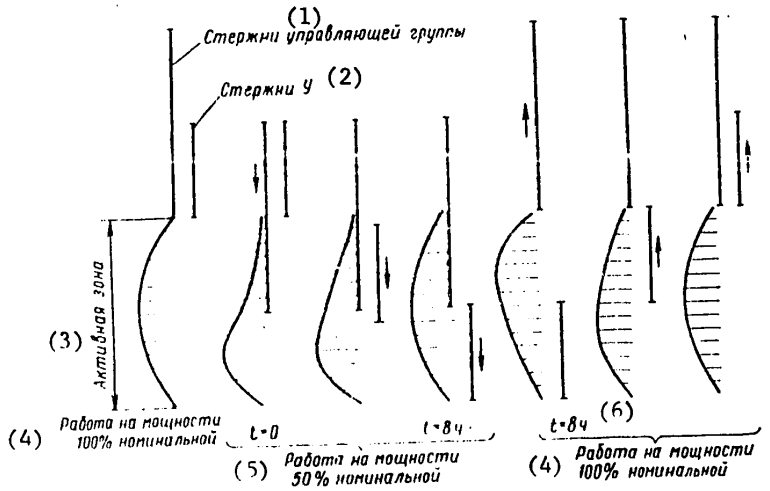

Figure 4.5. Movement scheme of control rods Y for suppressing spatial xenon oscillations along the height of the core of VVER-100.

Key: 1. Rods of the controlling group
2. Rods Y
3. Core
4. Work at 100% nominal power
5. Work at 50% nominal power
6. t = 8 hours

Evidently, in a number of cases, in order to reduce the dimensions of disturbances in power distribution, it is expedient to lower the regulating rods completely, and to compensate their influence by changing the concentration of boric acid during the entire operation time of the reactor at a lower power.

A sufficiently developed system of in-pile monitoring with results processed by a computer is a component part of the VVER-1000 control system. The operational information about the distribution of power over the core makes it possible to correct the developing deformations of the field in time. Radial and azimuthal deformations of power distribution can be corrected by withdrawing or lowering certain groups of absorbers. Height deformations can be corrected with the aid of a special group of control rods Y with a half-height of the absorbing substance by changing their position along the height of the core (Figure 4.5).

4.2. Changes in the Reactivity of the Reactor During Its Work at Full Power

When a reactor works at full power, besides the changes in the reactivity described in section 3.2, its reactivity changes as a result of the effects of poisoning and slagging of the core.

As a result of the fission of uranium and plutonium nuclei, there form various fission fragment nuclei and product nuclei of the radioactive decay of fragments. It is possible to isolate two main groups (see Chapter 1) among fission fragments and products of their decay whose accumulation in the core affects substantially neutron-physics characteristics of the reactor. The first group includes ^{135}Xe and ^{149}Sm nuclei which have large thermal neutron absorption cross sections. The decrease in the reactivity of a reactor as a result of the accumulation of ^{135}Xe and ^{149}Sm nuclei is called poisoning. Poisoning by ^{135}Xe is particularly important in transitional processes, because the half-life periods of ^{135}Xe and its predecessor ^{135}I are relatively small. The second group of fission fragments and products of their radioactive decay includes stable and long-lived isotopes which have relatively small neutron absorption cross sections. The decrease in the reactivity of a reactor caused by the appearance of fission products during the burnup of fuel is called reactor slagging.

Reactor Poisoning. Poisoning of a Reactor by ^{135}Xe. Chapter 1 gives the chain of the formation of ^{135}Xe from ^{135}I. A small portion of ^{135}I does not form directly during fission, but as a result of the radioactive decay of another fragment, ^{135}Te. The half-life of ^{135}Te is very short, therefore it is assumed in calculations that the entire ^{135}I forms directly during fission. Allowance is made in calculations that a small part of ^{135}Xe nuclei forms directly during fission. The balance of ^{135}I and ^{135}Xe nuclei in the reactor is described by the system of differential equations:

$$\frac{dN_I}{dT} = \gamma_I \Sigma_{fT} \varphi_T - \lambda_I N_I; \tag{4.5}$$

$$\frac{dN_{Xe}}{dT} = \gamma_{Xe} \Sigma_{fT} \varphi_T + \lambda_I N_I - (\sigma_{Xe} \varphi_T + \lambda_{Xe}) N_{Xe}, \tag{4.6}$$

where N_I. NXe -- concentration of iodine and xenon nuclei, respectively, cm^{-3}; γ_I, γ_{Xe} -- yield of iodine and xenon per one fission of a heavy isotope (^{235}U, ^{239}Pu, ^{241}Pu); Σ_{fT} -- macroscopic fuel fission cross section, cm^{-1}; φ_T -- current density of thermal neutrons, neutrons/($cm^2 \cdot sec$); λ_I, λ_{Xe} -- decay constants of iodine and xenon, sec^{-1}; σ_{Xe} -- microscopic absorption cross section of neutron by the isotope ^{135}Xe, cm^2.

For VVER, the following xenon process constants are taken: $\gamma_I = 0.061$; $\gamma_{Xe} = 0.003$; $\lambda_I = 0.287 \cdot 10^{-4}$ sec^{-1}; $\lambda_{Xe} = 0.207 \cdot 10^{-4}$ sec^{-1}.

In a rigorous examination, the values of Σ_{fT} and σ_{Xe} must be averaged over the spectrum of thermal neutrons in the reactor which is determined by the temperature of the fuel and coolant, concentration of boric acid in the coolant, layout of fuel assemblies in the core, concentration of ^{135}Xe nuclei, etc. As a rule, the neutron spectrum is calculated in one or another degree of approximation on a computer (see Chapter 7).

Under the condition that $\Sigma_{fT} = \text{const}$; $\varphi_T = \text{const}$ (i.e., under the condition of constancy of the power and the neutron spectrum), equations (4.5)-(4.6) can be solved analytically:

$$N_I = N_{0I}[1 - \exp(-\lambda_I T)], \tag{4.7}$$

where $N_{0I} = \gamma_I \Sigma_{fT} \varphi_T / \lambda_I$ -- equilibrium concentration of ^{135}I nuclei.

Equilibrium concentration of ^{135}Xe nuclei is determined from the expression

$$N_{0Xe} = \frac{(\gamma_I + \gamma_{Xe}) \Sigma_{fT} \varphi_T}{\lambda_{Xe} + \sigma_{Xe} \varphi_T}. \tag{4.8}$$

As follows from the above formulas, steady-state (equilibrium) concentration of ^{135}I and ^{135}Xe nuclei depends on the neutron flux density, and ^{135}Xe concentration depends on it nonlinearly.

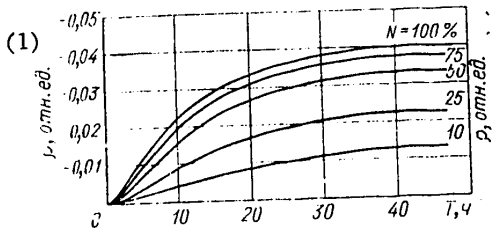

Figure 4.6. Steady-state xenon poisoning of VVER-440.
Key: 1. Per unit value

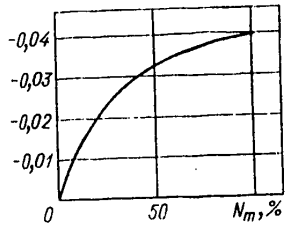

Figure 4.7. Dependence of steady-state xenon poisoning of VVER-440 on thermal power.

Figure 4.6 shows curves of steady-state ^{135}Xe poisoning of the core of VVER-440. When the reactor works at a steady power of 100%, the maximum steady-state poisoning equal to 4% is established approximately after 40 hours. At this moment, equilibrium is established in the formation of ^{135}Xe nuclei from ^{135}I and their disappearance as a result of radioactive decay and burnup by the neutron flux. Figure 4.7 shows the dependence of steady-state ^{135}Xe poisoning of VVER-440 on its power.

When the power of the reactor changes from N_1 to N_2, the balance of ^{135}I and ^{135}Xe nuclei is disturbed, which causes transient processes accompanied by changes in the reactivity of the reactor. When the power decreases, the reactivity of the reactor also decreases, because, as a result of the decrease in the neutron flux density,

the burnup of xenon by neutrons decreases, while its yield from ^{135}I, whose amount at the initial moment is determined by the former power level, does not change, which leads to an increase in the concentration of ^{135}Xe nuclei and increased poisoning. This phenomenon is called iodine pit.

The greatest depths of the iodine pit (4.5%) occurs when the load of the reactor is reduced from 100% to zero (Figure 4.8 a), which is achieved nine hours after the drop of load. Henceforth, as the number of ^{135}I nuclei and, consequently, the number of the forming nuclei of ^{135}Xe decrease, the reactivity increases. When the power is increased, the poisoning of the reactor by xenon first decreases (depoisoning takes place) due to intensive burnup by the increased neutron flux of ^{135}Xe, whose yield from ^{135}I remains for some time corresponding to a lower level of power. Then, the increased yield of xenon nuclei from iodine compensates the released reactivity and brings additional poisoning due to increased concentration of ^{135}Xe nuclei (see Figure 4.8d). The maximum depoisoning can reach 0.6-0.7% reactivity.

In plotting the curves in Figure 4.8, it was assumed that, before changing the power, the reactor operated in a steady-state mode for a long time (2-3 days). The origin of coordinates was selected as an initial point for all curves, and for determining the total poisoning of the reactor by xenon, it is necessary to shift all points of curves in the direction of negative reactivities to a corresponding steady-state poisoning. If the change in the power in the reactor occurred before the establishment of steady-state poisoning, then the following should be done for determining the total poisoning of the reactor by ^{135}Xe: to determine from curves in Figure 4.6 the poisoning of the reactor by xenon at a given power at a given moment of time and, using Figure 4.7, to find to what steady-state power level the obtained value of poisoning corresponds. Then, at the established value of the steady-state power, the parameters of the transient xenon process of interest to us are determined from Figure 4.8.

If the reactor was stopped for a longer time (more than 1.5-2 days), then practically the entire iodine and xenon decay, and curves in Figure 4.6 must be used in calculating the poisoning of the reactor after its startup. If the reactor stopped for less than 1.5 days, then for estimating its xenon poisoning after subsequent power increase, it is sufficient to have in mind that the total poisoning of the reactor tends to the steady-state poisoning at a given power. A method for a more accurate estimation of poisoning for such cases is given in work [32].

The time of attaining the maximum depth of the iodine pit depends on the percentage of the lowering of the reactor power. For example, if the total 100% load is dropped, the maximum of poisoning is attained after nine hours, but if the load is dropped from 100% to 50%, it is attained after five hours (see Figure 4.8a). The total time of ^{135}Xe processes is approximately equal to 40-50 hours.

Let us give an example of calculating the poisoning of a reactor by the ^{135}Xe isotope.

Problem. VVER-440 worked at 100% power (1375 Mw therm) in the course of 10 days. As a result of the triggering of the scram system, the power of the reactor dropped to 25%. After three hours, power was increased to 75%. Xenon poisoning of the reactor to be determined.

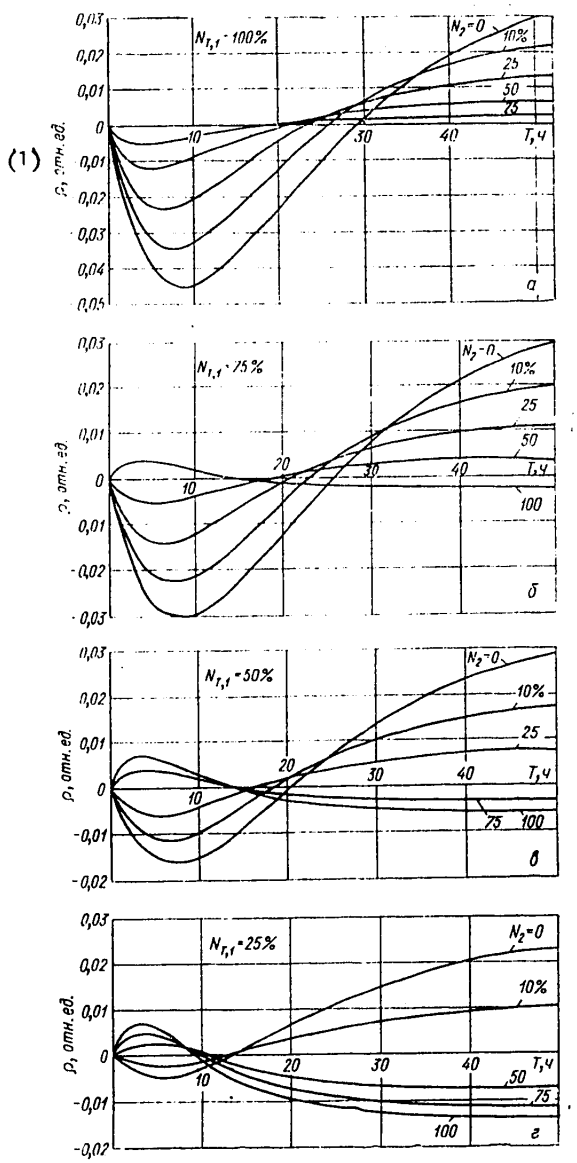

Figure 4.8. Nonsteady-state xenon poisoning of VVER-440 when power drops from 100 (a), 75 (b), 50 (c) and 25% (d) levels.

Key: 1. Per unit value

Solution. Before the shutdown of the reactor, steady xenon poisoning equal to -4% became stabilized (see Figure 4.6). Three hours after the drop of the load to 25%, the depth of the iodine pit reached -1.8% (see Figure 4.8a), and before the reactor power was increased to 75%, xenon poisoning was equal to (-4%) + (-1.8%) = -5.8% of reactivity. After 1.5-2 days of power operation of the reactor, xenon poisoning dropped to the steady-state value at this power, i.e., to -3.75%.

Transient xenon processes have a substantial effect on the maneuversbility of the AES.

Modern water-moderated water-cooled power reactors work, as a rule, in the boron regulation mode, which makes it possible in the steady-state mode to withdraw almost all SUZ assemblies from the core. Among the SUZ groups, only the controlling group remains in a semi-inserted state in the core, which compensates reactivity disturbances connected with the maintaining of the necessary power level of the reactor. The effective reactivity excess of the controlling group of the SUZ is equal to $\sim$0.5%. When the load variations are small, the effective reactivity excess is quite sufficient for compensating the temperature and power effects and the poisoning effect in the transient xenon processes. When the reactor power drops greatly, the depth of the iodine pit becomes greater, which can lead to the necessity of immediate removal of boric acid from loop I to compensate poisoning.

For an example, let us examine the above problem in a somewhat modified form.

Problem. VVER-440 operated at 100% power in the course of 10 days; the concentration of boric acid in the coolant was 2 g/kg, and the effective excess of the SUZ control group was 0.4%. As a result of the triggering of the scram system, the power of the reactor dropped to 25%. After three hours, power was increased to 75% of the nominal power. What actions must taken by the operating personnel for changing the reactivity in order to ensure the operation of the reactor at the above-mentioned power levels?

Solution. Steady-state ^{135}Xe poisoning and the power effect were compensated during the operation at 100% power by a boric acid solution and by the control group. When the load drops from 100 to 25%, a power effect equal to +1.2% is released (see section 3.3). However, this not enough for compensating xenon poisoning which will reach -1.8% after three hours (an iodine pit maximum equal to -2.25% is attained after six hours during operation at 25% power -- see Figure 4.8a). In addition, it is necessary to release the effective excess of the control group equal to +0.4%, and also +0.2% reactivity by removing boric acid from the reactor. Moreover, at the expense of the removal of boric acid, it is necessary to release +1.2% reactivity three hours later for compensating the power effect during the subsequent increase of power (if there are no other conditions, it is necessary to count on a power of 100%) and +0.45% of reactivity for fully compensating the iodine pit (-2.25%), since, as a rule, the exact moment of the emergence of the reactor to a higher power level is not known, and it is quite probable that this will occur at the moment when the maximum of the iodine pit is attained. Thus, in order to compensate +0.2+1.2+0.45% =+1.85% reactivity, it is necessary to lower the concentration of boric acid in the reactor by 1.38 g/kg ($\partial\rho/\partial C_{H_3BO_3} = -3 \cdot 10^{-2}$ kg/g) by delivering 67 m^3 of pure water to loop I [calculated by formula (4.20)]. When three feed pumps with a total capacity of 14 m^3/h are turned on, the delivery of such a volume of a volume of water requires

4.8 hours, in which case the concentration of boric acid will decrease by 1.58 g/kg after three hours and +1.26% of reactivity will be released which is temporarily compensated by inserting SUZ assemblies into the core.

Since the power of the reactor will increase to 75% after three hours, -0.8% of the reactivity released as a result of the removal of boric acid will be used for compensating the power effect and 0.2% -- for compensating poisoning. The effective excess of the control group will be +1.26-0.8-0.2% = +0.26%.

Reactor Poisoning by ^{149}Sm. Chapter 1 gave the chain of the formation of ^{149}Sm from ^{149}Pm directly during the fission of uranium and plutonium nuclei and, additionally, during the disintigration of the ^{149}Nd fragment nucleus. Usually, the presence of the intermediate ^{149}Nd isotope is disregarded in calculations due to its short half-life (1.8 h).

The change in the concentration of ^{149}Pm and ^{149}Sm is described by the following differential equations:

$$\frac{dN_{Pm}}{dT} = \gamma_{Pm}\Sigma_{fT}\varphi_T - \lambda_{Pm}N_{Pm}; \tag{4.9}$$

$$\frac{dN_{Sm}}{dT} = \lambda_{Pm}N_{Pm} - \sigma_{Sm}\varphi_T N_{Sm}, \tag{4.10}$$

where N_{Pm}, N_{Sm} -- concentrations of promethium and samarium nuclei, respectively, cm^{-3}; γ_{Pm} -- yield of promethium per one fission of heavy isotope; Σ_{fT} -- macroscopic fuel fission cross section, cm^{-1}; φ_T -- average density of the thermal neutron flux, neutron/(cm^2 X sec); λ_{Pm} -- promethium decay constant, sec^{-1}; σ_{Sm} -- microscopic cross section of the absorption of neutrons by the ^{149}Sm isotope, cm^2.

For VVER, the physical constants have the following values: $\gamma_{Pm} = 0.011$; $\lambda_{Pm} = 0.357 \cdot 10^{-5}$ sec^{-1}.

If φ_T = const (reactor power constancy condition), it is possible to obtain analytical solution of equations (4.10) and (4.9) for N_{Sm}:

$$N_{Sm}(T) = N_{nSm}\exp(-\sigma_{Sm}\varphi_T T) + \frac{\lambda_{Pm}(N_{0Pm} - N_{nPm})}{\lambda_{Pm} - \varphi_T\sigma_{Sm}}[\exp(-\lambda_{Pm}T) - \exp(-\sigma_{Sm}\varphi_T T)] + N_{0Sm}[1 - \exp(-\sigma_{Sm}\varphi_T T)], \tag{4.11}$$

where $N_{0Sm} = \frac{\gamma_{Pm}\Sigma_{fT}}{\sigma_{Sm}}$ -- equilibrium concentration of ^{149}Sm nuclei;

$N_{0Pm} = \frac{\gamma_{Pm}\Sigma_{fT}}{\lambda_{Pm}}\varphi_T$ -- equilibrium concentration of ^{149}Pm nuclei; $N_{П\ Sm}$ and $N_{П.\ Pm}$ -- concentrations of Sm and Pm at the moment of transition.

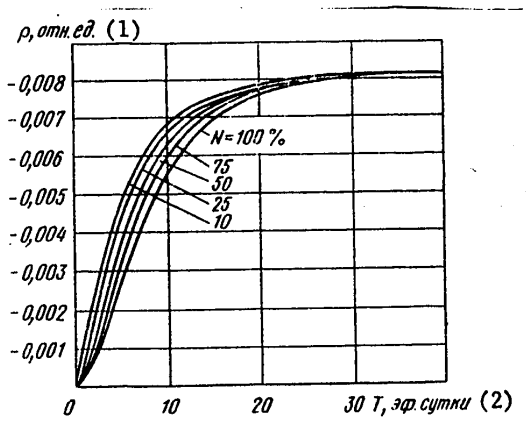

Figure 4.9. Steady-state poisoning of VVER-440 by samarium.
Key: 1. Per unit value
2. Effective days

Thus, the equilibrium concentration of the nuclei of samarium $N_{o\ Sm}$ does not depend on the neutron flux and, consequently, on the reactor power. However, the reactor power determines the time of the attaining of the equilibrium concentration of ^{149}Sm. Figure 4.9 shows the curves of the poisoning of the VVER-440 core by samarium for the first startup from which it follows that the equilibrium concentration of ^{149}Sm nuclei and steady-state (equilibrium) poisoning, which is 0.82% for VVER-440, is attained in the course of 30 effective days when operating at a steady power. The time of the onset of steady-state ^{149}Sm poisoning can also be estimated from the relation

$$T_{стац} \cong 10^{15}/\varphi_T, \qquad (4.12)$$

where $T_{стац}$ -- time of the onset of steady-state poisoning by samarium during power operation of the reactor, days; φ_T -- average density of the thermal neutron flux during reactor's operation at a steady power, neutron/(cm^2·sec).

The change in the reactor power from N_1 to N_2 (Figure 4.10) causes slow transient processes connected with the changes in the numbers of ^{149}Pm and ^{149}Sm nuclei in the core. The phenomenon of the lowering of the reactivity of the reactor when its power decreases due to the disturbance of the balance of ^{149}Pm and ^{149}Sm nuclei, by analogy with the iodine pit, is called promethium pit. The greatest depth of the promethium pit (of the order of -0.5%) is attained when the power of the reactor decreases from 100% to zero (see Figure 4.10a). and the total transformation of the formed ^{149}Pm into ^{149}Sm occurs approximately in 15 days after the drop of the load. During this time, the samarium nuclei formed from promethium during the shutdown time are added to the samarium nuclei accumulated during the time of power operation.

The ^{149}Sm isotope is stable, therefore, at the zero power of the reactor, the number of samarium nuclei remains constant. When the power drops partially, the depth of the promethium pit is smaller, because part of the accumulated samarium is burned up by neutrons.

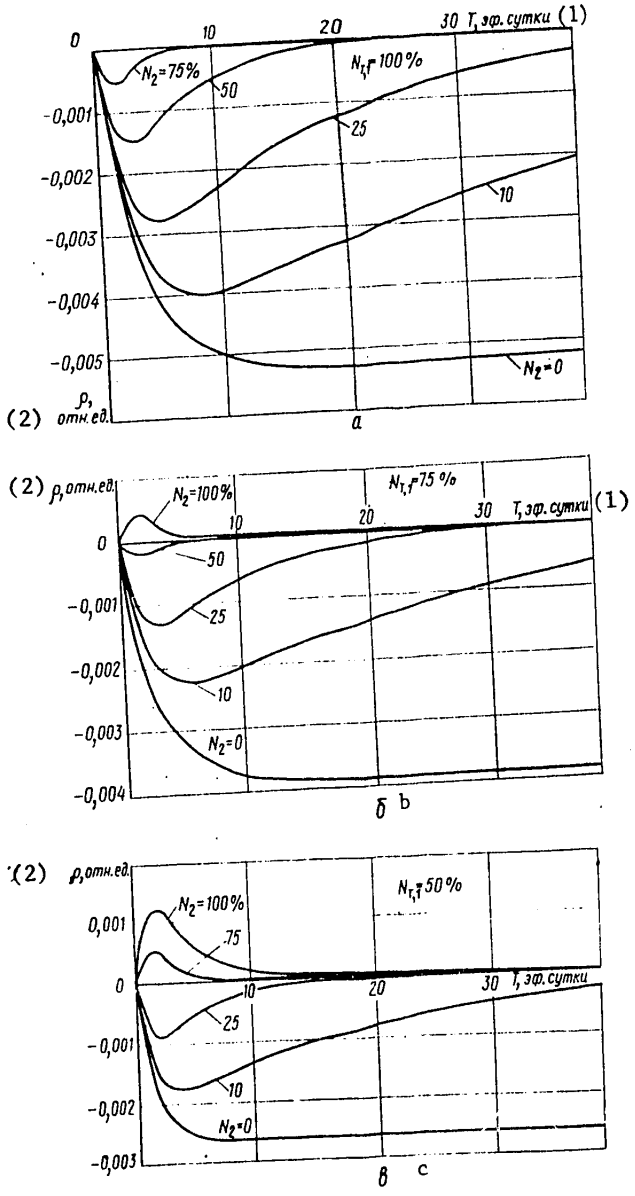

Figure 4.10 a, b, c
Key: 1. Effective days
2. Unit per value

The burnup of the "excess" of the samarium formed from the promethium after partial power drop gradually brings its concentration to a steady-state value which, as has been mentioned, does not depend on the power level. It should be kept in mind that

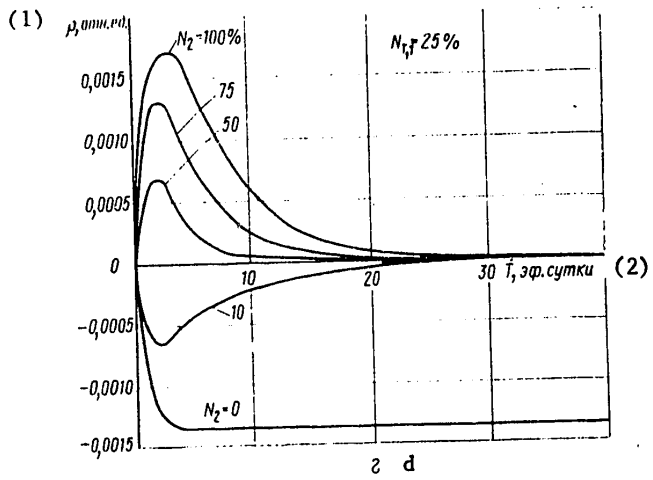

Figure 4.10. Nonsteady-state poisoning of VVER-440 by samarium when thermal power changes from 100 (a), 75 (b), 50 (c) and 25% (d) levels.

Key: 1. Per unit value
2. Effective days

the curves in Figure 4.10 presuppose that steady-state poisoning by ^{149}Sm is attained before the change in the reactor power.

The decrease in the time of the onset of the maximum of the promethium pit as the values of the power N_2 increase in Figure 4.10 should not be misleading, because the effective time is in question, and not the calendar time. The calendar time of the onset of the maximum of the promethium pit remains constant (15 days). As the power of the reactor increases, a samarium overshoot (reactivity increase) is observed, which is explained by the change in the rate of the burnup of samarium by neutrons and the rate of its accumulation from promethium. The maximum samarium overshoot can reach 0.25% during the time of the order of five hours after the rise of the reactor power from zero to 100%, assuming that the reactor was shut down for 15 days and the concentration of samarium stabilized as constant.

Let us give an example of the computation of the poisoning of a reactor by the ^{149}Sm isotope.

Problem. After 40 effective days of operation VVER-440 was shut down for two days. Before the shutdown the reactor operated in the course of 20 days at a 75% power. After the startup, the reactor was brought to a power of 50%. The poisoning of the reactor by samarium has to be determined.

Solution. Directly before the shutdown of the reactor, steady-state samarium poisoning was established in the core, since the transient process connected with the emergence of the reactor to the 75% power level occurred 20 days before the shutdown of the reactor (more than 15 days) and, moreover, in 40 effective days, steady-state

poisoning by ^{149}Sm became established. From Figure 4.9, we determine the steady-state poisoning by samarium equal to -0.82%. From Figure 4.10b, we find that during the two calendar days of the shutdown of the reactor (2 days· 75%/100% = 1.5 effective days) the depth of the promethium pit reached -0.2%. The total poisoning of the reactor by samarium directly before the startup is equal to -.82% + (-0.2%) = -1.02%. When the reactor reaches the 50% power level, samarium burns up and approximately after 30 effective days of operation (30 eff. days·100%/50% = 60 days) the poisoning drops to the steady-state value of -0.82%.

Reactor Slagging. The composition of stable and long-lived fission fragments -- slags -- forming during the fission of ^{235}U nuclei is given in Chapter 1. The accumulation of slags in the fuel is proportional to the neutron fluency and is an energy characteristic of nuclear fuel.

The unit of measurement of fuel burnup is the amount of thermal energy released from 1 t of fuel in terms of metal in 24 hours (Mw·days/tU). Another frequently used unit is the slag mass accumulating in 1 t of uranium (kg/tU). Fuel burnup is directly connected with the number of nuclear fissions of the fissionable isotope:

$$1\ \frac{(1)}{mU} = \frac{5{,}3916\cdot 10^{23}}{E}\ \frac{(2)}{дел/mU}, \qquad (4.13)$$

Key: 1. Mw· day
2. Fission/mW

E -- energy released in one isotope fission event, Mev: $5.3916\cdot 10^{23}$ -- coefficient of conversion of megaelectron volts into megawatt per day.

The energy carried away by neutrinos is not included in the value of the energy of one fission event in calculations, since it is not released in the volume of the reactor and is not a part of the thermal power of the reactor.

The recalculation between the burnup measurement units is done by a simple calculation of the mass of the split fuel nuclei with consideration of the fact that a mass of $1.6599\cdot 10^{-27}$ kg corresponds to the atomic mass unit:

$$1\ \frac{(1)}{mU} = \frac{A\cdot 1{,}6599\cdot 10^{-27}\cdot 5{,}3916\cdot 10^{23}}{E}\ \frac{(2)}{mU}, \qquad (4.14)$$

Key: 1. Mw·day
2. kg of slag

where A -- mass of the nucleus of the fissionable isotope, in atomic mass units.

Table 4.1 shows nuclear fission energies of 235U, 239Pu, 241Pu, as well as the number of fissions N_f and the mass of slags forming during the release of energy in 1 Mw·days/mU.

The relation of burnup units using the data of Table 4.1. can be writted in the form

$$1\ \text{kg slag/mU} = k_w^{-1}\ \text{Mw X days/mU} \qquad (4.15)$$

Table 4.1
Energy and Mass Characteristics of the Burnup Process

(1) Изотоп	(2) E, Мэв	$N_f \cdot 10^{21}$ дел/Мвт·сутки (3) (4)	$k_w \cdot 10^{-3}$ кг шлаков/Мвт·сутки (5) (4)
^{235}U	195 [9]	2,76	1,078
^{239}Pu	202 [9]	2,67	1,059
^{241}Pu	205 [16]	2,63	1,052

Key: 1. Isotope
2. Mev
3. Fission
4. Mw·day
5. kg of slag

In VVER, a considerable release of energy occurs due to the fission of the accumulating plutonium isotopes ^{239}Pu and ^{241}Pu in which case the ratio between the concentration of the isotope ^{235}U and content of the fissioning plutonium isotopes changes. Therefore, for a more accurate calculation of the accumulation of slag, it is necessary to consider the changes in the coefficient k_w in the course of the run. At the beginning of the run, when working with pure ^{235}U, the value of k_w is equal to $1.078 \cdot 10^{-3}$, while during the burnup of 28 kg/T with the corresponding accumulation of plutonium isotopes, its value decreases to $1.072 \cdot 10^{-3}$.

4.3. VVER Control and Maneuverability

In VVER, power control is facilitated by the negative temperature effect of reactivity. The temperature effect of reactivity in a number of practically important cases is capable of compensating power perturbation during emergency situations without the interference of control devices.

First, let us examine the processes in the reactor after a load perturbation without consideration for the influence of the power effect of reactivity. As the load of the turbo-generators increases at a constant power of the reactor, the flow rate of steam per turbine increases, and the steam pressure in the steam generators decreases. The decrease in the steam pressure and, consequently, of the saturation temperature increases the thermal head of the steam generator and the removal of heat from the I circuit, which, in turn, lowers the average temperature of the coolant in the core. The reactivity released during the lowering of the coolant temperature is spent on increasing the power of the reactor. After the termination of the transient process, the average temperature of the coolant in the core becomes equal to the original value, and the power of the reactor falls in line with the increased removal of heat from the steam generator. The self-regulation process has the nature of damped oscillations whose amplitude and period depend on the scale of changes in the load and the value of the negative temperature effect.

The negative power effect of reactivity, which appears when power increases, compensates to some degree the effect of the temperature effect. Therefore, the stabilization of the parameters of the reactor plant actually occurs at a lower medium temperature of the coolant than before the transient process and a power corresponding to the amount of heat removed from the steam generator. The change in the average water temperature in loop I is determined by the ratio of the temperature and power coefficients of reactivity. Figure 4.11 shows the curves of changes in the VVER-365 parameters in the process of self-regulation when one turbine is disconnected.

During the self-regulation of VVER, the power of the reactor eventually falls in line with the load of the turbo-generators. However, the process of the establishment of the steady state continuing for a relatively long period of time is aperiodic with large initial deviations of the parameters. Therefore, sufficiently simple and reliable forced control systems are installed in VVER.

VVER power control is accomplished according to the programs shown schematically in Figure 4.12.

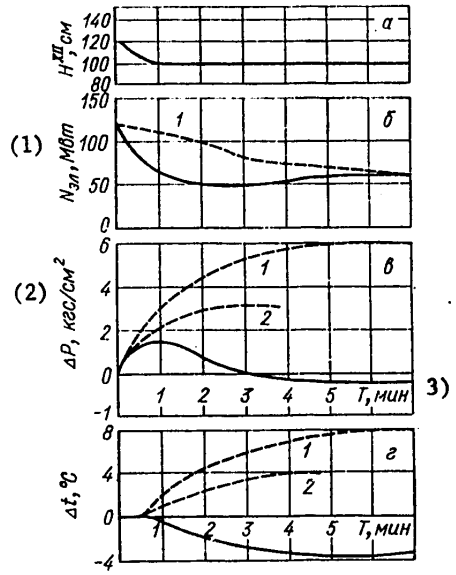

Figure 4.11. Changes in the parameters of VVER-365 in the case of a sharp load drop:
a -- position of the SUZ control group during the adjustment of a load perturbation by the regulator of the ARM [automatic power control]; b -- electrical power of the unit; c -- steam pressure in steam generators; d -- average coolant temperature in the reactor; ---- in the self-regulation process (1 -- $C_{H_3BO_3}$ = 2.3 g/kg; $\partial\rho/\partial t \simeq -1.7\cdot10^{-4}$ 1/°C; 2 -- $C_{H_3BO_3}$ = 0 g/kg; $\partial\rho/\partial t \simeq -4.3\cdot10^{-4}$ 1/°C; —— -- during regulation by ARM regulator.
Key: 1. $N_{electric}$, Mw
2. Kilogram-force/cm^2
3. Minutes

The maintenance of a constant average coolant temperature in the core while the load is decreasing is accompenied by a rise of steam pressure in the steam generators. The positive aspects of the program of maintaining a constant average temperature of circuit I are the maximum utilization of the self-regulation property of the reactor, less rigid requirements for the volume compensation system of circuit I, and insignificant changes in the amount of heat accumulated in circuit I. The latter is particularly valuable for dependable operation of AES in the mode of variable loads.

The negative aspect of the program of maintaining a constant average coolant temperature is the necessity of manufacturing heavier steam generators designed for the saturation pressure at the average temperature of circuit I, which is 15-20 kg-f/cm^2 higher than the nominal pressure.

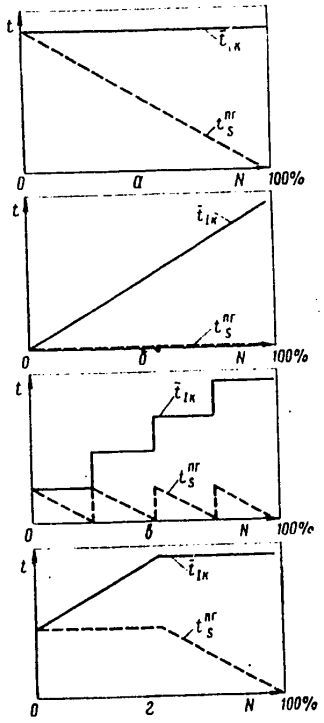

Figure 4.12. Programs of VVER power control:
a -- with constant average water temperature in the reactor;
b -- with constant steam pressure in circuit II; c -- stepped regulation by the average water temperature in the reactor;
d -- compromise program of regulation with maintaining constant steam pressure in circuit II at small loads and a constant average temperature in circuit I at large loads; ___ -- average water temperature in the reactor; ---- saturation water temperature of circuit II in the steam generator.

The advantage of the constant steam pressure program is the use of the least expensive casings of steam generators, as well as easier temperature conditions of the operation of circuit I at a lower power. However, this regulation program is characterized by the greatest changes in the thermal potential of circuit I as the load of the steam generator changes: when the load changes from 0 to 100%, the average temperature of the coolant of circuit I increases by 20-30 degrees C.

The disadvantages of the programs for maintaining a constant average temperature of the coolant in circuit I and a constant steam pressure in steam generators are partially eliminated in the compromise regulation programs.

VVER working in the basic load mode are regulated by using the regulation program with maintenance of a constant steam pressure in the steam generators. For example,

VVER-365 and VVER-440 use a two-pulse reactor power control system with an analog power control of the ARM (IRM) type [36]. Figure 4.11 shows the curves of changes in the VVER-365 parameters when the load drops from 120 to 60 Mw and the ARM regulator adjusts the perturbation. As can be seen from the curves, the ARM regulator steadily and rapidly adjusted the power of the reactor to the load.

During the regulation of the reactor, it is permissible to change the load of the unit at a rate of about 3-5% a minute. With respect to their regulation characteristics, AES are close to hydroelectric power stations and, in principle, can operate in the mode of variable loads. However, when a reactor is controlled by changing the concentration of boric acid, the rate of possible changes in the reactivity is considerably lower than when it is regulated by mechanical elements of the SUZ. The concentration of boric acid is changed by diluting the coolant of the reactor with pure water or, on the contrary, by feeding a highly concentrated boric acid solution into circuit I. Naturally, the time of the removal of boric acid from the coolant of circuit I and, consequently, release of reactivity, is much longer than the time of the withdrawal of SUZ assemblies, which limits the possibility of changing the reactor power in nonsteady-state transient xenon processes.

Let us estimate the rate of changes in the concentration of boric acid by solving the differential equation of acid balance in circuit I:

$$V\gamma dC = C_{\text{подп}} q_{\text{подп}} \gamma_{\text{подп}} dT - C q_{\text{пр}} \gamma_{\text{пр}} dT, \tag{4.16}$$

where V -- volume of circuit I of the reactor without volume compensators, m^3; γ -- water density at the average coolant temperature in circuit I of the reactor, kg/m^3; C -- concentration of boric acid in the water of circuit I, g/kg; $C_{\text{подп}}$ -- concentration of boric acid in the feed water of the reactor, g/kg; $q_{\text{подп}}$ -- volumetric flow rate of the feed water of the reactor, m^3/h; $\gamma_{\text{подп}}$ -- feed water density, kg/m^3; $q_{\text{пр}}$ -- volumetric flow rate of the blast water of the reactor, m^3/h; $\gamma_{\text{пр}}$ -- blast water density, kg/m^3; T -- operation length of the feed pumps, h.

Having solved equation (4.16), we obtain the expression

$$C(T) = C_{\text{подп}} \frac{q_{\text{подп}} \gamma_{\text{подп}}}{q_{\text{пр}} \gamma_{\text{пр}}} \left[1 - \exp\left(- \frac{q_{\text{пр}} \gamma_{\text{пр}}}{V\gamma} T \right) \right] + C_0 \exp\left(- \frac{q_{\text{пр}} \gamma_{\text{пр}}}{V\gamma} T \right). \tag{4.17}$$

Having used the condition of the material balance of the feed water and blast water in circuit I,

$$q_{\text{подп}} \gamma_{\text{подп}} = q_{\text{пр}} \gamma_{\text{пр}}, \tag{4.18}$$

we obtain

$$C(T) = C_{\text{подп}} \left[1 - \exp\left(- \frac{q_{\text{пр}} \gamma_{\text{пр}}}{V\gamma} T \right) \right] + C_0 \exp\left(- \frac{q_{\text{пр}} \gamma_{\text{пр}}}{V\gamma} T \right). \tag{4.19}$$

Expression (4.19) can be used for calculating the changes in the concentration of boric acid in the coolant when circuit I is fed with water with a high boric acid content and with pure water. For pure water, formula (4.19) is simplified:

$$C(T) = C_0 \exp\left(-\frac{q_{пр}\gamma_{пр}}{V\gamma} T\right). \quad (4.20)$$

If the initial concentration of boric acid in the coolant is equal to zero (pure water), then the changes in the concentration of boric acid in the case of feeding with boric water is described by the expression

$$C(T) = C_{подп}\left[1 - \exp\left(-\frac{q_{пр}\gamma_{пр}}{V\gamma} T\right)\right]. \quad (4.21)$$

Formula (4.17) also holds true for the case when the safety boron system is included into operation and when water from circuit I leaks. In this case, a high concentration solution of boric acid is delivered by high-efficiency safety feed pumps.

For maneuverability estimation, the concept of a relative rate of the lowering of the boric acid concentration with the dilution of the coolant of circuit I with water is used:

$$\beta = \frac{1}{C(T)} \frac{dC(T)}{dT} = \frac{q_{пр}\gamma_{пр}}{V\gamma}. \quad (4.22)$$

The maneuverability of VVER changes in the course of the run depending on the concentration of boric acid in the coolant (Figures 4.13 and 4.14).

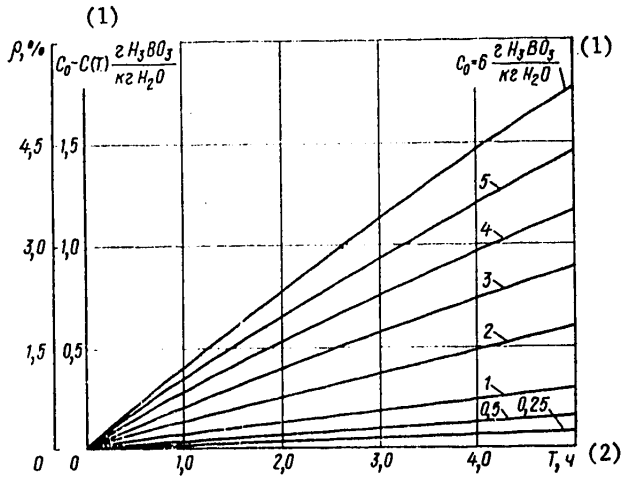

Figure 4.13. Changes in the concentration of boric acid in the coolant and the release of reactivity when circuit I is fed with pure water. The flow rate of the feed water is 13 m^3/h, and the volume of circuit I is 200 m^3.
Key: 1. gH_3BO_3/kgH_2O
2. T, h

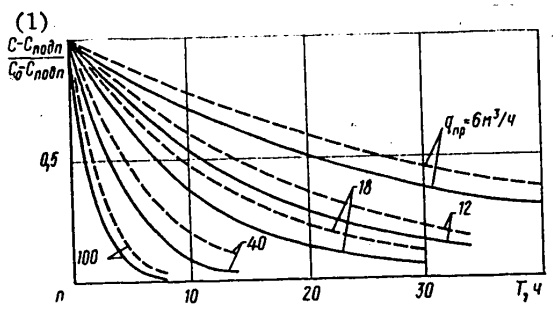

Figure 4.14. Relative changes in the concentration of boric acid in the coolant of circuit I of VVER-440 at various flow rates of pure feed water: ——— -- hot state (t=260°C); ---- -- cold state (t=100°C).
Key: 1. C_{feed}

As it follows from Figures 4.13 and 4.14, the withdrawal of boric acid from circuit I occurs slowly, which, however, does not create any inconveniences in the operation of the reactor at a steady-state power. When the power of the reactor changes, there occur difficulties in raising its power which are connected with a rapid decrease in the reactivity excess due to the poisoning of the core by ^{135}Xe (iodine pit). In such cases, provision can be made for switching on the standby ionite filter cleansed of boric acid which greatly increases the rate of boric acid removal [37]. Figure 4.15 shows the characteristics of the maneuverability of a unit with VVER-440 with consideration for the presence of the controlling group of SUZ assemblies in the core for various relative rates of the decrease of boric acid concentration. It can be seen from the curves that the maneuverability of the reactor gets worse toward the end of the run.

The maneuverability of a reactor depends on the speed of bringing it to its full power after a shutdown. For example, if a reactor is brought rapidly to its full power, the accumulated xenon is burned out intensively by the neutron flux, and the additional formation of Xe from iodine does not yet have any substantial effect on the reactivity. This fact can be used for increasing the power of the station temporarily, for example, to cover peak loads of the power system at the end of the reactor run when the reactivity excess is small. By lowering the power during the hours of low needs in energy, it is possible to accumulate a reactivity excess necessary for maintaining the full power of the reactor during peak hours. At the NVAES, this mode of operation at the end of the run was tested repeatedly on units II and III. Calculation show that it is possible to select an optimal mode of power variations ensuring the fulfillment of the daily load schedule of a power system.

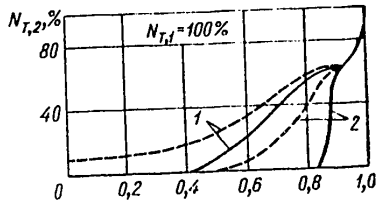

Figure 4.15. Characteristics of the maneuverability of an AES with VVER-440 with consideration for the presence of the controlling group of SUZ in the core:
—— -- reactor is maintained at the rated power, and attains the rated power in the case of a shutdown of the reactor for not more than one hour; ---- reactor is maintained at a lower power and can attain the rated power at any time; 1 -- β = 0.05 1/h; 2 -- β = 0.20 1/h.

The problems of the optimization of transient xenon-related processes are treated in detail in works [34, 35]. The basic mathematical method of the optimization of these processes is the Pontryagin maximum principle.

5.3. Permissible Power Level of Fuel Elements, Assemblies, and the Reactor

The main generally accepted initial prerequisites of determining the permissible level of the thermal power of a reactor are: a) impermissibility of the melting of the fuel even in individual, the most energy-intensive fuel elements; b) necessity of the absence of a heat exchange crisis on the surface of the fuel elements of the most energy-intensive assemblies in the steady-state and any transient mode of operation of the reactor.

The conditions of the absence of fuel melting were analyzed in work [3], where, among other things, it was shown that, for the fuel elements of VVER-440, in which slightly enriched uranium dioxide is used as fuel, the maximum linear load is ~ 500 w/cm. This load for the height distribution variation factor $k_z = 1.57$ corresponds to a maximum power of fuel elements of 0.08 Mw.

Permissible Power of Fuel Elements. The maximum power of fuel elements with respect to the heat-exchange crisis which is characterized by the appearance of critical phenomena even in one section of the fuel elements at prescribed physical and geometrical characteristics of fuel elements is determined by the flow rate, temperature, and pressure of the coolant. The condition of safe operation of a fuel element can be ensured if the heat flow in the steady-state and emergency modes does not exceed the critical flow over the entire height of the core. This condition determines the permissible power of the fuel element with respect to the heat-exchange crisis. Critical values of heat flows are calculated by the empirical formula (5.9). Finally, the permissible power of the fuel element $N^{\text{доп}}_{\text{твэл}}$ is established as the lowest of the maximum powers with respect to the melting of fuel and the heat-exchange crisis with a definite factor of assurance k (arbitrary to a certain degree due to insufficient understanding of the processes of heat removal in operating reactors).

Possible deviations of physical and geometrical characteristics of fuel elements are allowed for by a special factor which is called mechanical $k^{\text{твэл}}_{\text{мех}}$. With consideration for these two coefficients, the permissible power of fuel elements is equal to

$$N^{\text{доп}}_{\text{твэл}} = N^{\text{пред}}_{\text{твэл}} / k^{\text{твэл}}_{\text{мех}} k, \tag{5.30}$$

where $N^{\text{пред}}_{\text{твэл}}$ -- the lowest of the maximum powers of the fuel element with respect to the melting of fuel and the heat-exchange crisis.

The factor of assurance k for VVER-440 is taken to be 1.1.

The main limitations on the permissible power of fuel elements in VVER are imposed in analyzing emergency situations connected with decreases in the flow rate of water through the core (see section 5.5). In analyzing emergency conditions of this kind, it is necessary to calculate the law of changes of the flow rate of the coolant in the heated channel and the power of the fuel elements by using the formulas of section 5.1 which correspond to the appearance of a heat-exchange crisis at the initial and lowered values of the flow rate. Then the actual change in the energy release in the fuel elements after the operation of the safety system caused by the lowering of the flow rate of the coolant is calculated.

By comparing the curves of the changes in the flow rate of the coolant and the actual energy release in the fuel elements (see Figures 5.7 and 5.8), the initial level of power of the fuel elements is determined in the steady-state mode which makes it possible to prevent the heat-exchange crisis in the course of the entire transient process.

The actual power of the fuel elements and its changes in the course of the run are determined by calculations using, for example, programs BIPR-4 [45] and "Hexahedron" [46]. Due to the absence of a system for measuring this power during the operation of the reactor, the permissible rated power of fuel elements is decreased by the accuracy of calculations, i.e.,

$$N_{\text{твэл}}^{\text{доп.расч}} = N_{\text{твэл}}^{\text{доп}}/k_{\text{э(твэл)}}, \tag{5.31}$$

where $k_{\text{э(ТВЭЛ)}}$ -- factor of assurance for a possible deviation of the actual value of the relative power of the fuel element in the reactor from the calculated value. It is determined by the accuracy of the accepted calculation methods and programs, specifically, for the programs BIPR-4 and "Hexahedron" $k_{\text{э(ТВЭЛ)}}$ 1.14.

In VVER, the condition of the absence of the melting fuel is fulfilled in the majority of cases of operational modes and, therefore, the maximum power of the fuel elements is determined practically only by the danger of critical phenomena of heat removal.

Permissible Power of Fuel Assemblies. Knowing the permissible power of fuel elements, it is possible to determine the permissible power of fuel assemblies (clusters). It is determined by the condition of the absence of the heat-exchange crisis even on the most energy-intense fuel element.

For the convenience of the evaluation of the critical power of the assemblies, the concept of critical power N_k^{kp} of an assembly with mean physical and geometrical characteristics and equally intense fuel elements is introduced. Critical power is calculated with semiempirical formulas obtained by processing experimental data in bundles of heat-producing rods (see, for example, work [47]). Specifically, the critical power of a VVER-440 assembly at constant heat production along the height is determined by formulas

$$\left.\begin{aligned} N_{\text{к}}^{\text{кр}} &= 6{,}9\,(1 - 0{,}323 x Q_{\text{к}}^{0{,}4})^{1{,}3} Q_{\text{к}}^{0{,}2} \;\; \textit{Мвт}; \\ N_{\text{к}} &= (i_{\text{вых}} - i_{\text{вх}})\, Q_{\text{к}}/860 \;\; \textit{Мвт}; \;\; (\text{Mw}) \\ N_{\text{к}}^{\text{кр}} &= N_{\text{к}}, \end{aligned}\right\} \tag{5.32}$$

where $i_{вх}$, $i_{вых}$ -- coolant enthalpy at the inlet and outlet of the assembly, respectively, kcal/kg; x -- mass steam content at the outlet from the assembly; Q_k -- water flow rate through the assembly, t/h. The water flow rate through the assembly can be determined if we know its hydraulic characteristics (see section 5.2).

The maximum permissible power of an assembly when there is no boiling of the water ($x_{вых} = 0$) is found by the formula

$$N_к^{пр.доп} = (i' - i_{вх}) Q_к/860 \ Мвт. \tag{5.33}$$

In real assemblies, power is distributed nonuniformly among the fuel elements. This nonuniformity is characterized by the coefficient k_k which is equal to the ratio of the maximum power of the fuel element of the assembly to the mean power. This coefficient depends on the enrichment of the fuel, the position of the assembly in the core, the position of the regulating elements, and the concentration of the liquid absorber of neutrons (boric acid) in the coolant. The value of k_k is determined through calculations (see section 7.3).

With consideration for the mechanical coefficient $k_{мех}^{к}$ and the factor of assurance k, the expression for the permissible power of the assembly will assume the following form:

$$N_к^{доп} = N_к^{кр}/k_к k_{мех}^{к} k. \tag{5.34}$$

Here, $k_{мех}^{к}$ -- mechanical coefficient which, just as $k_{мех}^{твэл}$, allows for deviations in the physical and geometrical characteristics of the fuel elements from the mean values and, moreover, for deviations in the lattice pitch of the fuel elements. Consequently, $k_{мех}^{к} > k_{мех}^{твэл}$.

The connection of $N_к^{доп}$ with $N_{твэл}^{доп}$ is characterized by the relation

$$N_к^{доп} = \frac{N_{твэл}^{доп} n_{твэл} k_{мех}^{твэл}}{k_{мех}^{к} k_к} = \frac{N_{твэл}^{пред} n_{твэл}}{k_{мех}^{к} k_к k}, \tag{5.34'}$$

where $n_{твэл}$ -- the number of fuel elements in the assembly. For VVER-440 assemblies, $n_{твэл} = 126$.

In determining the permissible power of assemblies, sometimes it is taken into consideration that, due to the agitation of the coolant flow, the most intense fuel elements of the assembly are in better cooling conditions. The agitation effect is allowed for by the coefficients $k_п$ which depends on k_k. For example, for VVER-440 assemblies, $k_п \simeq 0.95$ at $k_k = 1.15$.

The permissible rated power of assemblies $N_к^{доп.расч}$, just as the permissible rated power of fuel elements $N_{твэл}^{доп.расч}$, is reduced by the accuracy of calculations, i.e.,

$$N_{к}^{доп.расч} = N_{к}^{доп.}/k_{з(кас)}, \qquad (5.35)$$

where $k_{з(кас)}$ -- factor of assurance for the deviation of the actual power of the assemblies from the rated power. For the BIPR-4 program, it is taken to be equal to 1.1. In this case, the relation $k_{з(твэл)}/k_{з(кас)}$ characterizes the inaccuracy of the calculated determination of the relative power of fuel elements in the assembly with a prescribed power, for example, for the program "Hexahedron" $k_{з(твэл)}/k_{з(кас)} = 1{,}04$.

In practical calculations, the relations $N_{к}^{кр} = f_1(Q_к)$ and $N_{к}^{доп.расч} = f_2(Q_к)$ found by formulas (5.32) and (5.35) are plotted on the chart of the family of the hydraulic characteristics of assemblies $N_k = f_o(Q_k)$ (for various values of pressure difference in the core $\Delta P_{а.з}$). The intersection points of the curves make it possible to determine the critical and permissible rated conditions of work of the maximally intense assemblies.

In the process of operation, the thermal power of the fuel assemblies is monitored by measuring the temperature of the coolant at the outlet from individual assemblies and average temperature at the inlet to the core. The permissible measured power of the assemblies is corrected with consideration for measurement errors.

The above evaluations are done in the following manner. The relative power of the fuel assemblies k_q^j is calculated with the relation

$$K_q^l = \frac{G_l}{\bar{G}_{контр}} \frac{i(t_{вых}^l) - i(\bar{t}_{вх})}{\frac{1}{m}\sum_{l=1}^{m} i(t_{вых}^l) - i(\bar{t}_{вх})} K_м. \qquad (5.36)$$

Here, $K_м = \sum_{l=1}^{s} K_{q\,расч}^l / s$ -- average rated relative power of the fuel assembly in a sample having a temperature control of the coolant at the oulet from the assembly; s -- number of the design numbers of fuel assemblies having a temperature control in at least one of the symmetry sectors (see Figures 3.9-3.11); $K_{q\,расч}^l$ -- relative rated power of a fuel assembly in a cell of the core with l-th design number; m -- number of fuel assemblies having a temperature control; $i(t_{вых}^j)$ -- coolant enthalpy at the outlet from the j-th assembly determined by the measured temperature $t_{вых}^j$, kcal/kg; $i(\bar{t}_{вх})$ -- coolant enthalpy at the inlet to the reactor core having the temperature $\bar{t}_{вх}$, kcal/kg; $G_j/\bar{G}_{контр}$ -- ratio of the rate of coolant flow through the j-th fuel assembly to the mean flow rate for the assemblies have a temperature control.

The value of $\bar{t}_{вх}$ is determined either by the direct measurements or by the relation

$$\bar{t}_{вх} = \frac{1}{m}\sum_{l=1}^{m} t_{вых}^l - \frac{\Delta\bar{t}_p \bar{G}_к}{k_{пр}\bar{G}_{контр}} K_м, \qquad (5.37)$$

where $\Delta \bar{t}_p$ -- average measured heating of the coolant in the reactor, °C; $\bar{G}_k/\bar{G}_{контр}$ -- ratio of the average rate of coolant flow through all fuel assemblies to the mean flow rate for assemblies having a temperature control; $k_{пр}$ -- coefficient of the rate of coolant flow through fuel assemblies (see section 5.2).

The advantage of using the relation (5.37) is the high accuracy of measurement of Δt_p due to the differential scheme of measurements which eliminates the error in the compensation of the cold junctions of the thermocouples. However, in this case it is necessary to know the $\bar{G}_k/\bar{G}_{контр}$ ratio.

Due to the absence of measurements of G_j in reactors not using shaped washers in the fuel assemblies with a temperature control, it is assumed that $G_j/G_{контр} \simeq 1$. Moreover, for a sufficiently representative sample of fuel assemblies with temperature control, $K_M \simeq 1$. In this case, the calculation of K_q^j by the relation (5.36) is simplified considerably.

The maximum relative error K_q^j can be determined by the relation

$$\delta[K_q^j] \simeq \left\{\delta^2[G_j/\bar{G}_{контр}] + \frac{\delta^2[t^j_{вых}]}{(1-\bar{t}_{вх}/t^j_{вых})^2} + \frac{\delta^2[\bar{t}_{вх}](K_q^j-1)^2}{(1-t^j_{вых}/\bar{t}_{вх})^2}\right\}^{1/2}, \qquad (5.38)$$

where $\delta[K_q^j]$, $\delta[G_j/\bar{G}_{контр}]$, $\delta[t^j_{вых}]$, $\delta[\bar{t}_{вх}]$ -- maximum relative errors of the values of K_q^j, $G_j/\bar{G}_{контр}$, $t^j_{вых}$, $\bar{t}_{вх}$.

According to [124], the error in the determination of temperature with the aid of chromel-copel thermocouples used in VVER-440 reactors is (without consideration for the errors of the measuring scheme) 2.6°C.

With consideration for the errors of the measuring circuits (0.3% for the $t_{вх}$ measuring system on each of the loops; 0.9% for the $t^j_{вых}$ measuring system with allowance for an additional error of the two-step circuit for compensating the temperature of the cold junction of the thermocouple), the corresponding maximum relative errors are equal to $\delta[t^j_{вых}] = 1{,}25\%$ and $\delta[t_{вх}] = 1{,}03\%$. Due to the nonuniform mixing of the coolant at the inlet to the reactor which is responsible for the nonuniformity of input temperatures, we assume that $\delta[\bar{t}_{вх}] \simeq \delta[t_{вх}]$. The value of $\delta[G_j/\bar{G}_{контр}]$, according to the available data, constitutes 2%.

The values of the maximum relative error $\delta[K_q^j]$ for typical operating conditions of the VVER-440 reactor ($\bar{t}_{вх} = 268°C$; $\sum_{i=1}^{m} t^i_{вых}/m = 295°C$) are given below.

K_q^j, отн. ед. (1)	0,4	0,6	0,8	1,0	1,1	1,2	1,3	1,4
$\delta[K_q^j]$, %	32,3	20,9	15,5	12,6	11,6	10,9	10,3	9,8

Key: 1. per unit value

It can be seen from these data that the error for the maximum values of K_q^j occurring during the operation of reactors (1.25-1.35) is $\sim$ 10%.

Permissible Power of a Reactor. The permissible power of a reactor is determined by the absence of critical phenomena even on the most intense fuel element of the most intense assembly of the core in a steady-state mode and in modes when the flow rate of water in circuit I decreases with simultaneous activation of the safety system. It is evident that the permissible power of a reactor can be increased if the nonuniformity of energy release is reduced. Nonuniformity of energy release in any assembly of the core is characterized by the calculated coefficient $k_{q,i}$, where i is the number of the assembly in the core. The maximum value of the coefficient

$k_{q,i}=k_q^{\text{макс}}$ characterizes energy release in the most intense assembly.

The coefficient of the nonuniformity of energy release of the most energy-intense fuel elements $k_{\text{МАКС}}$ can be represented in the form

$$k_{\text{макс}}=(k_{q,i}\,k_{\text{н}})^{\text{макс}}k_{\text{мех}}^{\text{к}}. \tag{5.39}$$

Since the coefficient k_k is not monitored during the operation of a reactor, this representation of $k_{\text{МАКС}}$ is not very convenient. Therefore it is usually assumed that

$$k_{\text{макс}}=k_q^{\text{макс}}k_{\text{к}}^{\text{р}}k_{\text{мех}}^{\text{к}}, \tag{5.40}$$

where k_k^p -- calculated value of k_k for an assembly with the maximum product $(k_{q,i}\,k_{\text{к}}^{\text{р}})^{\text{макс}}$.

Thus, the critical power and the maximum permissible power of the reactor will be defined as

$$N_{\text{р}}^{\text{кр}}=N_{\text{к}}^{\text{кр}}n_{\text{н}}/k_{\text{макс}}, \tag{5.41}$$

$$N_{\text{р}}^{\text{пред.доп}}=N_{\text{к}}^{\text{пред.доп}}n_{\text{н}}/k_{\text{макс}}, \tag{5.42}$$

where n_k -- the number of fuel assemblies in the core of the reactor.

The permissible power of the reactor must be reduced by a factor of assurance k.

Moreover, in order to ensure safe operation of the reactor, in addition to $k_{3(\text{ТВЭЛ})}$, the following additional factors of assurance are introduced: $k_{3(\text{N})}$-- allowing for deviations in the real power of the reactor from the design power; $k_{3(\text{ТГ})}$ -- allowing for the deviations of the power of the reactor from the prescribed level due to variations in the loads of the turbogenerators; $k_{3(\text{ВХ})}$ -- allowing for the degree of nonmixing of the water at the inlet to the core and the resulting macrononuniformity of the temperature field at the inlet to the core of the reactor.

For VVER-440, the above factors are taken to be: $k_{з(N)}=1{,}04$; $k_{з(ТГ)}=1{,}03$; $k_{з\,(вх)}=1{,}01\div1{,}03$ (the higher value is taken when the thermal power of the reactor is less than 50% of the rated power).

With consideration of all correction coefficients, the permissible rated power of the reactor is

$$N_{р}^{доп.расч}=N_{к}^{кр}n_{к}/k_{макс}k_{зап}, \qquad (5.43)$$

where $k_{зап}=k_{з\,(твэл)}k_{з\,(N)}k_{з\,(ТГ)}k_{з\,(вх)}k$ -- the aggregate factor of assurance. For VVER-440, $k_{зап}$ = 1.36. The total correction coefficient in determining the permissible power of the reactor with consideration for the mechanical coefficient $k_{мех}$ = 1.1, is 1.5.

It should be mentioned that the permissible power of the reactor also depends on the temperature (enthalpy) of the coolant at the inlet to the core. In calculating the critical thermal flow by formula (5.9), a proportionally greater channel power corresponds to the same critical flow (to the same output steam content) when the inlet temperature (enthalpy) drops. The change in the permissible power of the reactor when the inlet temperature (enthalpy) changes is determined by the relation*

$\Delta N_{р}^{доп}=\varphi G\Delta i/860\,k_{макс}k_{зап}$ kw, where G -- flow rate of the coolant through the core of the reactor, kg/h; Δi -- change of the coolant enthalpy at the inlet to the core, kcal/kg; φ -- coefficient allowing for the change in the flow rate of the coolant in transient modes. The coefficient φ is selected as a ratio of the coolant flow rate during transient modes corresponding to the moment of the maximum reactor power-flow rate ratio, to the initial coolant flow rate. For VVER-440 with a regular GTsN [main circulation pump] feed circuit, the worst transient (emergency) mode is the loss of the productivity of two GTsN without a change in the power (see section 5.7). In this case, $\varphi \simeq 0.7$.

The increase of the permissible power of the reactor during the lowering of the inlet temperature (enthalpy) of the coolant is limited by the critical heat flow at a zero steam content at the outlet from the channel with the highest thermal stress. This flow must not be exceeded in any section of the heated channel (which, apart from the power of the channel, is determined by the distribution of energy release along the channel). Moreover, the lowering of the inlet enthalpy is limited by the undesirable lowering of the parameters of the second (steam-turbine) circuit, potentialities of the heat exchangers (steam generators), and the growth of thermal stresses in the reactor vessel.

The values of the above-mentioned factors of assurance are taken and introduced arbitrarily in many respects due to insufficiently accurate measurements or calculations of the core parameters. Making them more accurate is a potential reserve for increasing the power of VVER which can be realized after conducting the necessary complex of studies and implementation of a number of technical measures.

*When the permissible power of the reactor is determined by equation (5.42)

7.1. Arrangement of Fuel Assemblies in the Core

The operating economy of an AES [atomic electric power station] is determined to a considerable degree by the effectiveness of the utilization of nuclear fuel which is characterized by the attained burnup fraction. It follows from the theoretical analysis conducted in the work [50] that the burnup fraction for a prescribed level of energy production depends on the mode of fuel reloading. The evaluation of the effectiveness of various reloading modes is done by introducing the concept of an ideal mode in which the depleated fuel is constantly replaced by fresh fuel with constant mixing in the volume of the core so that the burnup fraction would be identical for all assemblies being unloaded.

The VVER design makes it impossible to accomplish the ideal reloading mode, however, by comparing the selected real mode with the ideal mode, it is possible to evaluate its effectiveness and the degree to which it approaches the ideal mode.

Ideal Reloading Mode. The burnup fraction of the reloaded fuel in the ideal mode can be determined by introducing the concept of the mean factor of neutron multiplication in a core of infinite dimensions:

$$\overline{k_\infty(\rho_{шл})} = \int_0^{\rho_{шл}^{макс}} k_\infty(\rho_{шл})\,d\rho_{шл} \Big/ \int_0^{\rho_{шл}^{макс}} d\rho_{шл}, \qquad (7.1)$$

where $\rho_{шл}$ -- fuel burnup fraction for the moment of time being examined; $\rho_{шл}^{макс}$ -- maximum burnup fraction at which fuel is unloaded from the reactor in the ideal mode; $k_\infty(\rho_{шл})$ -- neutron multiplication constant for an infinite reactor at the burnup fraction $\rho_{шл}$ which corresponds with a sufficient degree of accuracy to the asymptotic multiplication constant $k_0(\rho_{шл})$ calculated by the programs POP and UNIRASOS (see section 7.2).

The characteristics of $k_\infty(\rho_{шл})$ for various degrees of enrichment of VVER-440 fuel are given in Chapter 2. These characteristics in the absence of burnable poisons are close to linear, and the rate of changes in $k_\infty(\rho_{шл})$ depends weakly on the enrichment of the fuel at an identical uranium-water ratio. The nonlinearity

of the characteristics of $k_\infty(\rho_{шл})$ in the first approximation can be disregarded, then

$$k_\infty(\rho_{шл}) = k_\infty^0 - A\rho_{шл}, \tag{7.2}$$

where k_∞^0 -- multiplication constant of the hot fuel lattice poisoned at the initial moment of power operation of the reactors; $\rho_{шл}$ -- amount of the slags at the moment of time being examined, kg/mU; A -- rate of changes in the characteristics of $k_\infty(\rho_{шл})$, $(kg/mU)^{-1}$.

After substituting the linear relation (7.2) in the integral of expression (7.1), we obtain

$$\bar{k}_\infty(\overline{\rho_{шл}}) = k_\infty^0 - A\rho_{шл}^{макс}/2. \tag{7.3}$$

As was mentioned in section 2.1, the reactor is critical when the mean multiplication constant of an infinite lattice analogous to the core of the reactor in its composition is equal to $k_\infty^{необх}$:

$$\bar{k}_\infty(\overline{\rho_{шл}}) = k_\infty^{необх} = k_\infty^0 - A\rho_{шл}^{макс}/2. \tag{7.4}$$

Hence, the maximum burnout fraction of the entire unloaded fuel is

$$\rho_{шл}^{макс} = 2(k_\infty^0 - k_\infty^{необх})/A. \tag{7.5}$$

The value of A which is determined from the graphical relations in Figure 2.6 is approximately equal to 0.01 $(kg/mU)^{-1}$. For more accurate calculations of the value of $\rho_{шл}^{макс}$, it is necessary to consider the nonlinearity of the characteristics of $k_\infty(\rho_{шл})$ which is represented in the form of polynomials. The values of the burnup fraction attained in the ideal mode without consideration for the nonlinearity of the characteristic of $k_\infty(\rho_{шл})$ are given in Table 7.1.

Table 7.1

Burnup Fraction $\rho_{шл}^{макс}$ of the Fuel Being Unloaded in the Ideal Reloading Mode for Assemblies of the VVER-440 Reactor for Various ^{235}U Content

$\rho_{шл}^{макс}$, кг/т U	10	32	50
^{235}U, %	1,6	2,4	3,6

Real or close-to-real fuel reloading modes are compared with the ideal modes by means of the burnup fraction disadvantage factor k_c:

$$k_c = \rho_{шл}^{макс}/\rho_{шл}^{к}, \tag{7.6}$$

where $\rho_{шл}^{к}$ -- finite burnup fraction of the fuel being unloaded in a mode different from the ideal.

Periodic Reloading Mode. The VVER design calls for periodic fuel reloading on a stopped reactor. It is evident that in order to increase the burnup fraction it is desirable to reload the reactor more often, approaching the ideal mode. On the other hand, frequent shutdowns of the reactor lower the production of electric energy and, therefore, are undesirable. Moreover, even with continuous reloading and radial mixing of the fuel during the power operation of the reactor, the ideal burnup fraction cannot be attained due to the nonuniformity of energy release along the height of the core, which follows from the formula [50]:

$$k_c = (k_z/\gamma)\left(1 - H_0^2/H^2\right), \tag{7.7}$$

where $k_z = \rho_{шл,0}^{макс}/\bar{\rho}_{шл}^{макс}$ -- nonuniformity factor of the burnup along the height of the core (index 0 refers to the center of the reactor); $\bar{\rho}_{шл}^{макс}$ -- average burnup in the assemblies being unloaded, kg/mU; H -- reactor height, cm; H_0 -- critical height of the reactor, cm, determined by the formula

$$H_0^2 = \pi^2/\varkappa_{z,0}^2. \tag{7.8}$$

Here, $\varkappa_{z,0}^2 = \varkappa_0^2 - \varkappa_r^2$ -- axial component of the material parameter, $см^{-2}$; $\varkappa_0^2 = (k_{\infty,0} - 1)/M^2$ -- material parameter of the core, $см^{-2}$; $\varkappa_r^2 = (2{,}405/R)^2$ -- radial component of the material parameter, $см^{-2}$; R -- core radius, cm.

The parameter γ (in formula (7.7)) is equal to

$$\gamma = \frac{A}{2}\,\frac{\rho_{шл,0}^{макс}}{M^2\varkappa_{z,0}^2}, \tag{7.9}$$

where M^2 -- migration area, $см^2$.

When $k_z = 1.20 \div 1.30$, which can take place in a real burnup situation, the disadvantage factor $k_c = 1.10 \div 1.20$, i.e., even in the mode of continuous reloading of the fuel assemblies with continuous rearrangement in the core (the fuel is not mixed along the height) the burnup fraction is approximately 20% smaller than in the ideal mode.

Under real operating conditions, the following periodic reloading modes can be accomplished.

Mode A. During each reloading, 1/n part of the core assemblies is replaced. In the course of the entire operation time of the assemblies T (total operating period of the fuel), n partial reloadings are done. The assemblies in the core are not rearranged during the reloadings. The disadvantage factor for this mode is estimated by the formula

$$k_c = \theta(1 + 1/n), \tag{7.10}$$

where θ -- nonuniformity function of energy release over the volume of the core. The value of θ in the general case is determined by numerical methods. In the

extreme case, when the radius of the core is very large, or when the fuel assemblies are continually rearranged, the value of θ coincides with the value of k_c determined by formula (7.7). In another extreme case, when the reactivity excess compensating the burnup is very small, θ has a maximum value equal to 2.25, i.e., $k_c^{\text{макс}} = 2{,}25(1+1/n)$.

The maximum value of the disadvantage factor (at n = 1) is 4.5.

Mode B. Part of the assemblies are rearranged during fuel reloading for equalizing the breeding properties of the core over the radius. During the total operating time of the fuel T, in each of the n reloadings of the core consisting of N assemblies, N/n of the most burned-out assemblies staying in the reactor during the T time are unloaded. The same number of N/n fresh assemblies are loaded in the core. The disadvantage factor for this mode (see work [50]) is

$$k_r = 2\theta_z / nB\bar{\varphi}, \tag{7.11}$$

where $\theta_z = (k_z/\gamma)\ (1 - H_0^2/H^2)$. The product $nB\bar{\varphi}$ is calculated by the formula

$$nB\bar{\varphi} = 0{,}415\left[\sqrt{(n-2)^2\,0{,}692 + 8(n-1)} - (n-2)\,0{,}831\right]. \tag{7.12}$$

The above mode is accomplished only at $n \geqslant 3$.

Mode C. The fuel assemblies in the core are not rearranged. Periodic reloading of the assemblies is done in proportion to the radial component of the energy-release field. The core consisting of N assemblies is divided into m circular subzones. Each circular subzone is divided into sections containing l_i assemblies each (i -- number of the subzone, $1 \leqslant i \leqslant m$); the number of assemblies in each section of the subzone is the same, and the number of these sections is proportional to the number of reloadings in a given subzone. The portion of the assemblies being reloaded in each zone $1/l_i$ is proportional to the radial component of the energy-release field in the subzone. Then, the number of the assemblies being reloaded, for example, in the first subzone can be found if the number of assemblies reloaded in the i-th subzone is known;

$$\frac{N_1/l_1}{N_i/l_i} = \frac{\bar{\varphi}_1}{\bar{\varphi}_i}, \tag{7.13}$$

where $\bar{\varphi}_1$, $\bar{\varphi}_i$ -- average densities of the neutron fluxes in the first and the i-th subzone; N_1, N_i -- number of assemblies in the first and the i-th subzone.

From expression (7.13) it is possible to find the total number of the assemblies being reloaded N/n in the entire core:

$$\frac{\bar{\varphi}N}{\sum_{i=1}^{m} \bar{\varphi}_i N_i} = \frac{N/n}{\sum_{i=1}^{m} (N_i/l_i)}, \tag{7.14}$$

where $\bar{\varphi}$ -- average density of the neutron flux in the core; n -- number of reloadings during the run.

The disadvantage factor for this reloading mode is equal to

$$k_c = 0_z(1 + 0_r/n), \tag{7.15}$$

where $0_z \approx (k_z + 1)/2$; $0_r \approx (k_r + 1)/2$; k_z -- nonuniformity factor of energy release along the height of the core; k_r -- nonuniformity factor of energy release along the radius of the core.

Under real conditions, mode B is used most widely because it makes it possible to improve the distribution of energy release over the core and thus to reduce the disadvantage factor k_c and to increase the fuel burnup fraction.

Selection of Fuel Loading Under Real Operating Conditions. When selecting the fuel reloading mode under real conditions, it is necessary to consider the technical potentialities of the VVER. As a rule, the reloading of a reactor is done simultaneously with routine maintenance of the equipment of the AES unit which takes approximately one month. The necessity of prolonged shutdown of a reactor for reloading lowers the utilization factor of its installed capacity, therefore, the number of shutdowns for reloading must be minimal. The needs of the power system which exclude possible shutdowns of AES units for reloading during the fall and winter energy load maximums should be considered as an additional condition. The mode of operation of AES units with one shutdown of the reactor a year for reloading during the spring floods when energy needs are satisfied by hydroelectric power stations is the most favorable for the energy system.

On the other hand, the reloading mode must ensure a sufficient burnup fraction which increases as the number of the reactor reloadings during a full fuel operating period increases.

With consideration for these conditions, the mode of three partial fuel reloadings during the run was accepted for VVER, which ensures the operation of the unit between reloadings in the course of one year (see section 12.2). In this case, as a rule, the number of the assemblies reloaded during each reloading time is close to one third of all the core assemblies, but it can also deviate from this number in individual units depending on the planned tasks of the AES as a whole.

In the first reactors -- VVER-210 (unit I of the NVAES) and VVER-70 (AES "Reinsberg", GDR) -- the loaded assemblies were distributed evenly in the core [3, 51]. In the new reactors -- VVER-440 and VVER-1000 which are equipped with boron control systems -- a zonal arrangement of the core is adopted, when the energy-release field is additionally leveled along the radius.

The special characteristics of the zonal method of fuel arrangement are as follows: 1) fresh fuel is arranged only at the core periphery; 2) the burned out fuel is in the central part of the core.

The fuel reloading mode with zonal arrangement is accomplished in the following manner: a) highly burned out fuel which remained in the reactor for three periods is removed from the central part of the core (approximately one third of all the assemblies); b) assemblies from the periphery and the its adjacent area which remained in the reactor for one or two periods are moved to the central part of the core; c) fresh fuel is loaded in the peripheral part of the core.

The zonal arrangement of the core makes it possible to achieve a considerable burnup fraction which is due to the lowering of the nonuniformity of radial energy release.

The loading of the fuel is determined by calculation according to special programs on a computer, the following requirements being fulfilled: 1) ensurance of the necessary length of reactor operation until the next reloading; 2) ensurance of the operation of the core at the rated power with minimum possible values of the nonuniformity factors over the radius and volume of the core; 3) ensurance of the necessary subcriticality of the stopped reactor in the cold state.

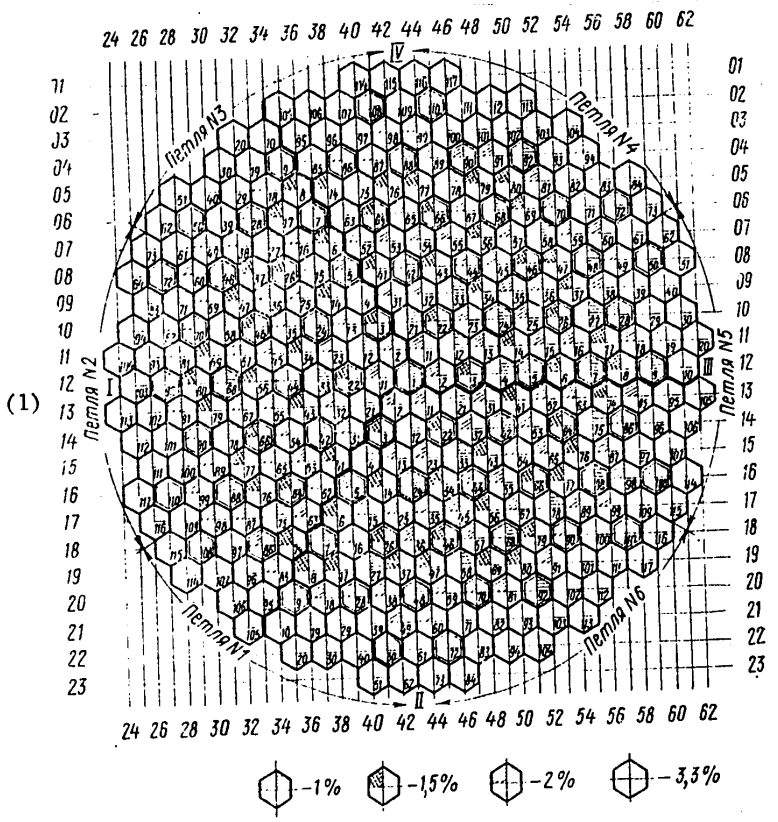

(1)

Figure 7.1. Cartogram of the first fuel loading of the VVER-440 of the III unit of the NVAES with assemblies with various degrees of fuel enrichment.
Key: 1. Loop

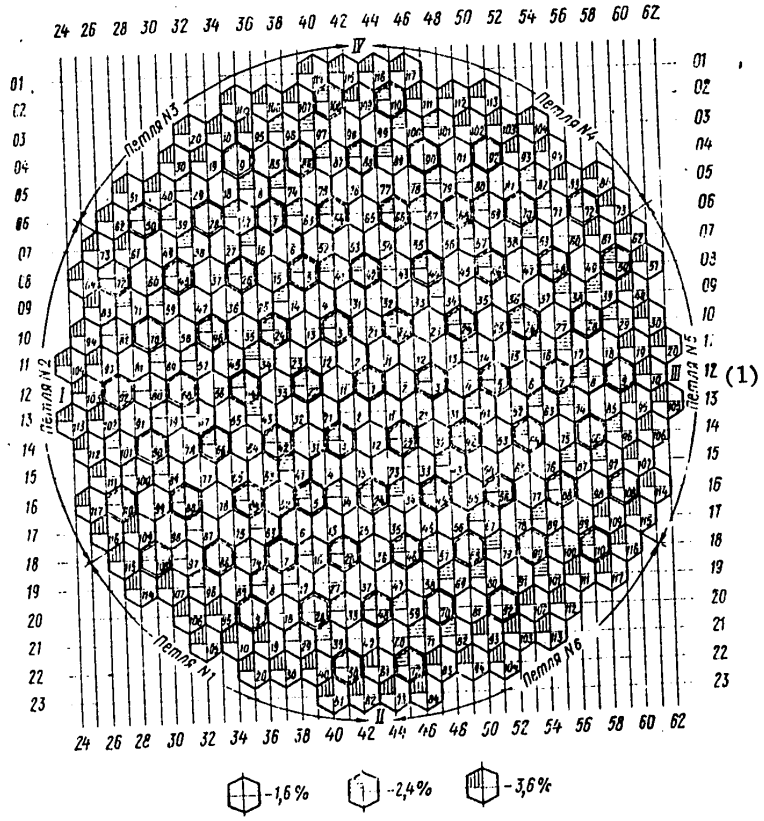

Figure 7.2. Cartogram of the first fuel loading of the VVER-440 of the IV unit of NVAES with assemblies with various degrees of fuel enrichment.
1. Loop

Special requirements are imposed upon the first fuel loading. In order to imitate in it a steady-state loading of the core containing partially burned out fuel mainly of the initial enrichment, assemblies with various degrees of enrichment are used. By using assemblies with 3-4 enrichments in the first loading, it is possible to achieve an acceptable nonuniformity of radial energy release ensuring the operation of the reactor at the rated thermal power. During further reloadings, the assemblies with the initial enrichment below the design enrichment are unloaded, and after 2-3 partial reloadings a mode is achieved when the reactor has assemblies only with the initial design enrichment. Figures 7.1 and 7.2 show cartograms of the first loadings of the VVER-440 at NVAES, and Table 7.2 shows their composition.

Table 7.2

Composition of the First Fuel Loadings of VVER-440 at NVAES

(3) Обогащение топлива по ^{235}U, %	(1) Количество кассет в первой загрузке				(3) Обогащение топлива по ^{235}U, %	(1) Количество кассет в первой загрузке			
	III блок (2)		IV блок			III блок		IV блок	
	(4) Рабочие кассеты	(5) Топливные части кассет СУЗ	(4) Рабочие кассеты	(5) Топливные части кассет СУЗ		(4) Рабочие кассеты	(5) Топливные части кассет СУЗ	(4) Рабочие кассеты	(5) Топливные части кассет СУЗ
1,0	24	25	—	—	2,4	—	—	78	49
1,5	48	18	—	—	3,3	108	12	—	—
1,6	—	—	114	24	3,6	—	—	84	—
2,0	96	18	—	—					

Key: 1. Number of assemblies in the first loading
2. Unit
3. ^{235}U fuel enrichment, %
4. Working assemblies
5. Fuel parts of SUZ assemblies

In VVER-440 reactors at NVAES, Kol'skaya AES, and other AES, fuel of two compositions -- 2.4 and 3.6% enrichment -- are used in the steady-state fuel makeup mode.

Cartograms of the first fuel loading of VVER-1000 of the V unit at NVAES are shown in Figures 2.10 and 2.11. In the mode of a three-year fuel cycle, the core is made up with a fuel with an initial enrichment of 4.4%, and in the mode of a two-year cycle -- with an initial enrichment of 3.3%.

As a rule, the selection of the first loadings of a VVER are checked and sometimes refined by physical experiments on critical assemblies in the Institute of Nuclear Energy imeni I. V. Kurchatov [24, 50, 52]. Such experiments make it possible to correct the calculation programs used in selecting subsequent loadings of reactor cores. The necessary experiments are also conducted during the startup and operation of VVER.

Physical experiments make it possible to determine: 1) critical positions of groups of SUZ assemblies and their effectiveness; 2) boric acid effectiveness, which is particularly important for VVER-440 in which the necessary subcriticality of the core is not ensured without boric acid in the coolant of circuit I; 3) temperature and power coefficients of reactivity, which is necessary for evaluating the self-regulation of reactors; 4) power distribution over the core assemblies; 5) ^{135}Xe and ^{149}Sm transient processes.

The loading of the core of VVER is symmetric over the azimuth with an order of symmetry of not less than 3 (sector of symmetry with a 120° angle in the plane). This makes it possible to calculate only one third part of the core when selecting the next loading of the reactor. However, in practice, it is possible to have cases when during the reloading of the fuel from the reactor, it is necessary for various

reasons to unload from some sector of symmetry one or several assemblies which are not subject to replacement. In this case, the symmetry of the loading cartogram is disturbed, because the empty cell is loaded with a fresh assembly of the same (or, perhaps, different) enrichment, or a burned-out assembly, but with a different slag content. In such cases, it is necessary to calculate the burnup of the entire core (360° in the plane), or be content with averaging the properties of the assemblies which are symmetric with respect to their asimuthal position, but are not identical with respect to their neutron-physics characteristics. The asymmetry in slag content can appear also in a symmetrically loaded core, if in the course of the burnup process the symmetrically arranged mechanical controls of the SUZ have different degrees of insertion into the reactor.

In conclusion, let us mention that at NVAES, where reactors with various specific powers are operating, it is possible, in principle, to increase the attainable burnup fraction by burning assemblies which are not completely depleted in a higher power reactor in a reactor of a lower power [53]. This is possible because the multiplication constant of a burned-out assembly is increased when it is placed in a reactor of a lower power resulting from a partial release of the power and temperature effects of reactivity and a decrease in the effect of xenon poisoning. Since an assembly reaches its maximal possible burnup fraction in a low power reactor, it is possible to unload a certain amount of not completely burned out assemblies from a high-power reactor. In other words, it is possible to reload more than one third assemblies in a high-power reactor and thus to increase the operation time between reloadings. The economical advantanges of this combined use of fuel are discussed in more detail in section 12.4.

7.2. Calculation of the Neutron Physics Characteristics of a Reactor

As was mentioned before, the selection of fuel loading is done with the aid of special calculation programs. The following basic programs are used in designing VVER and in predicting their characteristics in the process of operation*:

1) UNIRASOS (or ROR) -- a four-group program for calculating neutron-physics properties of low-enrichment uranium-water fuel lattices and changes in these properties as the nuclear fuel burns out [24, 54];

2) BIPR -- a single-group diffusion program for calculating a three-dimensional reactor as a whole [45];

3) RAGU -- a one-dimensional four-group diffusion program for calculating the neutron flux density on the external boundary of the core with a reflector and on the surfaces of the absorbers of the SUZ assemblies;

4) KR -- a single-group program using the perturbation theory for calculating the reactivity factors of a reactor, the lifetime of prompt neutrons, the effective fraction of delayed neutrons, and the time constant of delayed neutrons (this program works only in conjunction with the BIPR program) [25];

5) TWEL -- a program for calculating the temperature field and the margin until the melting of the fuel and pressure of gaseous fission products in the fuel elements of VVER reactors [55];

6) GDKH -- a program for calculating the hydrodynamic characteristics of fuel assemblies;

7) RASKhOD -- a program for analyzing emergency situations of the reactor in the case of a partial lowering of the coolant flow;

8) P-002 -- a program for solving the kinetic equations of the reactor with consideration for automatic control.

*The programs mentioned here were prepared by the following members of the Institute of Atomic Energy imeni I. V. Kurchatov: A. N. Novikov, V. D. Sidorenko, D. M. Petrunin, Ye. D. Belyayeva, V. S. Ionov, D. F. Strelkov, G. A. Bogachev, V. F. Ostashenko (deceased), Ye. V. Vinokhodov, V. D. Borisov, A. I. Belyayev, and others.

Other programs for some concrete problems of VVER operation are also being used.

The following programs are used for calculating the distribution of energy release fields within assemblies (for more detail see section 7.3):

1) ShESTIGRANNIK [Hexahedron] (or its variant -- TREUGOL'NIK [triangle]) -- a two-group diffusion program for calculating the distribution of energy release in individual fuel elements of hexahedral assemblies [46];

2) MIKRO -- a program for a simplified evaluation of specific thermal loads of individual fuel elements in an assembly (by the results of calculations using BIPR and ShSTIGRANNIK programs).

Simultaneous combined use of several programs made it possible to develop a method for physical calculation of the core and a method of thermohydraulic and dynamic calculations of reactors.

Let us examine the ideology of some of the above-mentioned programs used in the selection of cartograms of core loading of VVER.

UNIRASOS (ROR) Program. The four-group program ROR is used widely in designing VVER and in calculating regular fuel reloadings. This program makes it possible to determine the neutron-physics properties and the burnup of homogeneous low-enrichment fuel lattices of VVER [54]. The ROR program makes it possible to calculate lattices with local nonuniformities, when a small part of fuel rods is replaced with abosrbing elements (PEL), or when boron is contained in the jackets of the assemblies. It is possible to estimate indirectly the effect of the boric acid dissolved in the coolant of the first circuit. At the present time, this program is supplemented by a considerably improved program -- UNIRASOS.

The UNIRASOS (universal calculation of states) program makes it possible to calculate with the aid of computer small-group constants and their changes in the process of fuel burnup for a uniform fuel lattice (the presence of a small number of PEL is permitted) composed of identical assemblies, cells, or fuel elements, i.e., for a homogenized lattice of a given composition and geometry. This program makes it possible to calculate a series of individual states of the lattice, obtain and store (on a magnetic tape or on punched cards) the dependence of the neutron-physics constants of the lattice on the temperature of the coolant and the fuel, density of the moderator, power, and other parameters. The moderator can be in the form of a mixture of H_2O and D_2O and can contain a boric acid solution. The fuel is a mixture of isotopes from ^{231}Pa to ^{244}Cm of any composition which may also contain nonfissionable elements. The covering material of the fuel elements and PEL, assembly jackets, and PEL rods may contain, besides ^{10}B, 16 other burnable isotopes, including those with strong isolated resonances.

The UNIRASOS program, just as ROR, is based on splitting the neutrons spectrum into four groups (see section 2.3). With an appropriate approach, the three upper groups are combined into one group of epithermal neutrons. The first groups contains practically the entire fission spectrum. A noticeable portion of fission occurs on ^{238}U. The lower boundary of the group corresponds to the vanishing of the cross section of ^{238}U fission. The neutron spectrum within the second group is close to

the Fermi spectrum, and the resonance capture is weak. Resonances of the heavy isotopes are concentrated almost entirely in the third group: ^{232}Th, ^{233}U, ^{235}U, ^{238}U, ^{239}Pu, ^{240}Pu, ^{241}Pu, ^{242}Pu. In the fourth (thermal) group, a large portion of the fission takes place. In describing the processes in this group, the thermal motion of the nuclei of the medium is taken into consideration (approaching of a heavy gaseous moderator).

Within the above energy groups, effective group constants are practically constant for all reasonable variants of the properties of the medium. In a homogenized medium of a prescribed composition, the group constants are expressed in terms of effective microscopic cross sections calculated in the P_1-approximation. The homogenizing of the equivalent cell is done for each of the four groups.

The distinctive characteristic of VVER is the distribution of the fuel of a given degree of enrichment over the assemblies whose dimensions are sufficiently great in comparison with the characteristic path lengths of neutrons. Even in the hot state, the diffision length of thermal neutron is such (L $\approx$ 3 cm) that the dimentions of the assemblies are 4-5 L. Moreover, the dimensions of the assemblies are much greater than the moderation length. Therefore, each assembly can be considered to be isolated both with respect to thermal neutrons, and with respect to epithermal neutrons. When the enrichment is small, the spectrum of epithermal neutrons depends weakly on the enrichment, and it is taken to be identical in all assemblies. In all variants of the geometry of the lattice composition occurring in practice, the migration area M^2 even in the hot state is of the order of 60-80 cm^2, i.e., M $\simeq 8 \div 9$ cm. Since the dimensions of the assemblies are 2-3 M, it is sufficient to limit oneself to the P_1-approximation for determining the angular dependence of the neutron flux density.

With all of the above-mentioned characteristics of the fuel lattice, it is possible to consider that in the greater part of the assembly an approximation holds true at which the spatial distribution of the neutron flux density is identical for all energy groups. The length of the fuel elements of VVER is many times greater than their diameter, therefore, the conditions of the diffusion of neutrons along the axis of the rods and at right angles to them are different. The following system of equations is solved in the UNIRASOS program with consideration for the neutron diffusion anisotropy:

$$D_{zi} B_z^2 \varphi_i + D_{Ri} B_R^2 \varphi_i + (\Sigma_i^a + \Sigma_i^{yn}) \varphi_i = \frac{\chi_i}{k_{эф}} \left(\sum_{j=1}^{4} \nu_j \Sigma_j^f \varphi_j \right) + \\ + \Sigma_{i-1}^{yn} \varphi_{i-1}; \quad i = 1, 2, 3, 4, \tag{7.16}$$

where D_{zi}, D_{Ri} -- coefficients of diffusion along and across the axis of a fuel element (by groups); B_z^2, B_R^2 -- size-shape factor along and across the axis of a fuel element; φ_i -- group density of the neutron flux; Σ_i^a -- macroscopic absorption cross section for each group of neutrons; Σ_i^{yB} -- macroscopic cross section of the removal of neutrons from a given group to the next group; Σ_i^f -- macroscopic fission

cross section by groups; ν_j -- number of neutrons produced in one fission event; χ_i -- share of fission neutrons per given group; $k_{эф}$ -- effective multiplication constant of the lattice; i(j) -- neutron group index.

By solving this system at prescribed values of B_z^2 and B_R^2, it is possible to determine $k_{эф}$ and vice versa, if we take $k_{эф} = 1$, it is possible to determine the size-shape factor in the critical state. The system of equations (7.16) makes it possible to determine the neutron-physics characteristics of the fuel lattice also in a single-group and a two-group approximations. The determination of the heterogeneous effects is accomplished during the homogenizing of the equivalent cell.

The UNIRASOS program has a number of innovations in comparison with the ROR program which make it possible to take into account a number of effects more accurately and expand the potentialities of the program.

A list of fission products which are taken into consideration is given below in the order adopted in the standard variant of the UNIRASOS program:

1—4. ^{82}Kr—^{85}Kr
5. ^{85}Rb
6—7. ^{86}Sr—^{87}Sr
8. ^{86}Kr
9. ^{87}Rb
10. ^{88}Sr
11. ^{89}Y
12. ^{90}Zr
13. ^{90}Sr
14—17. ^{91}Zr—^{94}Zr
18—19. ^{95}Mo—^{96}Mo
20. ^{96}Zr
21—22. ^{97}Mo—^{98}Mo
23. ^{99}Tc
24. ^{100}Ru
25. ^{100}Mo
26—27. ^{101}Ru—^{102}Ru
28. ^{103}Rh
29. ^{104}Pd
30. ^{104}Ru
31—32. ^{105}Pd—^{106}Pd
33. ^{106}Ru
34—35. ^{107}Pd—^{108}Pd
36. ^{109}Ag
37—40. ^{110}Cd—^{114}Cd
41. ^{115}Zn
42—43. ^{116}Sn—^{117}Sn
44—46. ^{123}Te—^{125}Te
47. ^{124}Sn
48. ^{126}Sb
49. ^{126}Te
50. ^{127}I
51—52. ^{128}Xe—^{129}Xe
53. ^{128}Te
54. ^{129}I
55. ^{130}Xe
56. ^{130}Te
57—58. ^{131}Xe—^{132}Xe
59—60. ^{133}Cs—^{134}Cs
61. ^{134}Xe
62. ^{135}Cs
63—64. ^{136}Ba—^{137}Ba
65. ^{136}Xe
66. ^{137}Cs
67. ^{138}Ba
68. ^{139}La
69. ^{140}Ce
70. ^{141}Pr
71. ^{142}Nd
72. ^{142}Ce
73—76. ^{143}Nd—^{146}Nd
77. ^{147}Pm
78. ^{148}Sm
79. ^{148}Nd
80—81. ^{149}Sm—^{150}Sm
82. ^{150}Nd
83—84. ^{151}Sm—^{152}Sm
85—86. ^{153}Eu—^{154}Eu
87. ^{154}Sm
88. ^{155}Eu
89—90. ^{156}Cd—^{157}Cd
91. ^{159}Tb
92—95. ^{160}Dy—^{163}Dy

BIPR Program. This program is the basic program for the three-dimensional calculation of the VVER core. BIPR makes it possible to determine the reserves and reactivity factors of the core, to perform calculations of the integral and differential effectiveness of the control elements, to determine critical positions of the control elements and critical values of boron concentrations in the coolant, to obtain the three-dimensional distribution of the energy release fields in the core, and to calculate the fuel burnup in the core and ^{135}Xe and ^{149}Sm transient processes.

In the BIPR program, the reactor core is represented in the plan by several symmetric sectors in each of which the arrangement of assemblies with identical calculated neutron-physics properties and the same design number n repeats symmetrically ($1 \leq n \leq 117$ for three symmetry sectors for VVER-440).

This program makes it possible to calculate symmetry sectors with angles of 30, 60, 120 and 360 degrees. Due to the presence of symmetry, calculations are done for only one sector, which substantially simplifies and speeds up the calculation of the loading cartograms. Moreover, the "joining" conditions of the neutron flux densities on the inner boundaries of the symmetry sector are observed closely, i.e., the results of calculations are true for the entire core.

For mathematical description of physical processes, the real core in which the assemblies are arranged in plan over a triangular lattice is represented by a mathematical model, where continuous changes in the properties in the core volume are replaced by discrete changes over the points in which all physical properties averaged over the cross section of the assemblies are concentrated. Along the height of the assemblies, m cross sections (points, $1 \leq m \leq 10$) are taken and, thus, the core is represented in the form of a spatial lattice. At each lattice point with coordinates (n, m), a number of characteristics changing in time during the burnup are determined, breeding properties (k_∞) depending on the kind of fuel, local power effects, effects of poisoning by samarium and xenon, fuel burnup depth, neutron flux density field, energy release field, etc.

The working assemblies are represented as a stationary spatial lattice of points, the real lattice of SUZ assemblies is represented as a mobile spatial lattice of points. The movement of control elements is taken to be discrete with the movement pitch Δh_{SUZ} equal to the distance between the points along the height. In the process of the calculation of one state, the points of the mobile and stationary lattices always coincide. Unlike the points of the stationary lattice, the points of the mobile lattice can have either the properties of absorbers, or of the fuel, depending on the degree of the withdrawal of the SUZ assembly from the core.

The simulation of the process of power control by a liquid absorber is also accepted to be discrete (Δc_B).

The initial prerequisites of the BIPR program are as follows.

1. The distribution of the neutron flux density over an inhomogeneous core is found from the solution of the following one-group equation:

$$\Delta\varphi(r) + \varkappa^2(r, \lambda)\varphi(r) = 0. \qquad (7.17)$$

(Transition to discreteness is accomplished by replacing the radius vector r of the lattice point under consideration by its coordinates n, m). This equation can be reduced to the Poisson equation or to the diffusion equation (depending on the statement of the problem). It is solved by the iteration method according to the finite-difference scheme in a nine-point spatial lattice around each point.

Boundary conditions are given on the external boundaries of the core and on the surfaces of the SUZ assemblies:

$$\frac{1}{\varphi}\frac{d\varphi}{dl} = \frac{1}{d_{э\phi}}, \tag{7.18}$$

where $d_{э\phi}$ -- reciprocal value of the effective logarithmic derivative of the neutron flux density taken along the normal to external boundary of the region being examined; l -- direction of the normal.

2. The values of k_∞ and M^2 are calculated by the UNIRASOS (or ROR) program by the formulas

$$k_\infty = \frac{\int \nu\Sigma^f(E) f\left(E, B_0^2\right) dE}{\int \Sigma^a(E) f\left(E, B_0^2\right) dE}; \tag{7.19}$$

$$M^2 = \frac{\int D(E) f\left(E, B_0^2\right) dE}{\int \Sigma^a(E) f\left(E, B_0^2\right) dE}. \tag{7.20}$$

3. It is taken (and is confirmed experimentally) that all assemblies in the reactor are uniform with respect to their moderating properties, resonance capture and ^{238}U multiplication; $M^2 \approx \tau$ and is constant over the core.

4. Material parameter

$$\varkappa^2(r, k_{э\phi}) = \left(\frac{k_\infty(r)}{k_{э\phi}} - 1\right) \Big/ M^2, \tag{7.21}$$

where M^2 -- the value of square migration length averaged over the core; $k_\infty(r)$ -- multiplication factor of an infinite lattice with fuel of a given grade E; $k_{э\phi}$ -- effective multiplication factor.

5. The multiplication factor $k_\infty(r)$ at the points has its own definite value which depends on: a) enrichment of the fuel (grade E) in the assemblies; b) fuel burnup fraction at a given point $\rho_{шл}$; c) density γ and temperature of the moderator-coolant t; d) boron concentration in the coolant c_B; e) power of the assembly ψ; f) ^{135}Xe and ^{149}Sm poisoning, respectively, ρ_{Xe}, ρSm.

Thus, $k_\infty(r)$ is a composite function of many variables:

$$k_\infty(r) = k_\infty(n, m) = [1 + \Delta k_{0(E)} - \Delta k_{шл(n,m)} - \Delta k_{Sm(n,m)} - \Delta k_{\psi(n,m)}] \Pi_B \Pi_{\Delta t} \Pi_{Xe}. \tag{7.22}$$

Here $\Delta k_{0(E)} = k_{\infty(0,E)} - 1$ -- excess multiplication factor of a fresh, unpoisoned fuel lattice of grade E without power; $\Delta k_{шл(n,m)}$ -- slagging effect; $\Delta k_{Sm(n,m)}$ -- ^{149}Sm poisoning effect; $\Delta k_{\psi(n,m)}$ -- power effect; Π_{Xe} -- ^{135}Xe poisoning effect; $\Pi_{\Delta t}$ -- temperature effect; Π_B -- effect of poisoning by ^{10}B dissolved in the coolant-moderator.

Neutron flux density $\varphi(r)$ depends on the same parameters as $k_\infty(r)$:

$$\varphi = \varphi(n, m, E, \rho_{шл}, \rho_{Sm}, \rho_{Xe}, \Delta t, c_B).$$

6. In the BIPR program, the following definition of relative energy release is taken with a certain approximation:

$$\psi(r) = \psi(n, m) = k_\infty(r)\varphi(r) = k_\infty(n, m)\varphi(n, m). \quad (7.23)$$

7. It is assumed that slag formation is proportional to energy release in the segment of time when the characteristics of the reactor are practically constant:

$$\Delta\rho_{шл}(T) = k_{шл}\int_{T_1}^{T_2}\psi dT. \quad (7.24)$$

Here, $k_{шл} = (0.40 \div 0.45)\ 10^{-3}$ kg slag·1/(t·kw·day) -- conversion factor.

8. Nonsteady-state poisoning by xenon and samarium is taken into consideration.

A special control unit simulates the control of the reactor during the movement of the SUZ assemblies, which shows on the changes of the curvature of the neutron field $\varphi(r)$ with the changes in the concentration of boric acid allowed for in the value of the material parameter $\varkappa^2$ and in combined use of both control methods.

The BIPR program delivers the following information in the process of computations: 1) input characteristics of the core as a whole, as well as by the types of working assemblies and SUZ elements; 2) current moment of time T, eff. days; 3) average slag content in the core $\overline{\rho}_{шл}$, kg slag/t U; 4) $k_{эф}$ of the core; 5) nonuniformity factor of volume energy release $k_V^{макс} = (\psi_{m,n})_{макс}/\overline{\psi}$; 6) number of the calculated point with k_V^{max}; 7) nonuniformity factor of energy release of the assemblies $k_q^{макс} = (\int_0^H \psi dz)_{макс}/\int_0^H \overline{\psi} dz$; 8) number of the assembly with k_q^{max}; 9) boron concentration c_B, gB/kg H_2O; 10) withdrawal height of the working group of SUZ assemblies, cm; 11) number of the assembly in the operating group of SUZ; 12) reactivity in the given state $\rho = 1-1/k_{эф}$; 13) average content of slags $\overline{\rho_n}$, of energy release $\overline{k_{qn}}$, and heating Δt_n over the assemblies; 14) distribution of the slag content $\rho_{m,n}$, of neutron flux density $\varphi_{m,n}$, and energy release $\psi_{m,n}$ over the entire volume of the core; 15) concentration matrix of slag for all assemblies at ten points along the height; 16) concentration matrix of ^{149}Sm for all assemblies at ten points along the height; 17) concentration matrix of ^{149}Pm for all assemblies at ten points along the height.

In spite of the simplicity of its mathematical model, the BIPR program makes it possible to simulate with practically acceptable accuracy the work of a reactor in time and to obtain the necessary characteristics of the fuel burnup process in the core.

RAGU Program. This program makes it possible to determine the following in a small-group (up to four groups) diffusion approximation or P_1-approximation: 1) effective

multiplication factor of a multizonal (up to 10 zones) medium; 2) neutron flux density as a function of the coordinate r; 3) logarithmic derivative of the neutron flux density on the boundary surface of the SUZ absorber with the surrounding fuel part of the zone or the core with the reflector.

In order to perform calculations on SUZ absorbers, conversion is performed from a real hexahedral geometry to an equivalent cylindrical cell. The values of $k_{эф}$, B_r^2, d_{log} are determined, after which inverse conversion to the real geometry is performed, and single-group effective reciprocal value of the logarithmic derivative $d_{эф}$ suitable for using in the BIPR program is delivered.

Analogous operations are performed for determining the effective logarithmic derivative for a boundary with a reflector, but the entire core in this case is represented in the form of one equivalent cell.

The following is the initial system of equations in the program:

$$\left.\begin{aligned} &\frac{1}{r^\alpha}\frac{d}{dr}\left(r^\alpha \varphi_1^l\right) + \Sigma_0^l \varphi_0^l = f_0^{*l} + S_0^l; \\ &\frac{1}{3}\frac{d\varphi_0^l}{dr} + \Sigma_1^l \varphi_1^l = f_1^{*l} + S_1^l \end{aligned}\right\} \tag{7.25}$$

with boundary conditions for the core

$$\nabla\varphi_{0|r=0}^l = 0; \quad \varphi_{0|r=R}^l = 0 \tag{7.26}$$

and for the absorber cell

$$\nabla\varphi_{0|r=0}^l = 0; \quad \nabla\varphi_{0|r=R}^l = 0 \tag{7.27}$$

and the conditions of joining at the boundaries of the zones:

$$\varphi_i^l = \varphi_{i+1}^l; \quad D_i^l \nabla\varphi_i^l = D_{i+1}^l \nabla\varphi_{i+1}^l. \tag{7.28}$$

Here, i -- zone index; j -- number of the neutron group; α -- geometry parameter (plane, cylinder, sphere); r -- generalized coordinate; R -- size of the absorber cell or the core; φ -- neutron flux density;

$$\Sigma_0^l = \Sigma_a^l + \Sigma_{0ув}^{l\to l+1}; \quad \Sigma_1^l = \Sigma_{tr}^l + \Sigma_{ув}^{l\to l+1};$$

S_0^j and S_1^j -- isotropic and anisotropic sources of neutrons;

$$\left.\begin{aligned} &f_0^{*l} = \frac{\chi^l}{k_{эф}} Q + \Sigma_{0ув}^{l-1\to l}\varphi_0^{l-1}; \\ &f_1^{*l} = \Sigma_{1ув}^{l-1\to l}\varphi_1^{l-1}; \; Q = \sum_j (\nu\Sigma_f)^j \varphi_0^j \end{aligned}\right\} \tag{7.29}$$

(the same symbols as used earlier).

The initial constants for the fuel are found by the UNIRASOS (or ROR), and for other materials by the RAGU program. The RAGU program has been checked on a considerable amount of experimental material and showed that, in principle, it is applicable.

KR Program. The input constants for this program are calculated by the UNIRASOS (or ROR) and RAGU programs. The necessary data on three-dimensional density distribution of a single-group neutron flux in the core volume are taken from the BIPR program which operates jointly with the KR program.

The expression for the reactivity factor is represented in the form

$$\frac{d\rho}{dx} = \left[\frac{1}{k_{э\phi}}\int_V \frac{d\varkappa^2}{dx}\varphi^2 dV + \frac{1}{\overline{M^2}}\frac{\overline{dM^2}}{dx}\left(1-\frac{1}{k_{э\phi}}\right)\int_V \varphi^2 dV + \right. \\ \left. + \int_S \frac{1}{d^2_{э\phi}}\frac{d\,(d_{э\phi})}{dx}\varphi^2 dS\right]\left[(1/\overline{M^2})\int_V k_\infty \varphi^2 dV\right]^{-1}, \tag{7.30}$$

where $\varkappa^2$ -- material parameter of a homogeneous lattice; $\overline{M}^2$ -- average (independent of the coordinates) area of neutron migration; $d_{э\Phi}$ -- effective inverse value of the logarithmic derivative (for a single-group flux); x -- used to determine the changes in the reactivity factor (change in the coolant density, coolant temperature without changes in the density, average fuel temperature, coolant temperature including changes in the density and changes in the reactor power).

Other characteristics calculated by the KR program, their expression in terms of the determined parameters of the reactor, their caclulation and representation in the final form are given in work [25].

Appendix. Example of the Calculation of Loading (Reloading) of Fuel in the VVER-440 Reactor

The neutron energy spectrum averaged over the cross section of the assembly is found to be close to the asymptotic spectrum and is determined, primarily, by the properties of the assembly itself, which makes it possible to separate the problem of the calculation of small-group cross sections of fuel lattices and changes in the isotopic composition during the burnup of fuel from the calculation of the reactor as a whole. Thus, the final results of calculations by the UNIRASOS (ROR) program are the input parameters for the BIPR program.

Let us illustrate the selection of the cartogram of the loading (reloading) of nuclear fuel on an example of the calculation of the first loading of the VVER-440 of the IV unit of NVAES.

The three-dimensional calculation of the reactor is performed in the following sequence:

1. Calculation of the neutron-physics characteristics of the fuel assemblies to be used in loading, -- by the UNIRASOS (ROR) program.

2. Calculation of the reciprocal values of the logarithmic derivatives of the neutron flux density on the boundary of the core with a reflector and on the boundary of the absorbers of the SUZ with fuel -- by the RAGU program.

3. Calculation of the subcriticality (supercriticality) of the core in the cold state -- by the BIPR program.

4. Calculation of the distributions of the densities of neutron fluxes and energy releases, as well as of the fuel burnup over the volume of the core -- by the BIPR program.

5. Calculation of the effectiveness of the control elements -- by the BIPR program.

6. Calculation of the coefficients of the reactivity of the reactor -- by the KR and BIPR programs.

7. Thermohydraulic analysis of permissible operation modes -- by the GDKh, RASKhOD, ShESTIGRANNIK, TWEL programs.

Let us examine the process of calculations step by step.

1. Fuel assemblies of three degrees of enrichment were used in the reactor: 1.6, 2.4, and 3.6% (see Table 7.2). Consequently, it is necessary to perform three complete calculations of the burnup of such fuel lattices, as well as several short calculations of individual state for each fuel lattice (see Section 2.3) for various values of specific power, temperature of the coolant-moderator, and the boron concentration in it.

Calculations were done by the ROR program. The input parameter for this program are given below on the example of a fuel lattice of 3.6% enrichment.

k_T = 0.866 -- coefficient of the geometry of a hexagonal lattice;
h_T = 14.7 cm -- assembly spacing with consideration for the water gap;
d_T = 0.775 cm -- diameter of a fuel rod in a fuel element with consideration for the gas gap;
δ_{CT} = 0.065 cm -- wall thickness of the fuel element jackets;
Δ_k = 14.4 cm -- "box wrench" dimensions of the assembly;
δ_k = 0.15 cm -- thickness of assembly wall;
n = 126 -- number of fuel elements in the assembly;
d_{UO_2} = 0.755 cm -- diameter of the fuel pellet;
γ_{UO_2} = 10.2 g/cm^3 -- uranium dioxide density in the pellet;
T_{H_2O} = 293 degrees K -- temperature of the moderator (for an example, the cold state of the fuel lattice is taken);
γ_{H_2O} = 1.0 g/cm^3 -- density of the moderator at T_{H_2O};
m_{Zr} = 2 -- index indicating the material of the wall of the fuel element and the assembly (Zr);
$\overline{T}_{UO_2}$ = 293 degrees K -- average temperature of the fuel (cold state);
m_{UO_2} = 0 -- index indicating the type of fuel in the fuel element (UO_2);
w_{Xe} = 0.064 -- parameter indicating ^{135}Xe poisoning;
w_{Sm} = 0.011 -- parameter indicating ^{149}Sm poisoning;
$\overline{w}$ = 84.3 kw/l -- specific power in the volume of the core;
ρ_{25} = 0.036 -- initial concentration of ^{235}U;
ρ_{28} = 0.964 -- initial concentration of ^{238}U;
ρ_i = 0 -- initial concentration of ^{236}U, ^{239}Pu, ^{240}Pu, ^{241}Pu, ^{237}Np, ^{10}B, ^{242}Pu, and slag.

The remaining constants are tabular in nature and are not given here.

The dynamics of the fuel burnup is described by the following system of equations

$$d\rho_i/dT = S_i - \sigma_i^a \varphi \rho_i - \lambda_i \rho_i, \qquad (7.35)$$

where ρ_i -- concentration of the i-th isotope; T -- time; S_i -- source of the appearance of the i-th isotope (from the preceding isotope as a result of neutron capture or radioactive decay of some isotope); σ_i^a -- one-group absorption cross section of the i-th isotope; φ -- neutron flux density; λ_i -- radioactive decay constant.

Fission products are combined into a fictitious isotope (slags) with changes in the absorption cross section according to the 1/v law in the thermal region and having a resonance integral equal to 200 barns. Slags do not include isotopes ^{135}Xe and

^{149}Sm which are allowed for separately. The initial data are transferred to punched cards and are introduced into the computer. After completing machine computations, extensive output information is printed. The results of computations are shown graphically in Figures 2.5-2 9.

The next step is the processing of the obtained results in a form convenient for the BIPR prgram. For this purpose, the dependence of the multiplication constant of the fuel lattice of grade E on various effects of reactivity [see formula (7.22)] is approximated as follows:

$$\Delta k_{шл} = \sum_{i=1}^{8} a_{iE} \rho_{шл}^{i}; \tag{7.34}$$

$$\Delta k_{\psi} = \sum_{j=1}^{6} b_{jE} w^{j}, \tag{7.35}$$

$$\Delta k_{Sm} = e_{Sm,E} Sm; \tag{7.36}$$

$$\Pi_{Xe} = 1 + e_{Xe,E} Xe; \tag{7.37}$$

$$\Pi_{\Delta t} = 1 + d_{1E} \Delta t + d_{2E} \Delta t^2; \tag{7.38}$$

$$\Pi_{B} = 1 + C_{1E} C_B \gamma_{H_2O} + c_{2E} C_B^2 \gamma_{H_2O}^2. \tag{7.39}$$

Here, $\rho_{шл}$ -- slag concentration in the fuel lattice; w -- power at which the fuel lattice works; Sm, Xe -- concentration of ^{149}Sm and ^{135}Xe nuclei in the fuel lattice; Δt -- heating of the coolant over the length of the assembly; γ_{H_2O} -- coolant density (depends on the temperature); c_B -- boron concentration in the coolant-moderator; a_i, b_j, c_1, c_2, d_1, d_2, e_{Xe}, e_{Sm} -- approximation coefficients (Table 7.6).

2. The determination of logarithmic derivatives is particular in nature and is done one time for each reactor. Results for the cold and hot states of VVER are given on page 41, as well as below.

3. For the three-dimensional calculation of fuel burnup in the core: the symmetry sector of 120 degrees containing 117 assemblies. Preparations for computations according to the BIPR program begin with the selection of an arrangement scheme of assemblies in the core with various initial fuel enrichment levels and various degrees of burnup fractions. The initial prerequisites and the ideology of combining fuel assemblies are discussed in section 7.1. For this case, the loading cartograms are shown in Figure 7.2, its composition is given in Table 7.2.

Initial data for the BIPR program are given below:

$M^2 = 64.5$ cm^2 -- migration area;
$h_r = 14.7$ cm -- distance between centers of assemblies (in plane);
$m = 10$ -- number of calculation points along the height;
$H = 250$ cm -- core height;
$V_{a3} = 16{,}270$ l -- core volume;
$2d_R = 17.36$ cm; -- doubled reciprocal values of logarithmic derivatives for
$2d_H = 19.96$ cm the radial and the end reflectors;

Table 7.6
Approximation Coefficients for Fuel Lattices of VVER-440

Коэффициент (1)	(2) Значение коэффициента при обогащении топлива, %		
	3.6	2.4	1.6
Δk_0	+0,341800000	+0,248550000	+0,137180000
a_1	$-0,922801660 \cdot 10^{-2}$	$-0,680990342 \cdot 10^{-2}$	$+0,239969283 \cdot 10^{-2}$
a_2	$-0,883545897 \cdot 10^{-3}$	$-0,209788752 \cdot 10^{-2}$	$-0,543949452 \cdot 10^{-2}$
a_3	$+0,125842000 \cdot 10^{-3}$	$+0,365726456 \cdot 10^{-3}$	$+0,112442249 \cdot 10^{-2}$
a_4	$-0,839037485 \cdot 10^{-5}$	$-0,328936284 \cdot 10^{-4}$	$-0,131385367 \cdot 10^{-3}$
a_5	$+0,322736125 \cdot 10^{-6}$	$+0,175778354 \cdot 10^{-5}$	$+0,934433658 \cdot 10^{-5}$
a_6	$-0,733781061 \cdot 10^{-8}$	$-0,562023082 \cdot 10^{-7}$	$-0,400432270 \cdot 10^{-6}$
a_7	$+0,919482135 \cdot 10^{-10}$	$+0,993592319 \cdot 10^{-9}$	$+0,949278745 \cdot 10^{-8}$
a_8	$-0,489689719 \cdot 10^{-12}$	$-0,745453111 \cdot 10^{-11}$	$-0,953513678 \cdot 10^{-10}$
b_1	$-0,170750000 \cdot 10^{-3}$	$-0,168030000 \cdot 10^{-3}$	$-0,159630000 \cdot 10^{-3}$
b_2	$+0,308040000 \cdot 10^{-7}$	$+0,336040000 \cdot 10^{-7}$	$+0,252030000 \cdot 10^{-7}$
b_3	0,000000000	0,000000000	0,000000000
b_4	0,000000000	0,000000000	0,000000000
b_5	0,000000000	0,000000000	0,000000000
b_6	0,000000000	0,000000000	0,000000000
c_1	$-0,737600000 \cdot 10^{-1}$	$-0,104680000$	$-0,138130000$
c_2	$+0,409800000 \cdot 10^{-2}$	$+0,688100000 \cdot 10^{-2}$	$+0,112090000 \cdot 10^{-1}$
d_1	$-0,954190000 \cdot 10^{-3}$	$-0,759350000 \cdot 10^{-3}$	$-0,479170000 \cdot 10^{-3}$
d_2	$-0,296000000 \cdot 10^{-5}$	$-0,242000000 \cdot 10^{-5}$	$-0,161000000 \cdot 10^{-5}$
e_{Xe}	$-0,115000000 \cdot 10^{+1}$	$-0,185000000 \cdot 10^{+1}$	$-0,265000000 \cdot 10^{+1}$
e_{Sm}	$-0,121000000 \cdot 10^{-1}$	$-0,168000000 \cdot 10^{-1}$	$-0,218000000 \cdot 10^{-1}$

Key: 1. Coefficient
2. Coefficient value for fuel enrichment, %

$2d_r = 14.86$ cm; -- the same for the lateral side and the end part
$2d_T = 37.4$ cm of the controls;

$n_1 \div n_4 = 10$,
$n_5 \div n_8 = 11$,
$n_9 \div n_{10} = 10$,
$n_{11} = 9$; $n_{12} = 4$ -- number of assemblies in each of the 12 horizontal rows of the cartogram in the symmetry sector of 120 degrees $\left(\sum_{i=1}^{12} n_i = 117\right)$;

$h_{XII}^{CV3} = 125$ cm -- height of the initial withdrawal of the working group of the regulating rods (rods No 1, 7, 68);

$\Delta C_B = 0.01$ gV/kg H_2O -- step of the change in the boron concentration in the coolant during burnup;

$g_i = 1.0$ -- relative flow rates of the coolant through the assemblies (117 numbers);

$Q = 39{,}000$ m^3/h -- total flow rate of the coolant through the core;

$\bar{\gamma}_{H_2O} = 0.75 \cdot 10^3$ kg/m^3 -- average coolant density in the core;

$c_p = 1.249$ kcal/(kg·degrees) -- average specific heat of the coolant at a constant pressure;

$\gamma_{Pm} = 0.011$ -- ^{149}Pm fission yield;

$\gamma_{Sm} = 0$ -- ^{149}Sm fission yield;

$\lambda_{Pm} = 0.357 \cdot 10^{-5}$ sec^{-1} -- ^{149}Pm radioactive decay constant;

$\left.\begin{array}{l}\sigma^{*}_{Sm,1} = \\ = 0.202 \cdot 10^{6} \text{ barns} \\ \sigma^{*}_{Sm,2} = \\ = 0.337 \cdot 10^{6} \text{ barns} \\ \sigma^{*}_{Sm,3} = \\ = 0.464 \cdot 10^{6} \text{ barns}\end{array}\right\}$ -- effective microscopic cross sections of ^{149}Sm capture in the lattices 3.6, 2.4, 1.6%;

$P_U = 40.91$ t -- uranium charge in the reactor;
$\gamma_{UO2} = 10.2$ t/m^3 -- uranium dioxide density;
$N_T = 1375 \cdot 10^3$ kw -- total thermal power of the reactor;
$\Delta T = 5$ days -- burnup time spacing;

$\Delta k_{0,E}, a_{iE}, b_{jE}, c_{1,2,E}, d_{1,2,E}, e_{Sm,E}, e_{Xe,E}$ -- approximation coefficients for a fuel lattice of grade E: 1.6, 2.4, 3.6% (values are taken from Table 7.6);

T = 0 effective days -- beginning of burnup.

It is also necessary to give the values of ^{149}Pm, ^{149}Sm and slag concentrations in all 1170 points of the symmetry sector of the core. If the burnup of a fresh unpoisoned core is calculated, these values are equal to zero. The initial parameters are introduced into the computer and fuel burnup in a three-dimensional core is calculated. The following information is printed out at definite time intervals: distribution of slags, relative energy release and neutron flux densities over the entire volume of the core being calculated, as well as the average distribution of slags, energy releases and heating over the assemblies in the form of cartograms for the symmetry sector. For a typical case, some results of calculations are shown graphically in Figure 4.1. The diagrams reflect the peculiarities of conducting the burnup mode: first, with the aid of boric acid in the coolant with a fixed position of the controls of the working group, and then after the withdrawal of boron from the reactor, with the aid of SUZ assemblies.

The following are some characteristics of the burnup mode printed by the computer before the end of the boron regulation mode: T = 240 effective days; $\bar{\rho}_{шл}$ (over the core) = 8.146 kg slag/t U; $k_{эф} = 0.99976$ $k_V^{max} = 1.447$ at a point n,m = 41.3; k_q^{max} =1.259 in an assembly of n = 42; $c_B = 0.05$ g V.kg H_2O.

On completion of computations, the computer printed complete information for the core and punched networks for slags, ^{149}Sm and ^{149}Pm. Having supplemented the initial data with some constants, it is possible to calculate ^{135}Xe transient processes when the power rises or lowers.

If the computed characteristics of the burnup in the course of the operating period are unsatisfactory, the entire procedure is repeated, beginning with the change in the loading cartogram.

4. Due to the fact that the temperature effect of VVER reactivity is negative (see section 3.2), the cold state of the reactor is the most dangerous from the point of nuclear safety. The determination of the subcriticality (supercriticality) in the

cold state is particularly important for VVER-440 in which the total reactivity excess of the loaded (reloaded) core (see section 3.3) is sufficiently great and does not make it possible to operate it without boric acid in the coolant. Subcriticality (supercriticality) of the selected load is calculated by the BIPR program as a computation of one state of the reactor with initial data corresponding to the cold state.

The following results were obtained for the case in question for the cold state: k_{eff} = 1.2161 -- all upper SUZ assemblies, c_B = 0; k_{eff} = 1.03214 -- all lower SUZ assemblies, c_B = 0; k_{eff} = 10000-- all lower SUZ assemblies, c_B = 0.174 g V/kg H_2O; k_{eff} = 10000-- all upper SUZ assemblies, c_B = 1.347 g V/kg H_2O; k_{eff} = 0.9221 -- all upper SUZ assemblies, c_B = 2.1 g V/kg H_2O; k_{eff} = 0.8129 -- all lower SUZ assemblies, c_B = 2.1 g V/kg H_2O.

The last value of k_{eff} characterizes the allowed stopped condition of the reactor in the cold state.

5. It is important to know the differential and integral effectiveness of the controls (see section 3.3) for the evaluation of the capacity of the SUZ system (as a whole or for individual groups of assemblies) to compensate successfully various reactivity effects under any operating conditions, both steady-state, and nonsteady-state (transient and emergency).

The effectiveness of controls depends on the composition and the combination method of fuel assemblies in the core. Therefore, for a new reloaded (and in a number of cases for a reloaded) core, it is necessary to determine the effectiveness of the controls for various states of the reactor. Calculations are done by the BIPR program in a special mode of its operation. The results of the calculations are shown in Tables 3.5, 3.6 and in Figures 3.7, 3.8.

6. Computations of reactivity coefficients of the core (see section 3.2) characterizing the dynamics of changes in reactivity in nonsteady-states of the reactor are connected very directly with everything that was said above.

The necessary initial data prepared by the UNIRASOS (ROR) program together with the KR program are introduced into the computer for computations using the BIPR program. Thus, the determination of the coefficients of reactivity is combined with computations of individual states of the reactor or fuel burnup. Information on both programs is presented simultaneously, which is very convenient.

The results of the computations of coefficients of reactivity for various modes of VVER are shown in Tables 3.1, 3.2, and in Figures 3.3-3-6.

7. The selection of the cartogram of core loading is concluded by a thermohydraulic analysis of permissible operation modes of the reactor with this load for creating safe conditions for the fuel elements eliminating the melting of the fuel and the occurrence of a heat exchange crisis under any nonsteady-state conditions (see Chapter 5). This is a very important stage of calculations which can introduce definite corrections in the operating mode of the reactor.

The principles of the thermohydraulic analysis are explained in section 5.3. The initial materials are: results of calculation of the fuel load burnup by the BIPR program (see Figure 4.1), hydrodynamic characteristics of the assemblies and the reactor obtained by the GDKh program (see Figures 5.1, 5.2), charts for emergency reduction of the coolant flow rate when several GTsN are turned off (see section 5.5, Figure 5.10), coefficients of micrononuniformity of energy release for the fuel elements within the assemblies calculated by the programs ShESTIGRANNIK and MIKRO (see section 7.3, Figures 7.4-7.7, Tables 7.4, 7.5), and the method for calculating the margin to the melting of the fuel using the TWEL program.

The maximally energy-intensive fuel element is found in the core, and it is assumed that it limits the power level of the reactor. The maximum permissible power of the fuel element, the assembly, and the reactor are determined in successive order. As a result of these computations, a chart is obtained for the maximum permissible power of the reactor in the course of the run and a table of permissible power levels of the reactor depending on the number of operating GTsN and power supply circuits of GTsN (see Table 5.7) are obtained.

8.4. Studying Spent Nuclear Fuel in a Hot Chamber

The condition of fuel elements which reached the necessary burnup level and were unloaded from the reactor are studied in detail in a hot chamber. In the process of studies, the condition of spent fuel elements and other parts of the assembly is evaluated, defective fuel elements and causes of the appearance of the defects are revealed, possibilities of achieving an above-plan burnup level are evaluated, and ways of improving the assemblies are determined. Moreover, gamma-spectrometrics studies of spent fuel elements make it possible to determine experimentally the absolute value of fuel burnup and burnup distribution over the cross section and height of the assemblies and to obtain information about the migration of fission fragments, which makes it possible to evaluate indirectly the operating temperature of the fuel in the fuel elements.

VVER fuel elements work with high temperature differences between the central part of the fuel elements and the jacket, creating thermal stresses. Neutron fluences affecting fuel elements reach values of the order of 10^{21} neutrons/cm^2. Under these conditions of fuel element operation, the fuel swells, gaseous fission fragments accumulate under the jacket, and the strength properties of the fuel element jackets change.

Experimental studies of spent assemblies in a hot chamber made it possible to conclude that the design of the VVER assemblies and fuel elements and the technology of their manufacturing ensure a sufficient working capacity of the fuel to the rated burnup level and higher.

When studying spent assemblies in a hot chamber, they are first examined visually in order to reveal possible defects and to evaluate the nature of the deposits of corrosion products. The equipment of the hot chamber makes it possible to measure the diameter and length of the fuel element, pressure of gaseous fission products under the jacket, ultimate strength, and relative lengthening of the fuel element jackets and to determine the chemical composition of the detected deposits.

For an example, Table 8.6 gives the experimental data about the changes in the diameter and length of the fuel elements of VVER-365 assemblies of the unit II of NVAES [67]. Changes in the fuel element diameter are within the limits of the manufacturing tolerance, i.e., there is actually no transverse swelling of the jackets. The increase in the fuel element length is somewhat higher than the manufacturing tolerance. The design of the assemblies makes it possible to compensate the temperature elongation of the fuel elements, and the absence of their bending indicates a normal compensation of such elongations.

Table 8.6
Changes in the Geometrical Dimensions of Fuel Elements Under Irradiation

(1) Выгорание, Мвт·сутки/тU · 10^{-3}	(2) Изменение размеров твэла, %	
	(3) диаметра	(4) длины
7,5	—0,55	0,16
19,1	—0,22	0,17
25,6	0,33	0,24

Key: 1. Burnup, Mw·day/mU · 10^{+3}
2. Changes in the dimensions of fuel elements, %
3. Diameter
4. Length

The pressure of gaseous fission fragments under the fuel element jacket is determined by puncturing the jacket. In the VVER-365 assemblies which were studied, the gas pressure under the fuel element jackets under operating conditions is about 10 kg-force/cm^2. This value of the pressure under the jacket indicates that the temperature of the fuel pellets during the operation of the fuel elements does not exceed 1600 degrees C [68].

Special attention is given to the study of fuel elements with detected defects in the jackets.

The following are the possible causes of damages of fuel element jackets: 1) local overheating; 2) cracking connected with stresses or fatigue, as well as with the effect of thermal cycles of the core and jacket of the fuel element during rapid and considerable changes in the power of the assemblies and the reactor as a whole; 3) swelling or excessive elongation of the fuel elements caused by the accumulation of gaseous fission products or structural changes in the fuel pellets; 4) development of microdefects in the jackets of fuel elements which were not detected in the process of the manufacturing of assemblies at the plant.

The main cause of the appearance of damages in fuel element jacket is, evidently, the development of hidden defects which are not revealed during inspection at the plant.

The amount of deposits of corrosion products on the fuel element surface is insignificant [69] and cannot lead to serious disturbances in the heat removal. This is explained to a considerable degree by the absence of stagnant zones in the assemblies. The detected deposits have a dark brown color against the background of a dark grey oxide film of the fuel element jackets and are removed easily with a wad of cotton. Stagnant zones appear in the gaps between the covers of the assemblies. Therefore, there are more corrosive deposits on the surfaces of the covers of assemblies which are activated in the neutron flux. If the water regime is disturbed, the activated corrosion products deposited on the covers of the assemblies and devices within the vessel can spread over the entire I circuit and increase the radioactive contamination of the equipment.

Studies of spent assemblies make it possible to obtain information about the working conditions of the fuel in the reactor.

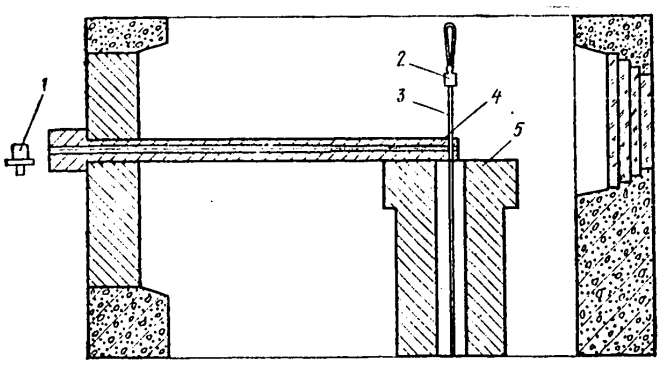

Figure 8.3. Diagram of a Device for Gamma-Spectrometic Studies of Fuel Burnup:
1 -- Ge(Li)-detector; 2 -- capture; 3 -- fuel element;
4 -- collimator; 5 -- table for separating the assemblies.

Gamma-spectrometric studies of spent fuel elements make it possible to determine the absolute values of fuel burnup, burnup distribution over the cross section and the height of the assemblies, and a number of other characteristics [70-72]. The method of gamma-spectrometry of fission fragments makes it possible to conduct burnup measurements without preliminary radiochemical reprocessing of the irradiated fuel. For the burnup evaluation, fission fragments and the products of their decay having a high yield and a sufficiently large half-life are selected (Table 8.7).

In the hot chamber of NVAES, gamma-spectra of fission fragments are determined by a semiconductor germanium-lithium detector with the use of a multichannel analyzer. When an assembly is taken apart, fuel elements are installed in front of the collimator and are moved along the height in relation to the detector (Figure 8.3). By using the multichannel analyzer, it is possible to resolve well gamma-lines of 513 kev from ^{85}Kr and ^{106}Ru; 605 and 796 kev ^{134}Cs, 622 kev ^{106}Ru, 724 and 757 kev ^{85}Zr, and others.

Nuclear fuel burnup is determined by using gamma-lines of isotopes ^{137}Cs and ^{106}Ru. Isotope ^{137}Cs has a large yield during the fission of ^{135}U and ^{239}Pu. ^{106}Ru has a preferential yield from the fission of ^{239}Pu and ^{241}Pu nuclei. The absolute burnup is determined by comparing the intensity of the gamma-line of ^{137}Cs of the fuel being studied and the standard cesium source.

Table 8.8 shows an example of the results of measurements of fuel burnup in assemblies of VVER-210 and VVER-365. The error in the determination of ^{235}U burnup does not exceed $\pm 10\%$, and that of ^{239}Pu -- $\pm 15\%$.

The gamme-spectrometric method of burnup determination is checked by the mass-spectrometric method.

Table 8.7

Nuclear Physical Properties of Characteristic Fission Fragments

Изотоп (1)	$T_{1/2}$	E_γ, кэв (2)	(3) Выход γ-квантов на один акт β-распада, %	(4) Выход на один акт деления, %			σ_a нейтронов, барн (5)	
				^{235}U	^{239}Pu	^{241}Pu	(6) тепловых	надтепловых (7)
^{95}Zr	63,98±0,06 суток (8)	724,23±0,04 756,74±0,04	43,5±0,5 54,3±0,5	6,455±0,032	4,9±0,25	—	—	—
^{106}Ru	368,3±2 суток	511,8±0,2 622,1±0,2	20,6±0,6 9,94±0,11	0,39±0,03	4,34±0,145	6,08±0,608	9	1,72
^{135}Cs	Стабилен (9)	—	—	6,72±0,0336	7,18±0,15	6,64±0,199	29,5±2.0	46,2
^{134}Cs	2,058±0,012 лет (10)	604,62±0,05 795,84±0,03 802,06±0,08	97,5±0,1 85,4±0,9 8,73±0,15	—	—	—	134,0	5,83
^{137}Cs	29,901±0,045 лет	661,64±0,8	34,6±0,4	6,27±0,314	6,48±0,194	6,52±0,196	0,11	—
^{144}Ce	284,5±0,4 суток	696,48±0,09 1489,14±0,07 2185,72±0,05	1,51±0,05 0,29±0,02 0,74±0,03	5,42±0,0272	3,85±0,012	4,09±0,04	1	2,2

Key: 1. Isotope
2. kev
3. Yield of gamma-quanta per event of beta-decay,%
4. Yield per fission event, %
5. Neutrons, barn
6. Thermal
7. Epithermal
8. Days
9. Stable
10. Years

Table 8.8
Experimental Values of the Nuclear Fuel Burnup Fraction in Assemblies of VVER-210 and VVER-365

(1) Измеряемая величина	(2) ВВЭР-210	(3) ВВЭР-365
Средняя интенсивность γ-линий, *имп/сек*: (4)		
^{106}Ru (622 *кэв*) (5)	2,51	5,86
^{137}Cs (662 *кэв*)	20,68	24,46
Среднее число ядер в 1 *см*^{3}: (6)		
^{106}Ru	$7,58 \cdot 10^{18}$	$9,68 \cdot 10^{18}$
^{137}Cs	$2,72 \cdot 10^{19}$	$3,268 \cdot 10^{19}$
Число разделившихся ядер в 1 *см*^{3}: (7)		
^{235}U	$2,81 \cdot 10^{20}$	$3,225 \cdot 10^{20}$
^{239}Pu	$1,42 \cdot 10^{20}$	$1,844 \cdot 10^{20}$
Выгорание, *кг* шл/*т* U: (8)		
^{235}U	$12,465 \pm 1,135$	$14,362 \pm 1,044$
^{239}Pu	$6,404 \pm 0,665$	$8,314 \pm 0,651$
Полное выгорание, *кг* шл/*т* U (9)	$18,869 \pm 2,624$	$22,616 \pm 2,420$

Key: 1. Measured value
2. VVER-210
3. VVER-365
4. Average intensity of gamma-lines, pulse/sec
5. kev
6. Average number of nuclei in 1 cm^3
7. Number of split nuclei in 1 cm^3
8. Burnup, kg slag/t U
9. Total burnup, kg slag/t U

By measuring the distribution of isotopes of cesium and ruthenium, it is possible to make a conclusion about the working temperature mode of the fuel elements. Migration of cesium isotopes is observed at temperatures of uranium dioxide above 1600 degrees C [68], and isotope ^{106}Ru migrates during the melting of the fuel. Studies on the fuel elements of VVER-210 and VVER-365 assemblies showed that the fuel temperature does not exceed 1600 degrees C.

11.1. Reactor Plant

The reactor plant VVER-1000 of block V at NVAES (Figure 11.1) contains, as compared to VVER-440, a number of changes in its design, layout and technological features which reflect the modern level of the development of VVER-type reactors.* These changes improved substantially the reliability and safety of operation, as well as improved the technical and economic indexes of the power unit as a whole. At the same time, there is a certain continuity with respect to its design and a technological solution which demonstrated its high effectiveness [130-132].

The development of highly productive equipment, primarily the main circulation pumps GTsN-195 and steam generators PGV-1000, made it possible to increase considerably the thermal power of the reactor and switch to a four-loop scheme of the reactor plant.

GTsN-195 is a vertical centrifugal-type pump with a sealed shaft and an external asynchronous electric motor equipped with flywheel masses. The basic characteristics of GTsN-195 are as follows:

Pump capacity, m^3/h	20,000
Pressure differential at nominal parameters (160 kg-force/cm^2, 290°C), kg-force/cm^2	6.75±0.25
Power consumption:	
for nominal parameters, kW	5300
on cold water (20-60°C), kW	7000
Number of revolutions (synchronous), rpm	1000
Inertia moment of the rotor of the motor with a flywheel, tm^2	7.25
Efficiency of pump with electric motor, per unit value	0.74
Weight of the set (pump+electric motor), t	156

The pressure in circuit I at which it is permissible to turn on the GTsN for preventing cavitational wear of the rotating blades increases when the temperature rises and

*The material presented here is based on the studies conducted by a team headed by V. V. Stekol'nikov.

is 15-20 kg-f/cm^2 at a temperature of 150°C. At 250°C, the above minimum permissible value of pressure increases to 50 kg-f/cm^2.

The presence of a flywheel increases substantially the rotor's moment of inertia, which ensures the required cooling of the reactor core in transient modes without taking special measures for increasing the reliability of electric power supply. For example, in a no-current mode, the delivery of the GTsN-195 decreases to 10/27 in 30 seconds, while the effective delivery of the low-inertia GTsN-310 used in the reactor plants VVER-440 drops practically to zero in three seconds.

The presence of the GTsN with flywheel masses increases the permissible power of the reactor in comparison with VVER-440 during operation on an incomplete number of loops, which, for VVER-1000, is 75% of the nominal value when working on three loops and 50% in working on two loops. In order to prevent the escape of radioactive coolant of circuit I through the stuffing-box seal of the GTsN shaft, provisions are made for delivering blocking water into the chamber of the stuffing-box seal. The flow rate of the blocking water after the main stages and the end sealing delivered by a system of organized streams is not over 3.5 m^3/h. The flow rate of the blocking water into the first circuit is not over 0.6 m^3/h.

Steam generator PGV-1000 is a horizontal single-hull heat exchanger with a submerged pipe bundle. The basic characteristics of PGV-1000 are as follows (also see Introduction):

Thermal power, MW	750
Average heat transfer coefficient (without consideration for deposits), kW/(m^2·°C)	6.03
Average thermal head, °C	24.7
Number of heat-exchange pipes, items	11,000
Length of pipes 16X1.5 mm of the heat-exchange bundle (average structural length) m	11.1
Margin with respect to the area of the heat-exchange surface in relation to the design area, %	21.4
Hydraulic resistance along the heat-transfer channel of circuit I, kg-f/cm^2	1.3
Heat flux density, kW/m^2:	
average	148.9
maximum	226.8
Steam moisture content at the outlet of the steam generator, %	0.2
Weight of dry steam generator (without supports), t	321.2

The main circulation pipelines of VVER-1000 of unit V at NVAES, as well as on VVER-440 have main shut-off gate valves (GZZ) which make it possible to shut off loops with malfunctioning equipment and to operate the reactor at intermediate power levels. The GZZ of VVER-1000, unlike the GZZ of VVER-440, has a parallel-plate shut-off gate. The main characteristics of the GZZ of VVER-1000 at the nominal parameters of the heat-transfer agent are as follows:

Normal pressure differential on the shut-off gate during opening and closing of the gate valve, kg-f/cm^2	18

Hydraulic losses on the fully opened gate, kg-f/cm^2:	
on a "cold" thread	0.16
on a "hot" thread	0.18
Electric motor power, kW	22
Rotation speed of the output shaft of the electric drive, RPM	20
Shutting time of the gate by the electric drive, sec	90
Diameter of the narrowed cross section in the seats, mm	630
Leakage through the shut-off gate with the closed position of the gate, cm^3/ min	5.2
Leakage through the stuffing box along the rod, cm^3/min:	
with the lower position of the gate	11
with the upper position of the gate	3

When the gate is in the closed position, in order to prevent the leakage of radioactive coolant into the shut-off part of the loop, provision is made for the delivery of sealing water into the space between the plates. The leakage of sealing water through the stuffing box along the rod of the electric drive is diverted by an organized leakage system.

VVER-1000 has a steam-type volume compensator (KO) which is an effective stabilizer and regulator of pressure in circuit I in the units of the preceding generation (VVER-365 and VVER-440). The basic characteristics of the KO of VVER-1000 are as follows:

Volume, m^3:	
total	79
of steam in the rated mode	24
corresponding to the shifting of the level by 10 cm along the height	0.707
Working parameters:	
pressure, kg-f/cm^2	160
temperature, ^{o}C	346
Safety valve triggering pressure, kg-f/cm^2:	
first	185.0
second and third	190.0
Power of electric motors, kW	2520
Number of electric heater units	28
Inner diameter of the cylindrical part of the body,m	3.0
Height (without support),m	13.66
Weight (without water), t	212

KO of VVER-1000 is connected by pipeline Du-350 with the permanently connected part of the "hot" thread of one of the loops of circuit I. The upper part of the KO has a Du-175 sleeve connected with the "cold" thread of one of the loops of circuit I which serves for injecting "cold" coolant if it is necessary to lower the pressure in the KO. There is also a Du-175 sleeve for removing excess steam through pulsed safety devices into the bubbler tank (BB).

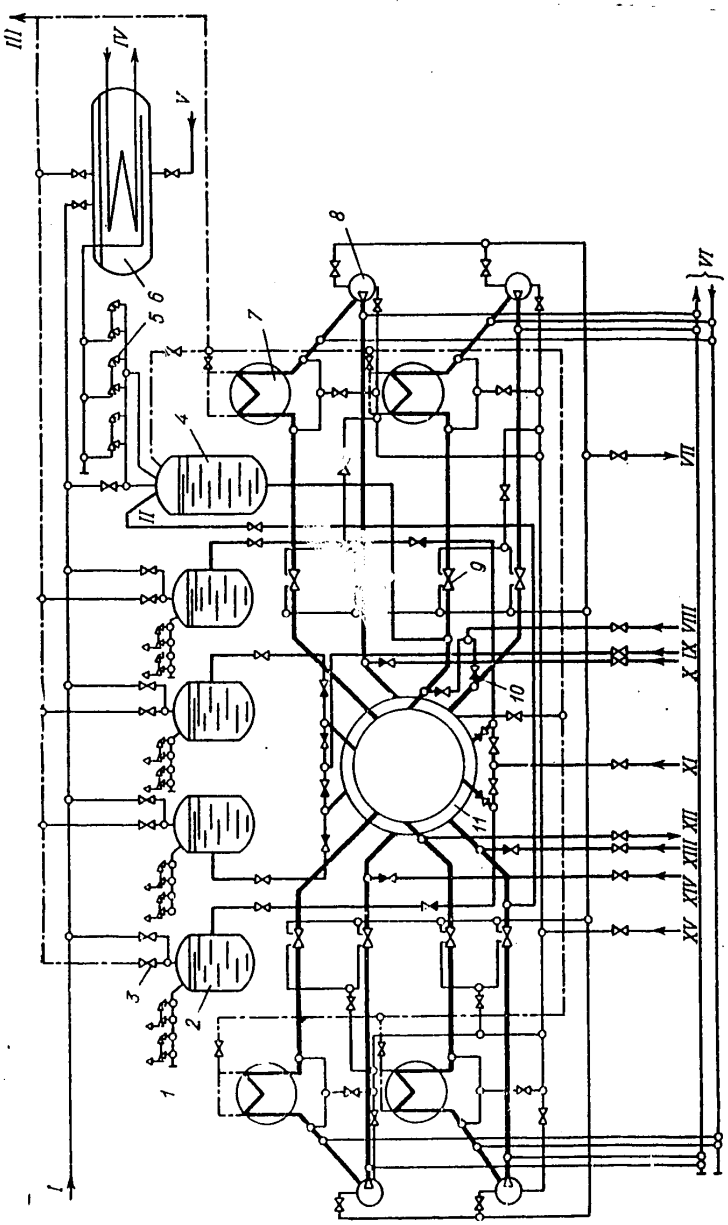

Figure 11.1. Basic Diagram of the Reactor Plant VVER-1000 of Unit V at NVAES:

I -- Nitrogen feed line; II -- line of injection of "cold" coolant into KO; III -- removal of blown-off gas; IV -- supply and removal of cooling water of the intermediate circuit; V -- pure condensate supply line; VI -- to the unit for purifying scavenging water of circuit I; VII -- to the heat exchanger of organized leakage system; VIII, IX, XI -- from ARN; X, XIII, XIV -- from AVN; XII -- to emergency shutdown heat exchangers; XV -- supply line of sealing water to GTsN and GZZ as well as for filling the loops of circuit I; 1 -- emergency hydraulic capacity safety valves; 2 -- emergency hydraulic capacity; 3 -- gating valve fixtures; 4 -- volume compensator; 5 -- KO safety valves; 6 -- bubbler tank; 7 -- steam generator; 8 -- main circulation pump; 9 -- main shut-off gate valve; 10 -- nonreturn valve; 11 -- reactor.

A substantial difference of the reactor plant VVER-1000 of unit V of NVAES from the plants of the preceding generation is the presence of safety systems ensuring emergency cooling of the reactor core in the case of a seal failure of the main circulation circuit (down to a failure with instantaneous bursting of the main circulation pipeline Du-850) and localization of the aftereffects of the failure within the limits of the reinforced-concrete protective shielding of the reactor [132].

The system of emergency cooling of the reactor core (SAOZ) includes a passive assembly (hydrocapacities) and emergency shutdown cooling pumps (ARN). Moreover, cooling water can be delivered to the loops of the reactor by emergency injection pumps (AVN) whose main purpose is to ensure the subcriticality of the core, as well as by makeup pumps (PN) through the scavenging return line.

The passive assembly of SAOZ consists of four cavities filled with borated water with the concentration of boric acid of 16 g/kg H_2O. The cavities are connected in pairs by Du-300 pipelines with the upper and lower mixing chambers of the reactor. The pipelines have nonreturn valves separating the cavities of the SAOZ from the reactor during normal operation. The cavities have safety valves protecting them from excessive rise of pressure in the case of a seal failure of the nonreturn valves. The pipelines connecting the cavities with the reactor also have quick-action gate valves which cut off the cavities from the reactor when the valves are triggered after the level of the borated water in the cavities drops to the minimum level, which prevents the entry of nitrogen into circuit I and the impairment of heat exchange in the reactor core. The main characteristics of the hydrocavities are as follows:

Total volume, m^3	60
Water volume, m^3	50
Working parameters:	
pressure, $kg\text{-}f/cm^2$	60
temperature, ^oC	40 - 60
Pressure in circuit I at which water from the hydrocavity enters the reactor, $kg\text{-}f/cm^2$	60
Pressure triggering safety valves, $kg\text{-}f/cm^2$:	
first	68
second	70
Internal diameter of the body, m	3.2
Height of the tank (with sleeves), m	8.7
Weight of the tank (without water), m	62.8

Emergency shutdown cooling pumps serve for delivering cooling water into the reactor vessel, as well as into one of the loops of circuit I after the triggering of hydrocapacities under emergency conditions when there is a seal failure in circuit I, and for planned cooling of circuit I to temperatures below 150 degrees C. The main characteristics of the ARN of VVER-1000 are as follows:

Number of pumps per unit	3
Delivery capacity of one pump, m^3/h	750
Pressure in circuit I at which ARN is turned on, $kg\text{-}f/cm^2$	15
Temperature of pumped liquid, ^oC	40 - 60
Weight of one unit, t	8.74

Under emergency conditions, ARN pump borated water with the concentration of boric acid of 16 g/kg H_2O from three tanks with emergency reserves of boron solution, each of 582 m^3 effective volume. When these tanks are emptied, the ARN switch to operation according to the following scheme: adjoining basement of the reactor room -- emergency shutdown cooling heat exchangers -- reactor. When ARN are used in the mode of planned shutdown cooling, the coolant of circuit I is pumped from the "hot" thread of one of the loops and delivered to the emergency shutdown cooling heat exchangers. After cooling, the coolant is returned by the ARN pumps to the lower mixing chamber of the reactor through the emergency cooling pipelines or to the "cold" thread of one of the loops of circuit I.

Emergenct injection pumps deliver boric acid solution with the concentration of 30 g/kg H_2O from the tank with a concentrated boric acid solution of 150 m^3 to the "cold" threads of three loops of circuit I. AVN are turned on in the modes with emergency shutdown cooling of circuit I and maintain the core of the reactor in the subcritical state. The main characteristics of AVN are as follows:

Number of pumps per block	3
Delivery capacity of one pump, m^3/h	150
Temperature of pumped liquid, ^oC	20 - 60
Pressure in the pressure nozzle, kg-f/cm^2	104
Weight of one unit, t	7.75

Makeup pumps (PN) regulate the water and chemical conditions of circuit I. PN deliver scavenging water into the return line with necessary additions of chemical reagents, such as boric acid, from the feed water deaerators of circuit I. The main characteristics of PN are as follows:

Number of pumps per block	3
Delivery capacity, m^3/h	10 - 60
Maximum output pressure, kg-f/cm^2	200
Temperature of pumped liquid, ^oC	70
Weight of one unit, t	12.3

The necessity in the inspection and repairs of radioactive equipment during preventive maintenance and major overhaul jobs and reloading of the reactor core is taken into consideration in the layout of the equipment of the VVER-1000 reactor room of the unit V of NVAES to a considerably greater degree than in the previous designs. For example, there are inspection shafts for the upper block of the reactor vessel, the block of protective pipes, devices and structures of the reactor with the necessary protective, maintenance and crane equipment.

The reliability and operational safety of the reactor plant are improved considerably by a regular tensiometric system for the equipment of circuit I (vessel and lid of the reactor, pins, gate valves, steam generators) which has a total of 349 tensioresistors, as well as an external inspection system and nondistructive ultrasound inspection system of the reactor vessel.

Generally, the VVER-1000 reactor plant of unit V at the NVAES meets the modern requirements for the technucal characteristics, operating conditions and safety for VVER-type reactor plants.

Accelerated introduction of AES power capacities planned for the next few decades will be ensured by standardization of the main equipment of VVER-1000 reactor plants. In the near future, it is planned to construct series blocks with VVER-1000 in which the main equipment of the reactor department will be practically analogous to the equipment of unit V of NVAES. The differences are due to the changes in the design of the core and the internal vessel equipment, the absence of GZZ on main circulation pipelines, further improvement of SUZ, and others.

Later, it is planned to use modernized series-produced reactor plants with vertical-type steam generators and new GTsN [132].

11.2. Steam Turbine Plant

The basic diagram of the steam turbine plant of the energy block of VVER-1000 of unit V of NVAES is analogous to the traditional thermal circuits of AES with VVER. The differences in the designs are connected with the improvement of the parameters of steam-power equipment and ensuring a safer and reliable operation of turbine units [128-130].

The steam from the steam generators is delivered to two turbines through four high-pressure steam pipelines which have the following characteristics:

Rated pressure, kg-f/cm^2	86
Rated temperature, ^{o}C	300
Hydraulic test pressure, kg-f/cm^2	110
Size of the pipe of the pipeline (diameter X wall thickness), mm	630X25

In the rated operation mode of the energy unit, each turbine receives steam from two steam generators. The turbine unit consists of a K-500-60/1500-type condensing turbine, a TGV-500-4 generator and a BTV-500-4 brushless exciter. The turbine (Figure 11.2) consists of two cylinders. The first combines parts of high (ChVD) and medium (ChSD) pressures. The second cylinder is a low pressure cylinder (TsND) [128]. The basic rated characteristics of the turbine are:

Specific heat consumption (gross), kcal/kW·h	2563
Frequency of shaft rotation, rpm	1500
Steam consumption per turbine, t/h	3135
Rated pressure of life steam in front of combined valves, kg-f/cm^2	60
Temperature of live steam in front of valves, ^{o}C	274.3
Steam dryness degree in front of valves, per unit value	0.995
Steam pressure at the exit from ChVD, kg-f/cm^2	11.71
Steam pressure after intermediate superheating (at the inlet to ChSD), kg-f/cm^2	10.77
Steam temperature after intermediate superheating (at the inlet to ChSD), ^{o}C	250
Number of:	
regenerative steam bleedings	7
stages in ChVD	7
stages in ChSD	5
stages in TsND	2X4

External diameter of the last stage of TsND, mm	5600
Feed water temperature, °C	220
Addition of desalinized water into the circuit, t/h	50

After the ChVD, intermediate separation and two-stage steam superheating in two separators-superheaters (SPP) are organized. They have the following characteristics:

Steam flow rate at the inlet, t/h	1180
Flow rate of heating steam of the first stage to steam superheater PP-1, t/h	37.7
Flow rate of heating steam of the second stage to the steam superheater PP-2, t/h	64.9

After each TsND of each turbine, the dead steam is condensed in two K-22550-type condensers. The condenser is a surface, two-pass, two-stream, lateral-type condenser. The cooling circulation water is delivered to the upper and lower halves of the condensers by pumps. The basic characteristics of the condenser are:

Rated steam pressure at the inlet, kg-f/cm^2	0.06
Temperature of cooling water, °C	22
Flow rate of cooling water to two condensers of one turbine, m^3/h	91650
Cooling water pump head, m:	
into upper halves of condensers	15-22.2
into the lower halves of condensers	13.5
Number of cooling tubes with dimensions (diameter X wall thickness, mm):	
28 x 1	12752
28 x 2	214
Length of cooling pipes, m	10
Pressure differential on the condenser in the rated mode, kg-f/cm^2	0.4
Maximum permissible excessive pressure inside the water space of the condenser, kg-f/cm^2	2
Steam flow rate through the receiving-discharging device (PSU), t/h	1800
Oxygen content in water after the condensator, µg/l	$\leq$20

The condensate is delivered by pumps (three items) into the regeneration circuit consisting of four low-pressure heaters (PND), a deaerator (D) for removing gases (chiefly oxygen) dissolved in the feed water and three high-pressure heaters (PVD) (Table 11.1). The draining of the condensate of the heating steam (drainage) of PVD progresses in stages: from PVD-7 to PVD-6, from PVD-6 to D, from PVD-5 to PND-4; provision is made for switching the drainage of PVD-6 to PVD-5. The drainage from PND-4 is directed to the external drainage cooler OD-4, from there to PND-3, from which condensate is pumped by the drainage pump DN-2 to the main condensate line. The drainage from PND-2 is directed to OD-2, from there to PND-1, from which the condensate is pumped by the drainage pump DN-1 to the main condensate line. The condensate of the heating steam from PP-2 gravitates into PVD-7, and the condensate

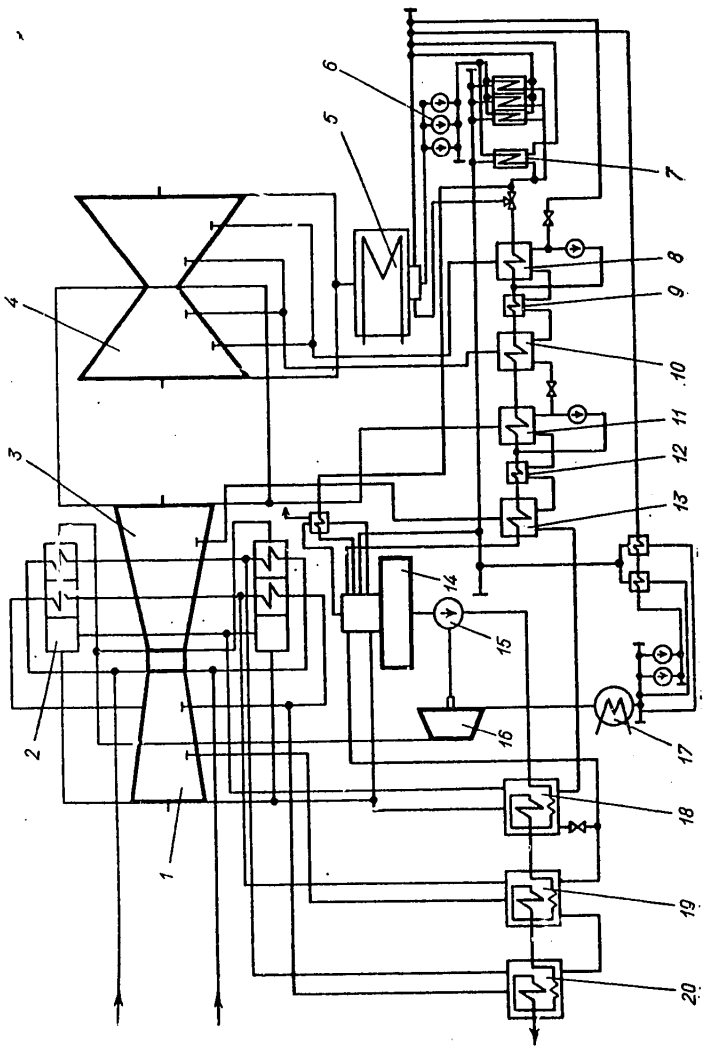

Figure 11.2. Basic Thermal Diagram of the Turbine Unit K-500-60/1500:
1 -- high pressure part (ChVD); 2 -- separators-steam superheaters (SPP); 3 -- medium pressure part (ChSD); 4 -- low-pressure cylinder (TsND); 5 -- turbine condensator; 6 -- condensate pumps; 7 -- ejector coolants (OE); 8 -- low pressure heater No 1 (PND-1); 9 -- drainage cooler (OD-2); 10 -- PND-2; 11 -- PND-3; 12 -- drainage cooler (OD-4); 13 -- PND-4; 14 -- deaerator (D); 15 -- feeding pipe pump; 16 -- driving steam turbines; 17 -- condensator of driving turbines; 18 -- high pressure heaters No 5 (PVD-5); 19 -- PVD-6; 20 -- PVD-7.

Table 11.1

Characteristics of Heat Exchange Equipment of the Turbine Plant K-500-60/1500

(1) Наименование оборудования	(2) Тип оборудования	(3) Поверхность теплообмена, м²	(4) Гидравлическая характеристика: (5) расход воды, м³/ч	(6) перепад давлений, кгс/см²	(7) Пробное давление гидроиспытаний, кгс/см²: (8) в корпусе	(9) в трубках
ПНД-1 (10)	(14) ПН-1700-25-0,3	1500	1739	0,94	20	32
ПНД-2	ПН-1700-25-1,3	1700	2043	1,17	20	32
ПНД-3	ПН-1700-25-2,5	1500	2043	1,14	20	32
ПНД-4	ПН-1700-25-6	1700	2608	1,76	20	32
ПВД-5 (15)	ПВ-2000-120-12	2300	3241	0,203	80	160
ПВД-6	ПВ-2000-120-19	2300	3241	0,203	80	160
ПВД-7	ПВ-2000-120-29	2300	3241	0,203	80	160
ОД-2 ПНД-2 11)	ОД-600-25-4	600	2043	0,77	20	32
ОД-4 ПНД-4	ОД-600-25-16	600	2608	0,53	20	32
(12) Колодильники эжекторной установки	ЭУ-16-2 (16)	280	1730	0,5	1,5	30
То же (13)	ЭП-3-55/150-2 (17)	153	900	0,5	1,5	30

Key: 1. Name of equipment
2. Type of equipment
3. Heat-exchange surface, m^2
4. Hydraulic characteristics
5. Water flow rate, m^3/h
6. Pressure differential, $kg\text{-}f/cm^2$
7. Test pressure of hydraulic tests, $kg\text{-}f/cm^2$
8. In the vessel
9. In the pipes
10. PND
11. OD
12. Coolers of the ejection unit
13. Same
14. PN
15. PV
16. EU
17. EP

from PP-1 is directed to PVD-6. The steam separated from the steam-water mixture is delivered from SPP into PVD-5.

The full-flow condensate of each turbine passes through two thermal deaerators of the DSP-1600-1 type consisting of a tank and a deaeration column. The parameters of the deaerator are given below:

Tank weight, t	30.1
Column weight, t	17.164
Working pressure in the column and the tank $kg\text{-}f/cm^2$	6

Permissible pressure in the column and the tank during the operation of safety valves, kg-f/cm^2	7.5
Hydraulic test pressure of the column and the tank, kg-f/cm^2	9
Working temperature in the column and the tank, °C	164
Geometrical volume, m^3:	
column	52
of the tank	150
Working volume of the tank, m^3	120
Rated output, t/h	1600
Specific evaporation per ton of deaerated water, kg	≤ 2
Stable deaeration under load (at an average water heating $\Delta t = 10 \div 40$°C), t/h	480-1600
Concentration of oxygen in deaerated water (at initial concentration of 1 mg/kg), µg/kg	≤ 15
External diameter of the column, mm	3442
Wall thickness of the column, mm	16
Height of the column, mm	8155
External diameter of the tank, mm	3442
Wall thickness of the tank, mm	16
Tank length, mm	17000

The deaerated water is pumped along the line by a PT-3750-75-type three-step centrifugal turbopump with a superimposed (booster) one-step centrifugal pump PD-3750-200. Due to the large flow of feed water, an OK-12A-type turbine is used as a drive of the feed pump. The turbine is supplied with steam bled after the SPP. Such a turbopump unit was used for VVER for the first time in the Soviet Union. The main parameters of the feed turbopump unit are as follows:

Driving Turbine

Rated power, kW	11600
Rotation frequency of the rotor, rpm	3500
Rotation frequency of the output shaft of the reductor, rpm	1800
Rated steam pressure in front of the check valve, kg-f/cm^2	9.9
Rated temperature of cooling water, °C	22
Counterpressure in the condenser at the rated power, kg-f/cm^2	0.06
Full rundown time of the rotor of the turbopump unit, min	$\sim$20

Feed Pump

Delivery power, m^3/h	3760
Head, m	808

Pressure, kg-f/cm^2:	
at inlet	27
at outlet	100
Power, kW	9130
Rotation frequency, rpm	3500
Feed water temperature (before the pump), °C	170
Pump weight, t	20
Pump dimensions, mm:	
length	3415
width	2020
height	2130

Booster Pump

Delivery power, m^3/h	3815
Head, m	214
Pressure, kg-f/cm^2:	
at inlet	7.7
at outlet	27
ultimate	37
Power, kW	2435
Rotation frequency, rpm	1800
Pump weight, t	6.48
Pump dimensions, mm:	
length	~2380
width	1760
height	~1880

The dead steam of the driving turbine is condensed in a special condenser from which the condensate is directed by two pumps into the full-flow condensate regeneration circuit. Provision is made in the turbine K-500-60/1500 for nonregulated steam bleeding: a) for covering the district heating load in the amount of 30 Gcal/h (a network water temperature of 130/70 degrees °C is ensured at 60-100% loads of the main turbine); b) for the power station needs in the amount of 75 t/h from the III bleeding of the turbine; c) for feeding the deaerator from the III bleeding at a turbine load of 75-100%, at loads below 75%, the deaerator is fed through a high-speed reduction unit of the deaerator (BRU-D).

For emergency situations, the turbine plant has high-speed reduction devices for discharging steam into the atmosphere (BRU-A) and into the condenser of the turbine (BRU-K). The parameters of the BRU are as follows:

Delivery power, t/h	900
Working pressure, kg-f/cm^2:	
in front of BRU-A (K)	78
after BRU-A (K)	15
Working steam temperature, °C	
in front of BRU-A (K)	292
after BRU-A (K)	197

Generator TGV-500-4 producing electrical current is connected coaxially with the turbine. The main parameters of the generator are as follows:

Power, kW	500,000
Voltage on the stator, kv	20
Power coefficient	0.85
Rated rotation rate of the rotor, rpm	1500
Current frequency, Hz	50
Current, a:	
stator	17,000
rotor	~4380
Weight, t:	
stator	235
rotor with fitting accessories	166

In the series-produced block, the VVER-1000 reactor is combined in a single block with a steam condensation turbine with a power of 1000 MW of the K-1000-60/1500 or K-1000-60/3000 type. In the future, the possibility of using turbines of the K-1000-70/1500 and K-1000-70/3000 types is considered.

12.4. Utilization of Spent Fuel of VVER

Reusing the fuel unloaded from reactors is one of the reserves for lowering the fuel component of the cost of electric energy, because spent fuel assemblies stored in cooling ponds can be considered as a potential reserve of additional nuclear fuel.

As a rule, some of the unloaded fuel assemblies still have sufficiently high breeding properties ($k_\infty > 1.0$). This depends greatly on the ways the reactor is operated, for example: the presence of a range in the burnup fraction of the unloaded fuel assemblies and average burnup fraction of the fuel in the core by the moment of the shutdown of the reactor for replacing the fuel; distribution of energy release in the fuel assemblies in the course of the last run; the assumption of the necessary length of the next run; the assumption of the necessary distribution of energy release in the fuel assemblies in the course of next run of the reactor and the requirements of maintaining the symmetry in loading connected with this, particularly in rejecting individual underfired fuel assemblies, for example, by the results of the inspection of the sealing of fuel element jackets.

The underfired nuclear fuel unloaded due to the above reasons, can be reused in one of the following loadings of the same reactor when, for example, it is required to replace an underfired fuel assembly with a revealed leaky condition of its jacket.

Underfired fuel assemblies kept for a certain period of time in the cooling pond are reloaded into the reactor after an additional nondistructive inspection of the condition of the fuel elements. For example, incompletely burnt assemblies were reused on many occasions in the reactors of units I and II at NVAES, as a result of which experience was accumulated, confirming a high effectiveness of the fuel elements used in VVER [53]. Incompletely burnt fuel assemblies were reused in the same reactor although, as was mentioned in section 12.3, it is more practical to reuse assemblies unloaded from reactors with a higher average working temperature of the core, i.e., with a higher water and fuel temperature, in reactors with a lower average temperature of the core and lower specific energy release.

The burnup fraction of the nuclear fuel of VVER can also be increased by using spent assemblies unloaded from the reactor for producing thermal energy at atomic boiler plants, which makes it possible to increase the average burnup fraction in assemblies by 3000-4000 MW·day/t U [53, 121]. Evaluations of the neutron-physics characteristics of the reactor of the atomic boiler plant indicate that each energy unit of an AES with VVER-440 can provide fuel for a rayon boiler plant of 250 MW with a reactor containing 349 spent assemblies of the supplier reactor operating in the annual reloading mode. The power unit of an atomic boiler plant can be put into operation

4-5 years after the starting of an AES reactor, i.e., after the accumulation of a sufficient number of assemblies for the first loading of the boiler plant reactor.

It is possible to lower the fuel component of the cost of VVER energy by industrial-scale chemical reprocessing of unloaded nuclear fuel containing ^{235}U, plutonium and other transuranium elements of great practical value. Uranium and plutonium separated from radioactive fission products can be used in producing fuel elements for thermal and fast neutron reactors. The possibility and economic practicality of using plutonium as a nuclear fuel without violating the safety requirements of the operation of atomic power and heat generating plants have been proven both theoretically and experimentally [122]. Moreover, exposed nuclear fuel, among all fission products of uranium and plutonium isotopes, contains individual radioactive isotopes or groups of isotopes which, having been separated from the spent nuclear fuel, can be of practical value in using them as radiation sources in various areas of science, as well as in industry, agriculture and medicine.

Table 12.2
Some Data on Radioactive Isotopes Obtained in Reactors for Creating Thermal Energy Sources

Показатель (1)	^{60}Co	^{90}Sr	^{137}Cs	^{144}Ce	^{147}Pm	^{170}Tm	^{209}Po	^{238}Pu	^{241}Am	^{242}Cm	^{244}Cm
Период полураспада, годы (2)	5,3	28	30	0,78	2,7	0,35	0,38	89	458	0,45	18
Изотопная чистота, % (3)	10	24	16	15	82	6,57	95 10)	70	90	82	82
Форма изотопа (4)	Металл	$SrTiO_3$	Стекло	CeO_2	Pm_2O_3	Tm_2O_3	Металл	PuO_2	Металл	Cm_2O_3	Cm_2O_3
Плотность, $г/см^3$ (5)	8,9	4,6	3,2	6,4	6,6	7,7	9,3	10	11,7	11,75	11,75
6) Удельное тепловыделение, $вт/г$:											
7) изотопа (включая дочерний)	17,4	0,95	0,42	25,6	0,33	15,6	141	0,56	0,11	120	2,8
(8) соединения	1,7	0,23	0,057	3,8	0,27	1,03	134	0,39	0,1	98	2,3
(9) Примерная стоимость 1 г соединения [13], долл.	56,1	4,4	1,4	3,8	24,6	10,3	2680	348,7	182	1666	821

Key: 1. Index
2. Half-life period, years
3. Isotopic purity, %
4. Isotope form
5. Density, g/cm^3
6. Specific heat release, W/g:
7. isotope(including daughter isotope)
8. compound
9. Approximate cost of 1 g of compound [13], dollars
10. Metal
11. Glass

The most promising fission product used for producing gamma-sources include ^{137}Cs which has a half-life of 30 years. ^{137}Cs is used as a radioactive indicator and tag for stable cesium in various physicochemical studies. Low-activity cesium sources are used widely in industry in instruments for measuring thicknesses, density, concentration and levels of various substances. Cesium sources of medium and high activity are used widely in gamma-defectoscopy of materials and weld seams, in gamma-ray therapy, for processing foodstuffs and sterilization of medical materials. The heat released during radioactive decay of ^{137}Cs is used very widely in isotopic generators of thermal and electrical energy which are long-life sources of electric power supply for navigational and meteorological instruments and stations. Another fission-fragment isotope used for practical and scientific purposes is ^{90}Sr; together with its daughter isotope ^{90}Y, it is an excellent beta-radiator and is used widely

for manufacturing beta-sources for various technological monitoring instruments, for removing electrostatic charges, as well as for making thermal units of isotopic generators of electric energy, including those for communication satellites.

Among fission-fragment radioactive isotopes of rare-earth elements, ^{144}Ce and ^{147}Pm are of practical interest. They can also be used for creating thermal generators of electric energy.

In spite of the fact that some other elements obtained in reactors, such as ^{60}Co, ^{170}Tm, ^{210}Po, ^{238}Pu, ^{241}Am, ^{242}Cm and ^{244}Cm, can be used in radio-isotopic generators of energy, fission fragment isotopes are used more widely because of their considerably lower costs (Table 12.2).

Fission-fragment isotopes ^{106}Ru, ^{95}Zr and ^{140}Ba which are used with their daughter isotopes ^{106}Rh, ^{95}Nb and ^{140}La, respectively, are of interest as sources of gamma-radiation. Radioactive isotopes of iodine containing in fission products have many practical applications, particularly in medicine.

Contents

END

10,233
CSO: 8144/1845